

POLITECNICO DI TORINO

Collegio di Ingegneria Chimica e dei Materiali

**Corso di Laurea Magistrale in Ingegneria Chimica e dei  
Processi Sostenibili**

Tesi di Laurea Magistrale

**Production of micro-particles by  
photo-polimerization in aerosol through cationic  
and radical mechanism**



**Relatori:**

Prof. Roberto Pisano  
Prof. Marco Sangermano  
Marco Bazzano

**Candidato:**

Martina Zappitelli

Ottobre 2017



# Contents

<b>Abstract</b>	<b>i</b>
0.1 Obiettivo della tesi . . . . .	i
0.2 Introduzione . . . . .	i
0.3 Risultati . . . . .	iii
0.3.1 Polimerizzazione cationica . . . . .	iii
0.3.2 Polimerizzazione radicalica . . . . .	v
0.3.3 Polimerizzazione tiolenica . . . . .	ix
0.4 Conclusioni . . . . .	x
<b>1 Introduction</b>	<b>1</b>
1.1 Micro-particles and Nano-particles . . . . .	1
1.2 Polymerization Techniques . . . . .	2
1.3 Aerosol Photo-Polymerization . . . . .	4
1.3.1 Atomization of liquid solutions . . . . .	4
1.3.2 Formation of solid particles . . . . .	5
1.4 Mechanisms of reaction . . . . .	7
1.4.1 Acrylic radical chain polymerization . . . . .	7
1.4.2 Cationic polymerization . . . . .	12
1.4.3 Thiol-ene radical polymerization . . . . .	14
1.4.4 Aim of the thesis . . . . .	15
<b>2 Experimental section</b>	<b>17</b>
2.1 Materials . . . . .	17
2.1.1 Cationic polymerization . . . . .	17
2.1.2 Acrylic radical polymerization . . . . .	19
2.1.3 Thiol-ene radical polymerization . . . . .	20
2.2 Equipment and Instrumentation . . . . .	21
2.3 Analysis techniques . . . . .	23
2.3.1 Field emission scanning electron microscopy . . . . .	23
2.3.2 Fourier transform infrared spectroscopy . . . . .	23
<b>3 Results and discussion: Cationic Polymerization</b>	<b>25</b>
3.1 Production of full micro-particles . . . . .	25
3.2 Production of porous micro-particles . . . . .	27
3.3 Production of micro-capsules . . . . .	29
3.3.1 Use of Iso-Octanol . . . . .	29
3.3.2 Use of co-monomers . . . . .	36
3.4 Conclusion cationic polymerization . . . . .	38

<b>4 Results and discussion: Radical Polymerization</b>	<b>39</b>
4.1 Acrylic Polymerization . . . . .	39
4.1.1 Production of full micro-particles . . . . .	39
4.1.2 Production of porous micro-particles . . . . .	43
4.1.3 Production of micro-capsules and micro-caps . . . . .	47
4.2 Conclusion acrylic polymerization . . . . .	60
4.3 Thiol-ene Polymerization . . . . .	62
4.3.1 Production of full micro-particles . . . . .	62
4.3.2 Production of porous micro-particles . . . . .	65
4.4 Conclusion thiol-ene polymerization . . . . .	66
<b>List of Figures</b>	<b>66</b>
<b>List of Tables</b>	<b>68</b>
<b>Acronyms</b>	<b>71</b>
<b>List of Symbols</b>	<b>73</b>
<b>Bibliography</b>	<b>75</b>
<b>Acknowledgments</b>	<b>77</b>

# Abstract

## 0.1 Obiettivo della tesi

La tesi sperimentale è stata condotta presso i laboratori del Karlsruhe Institute of Technology (KIT), Karlsruhe, Germania.

L'obiettivo di questo lavoro è stato lo studio e la produzione di micro-particelle polimeriche utilizzabili per fini farmaceutici. La loro produzione è avvenuta attraverso una polimerizzazione in aerosol foto-attivata sfruttando tre diversi meccanismi di reazione: cationico, radicalico acrilico e radicalico tiolenico. Per ogni meccanismo di reazione si è cercato di produrre particelle piene, porose e a forma di capsula o a forma di caps.

Inoltre sono state ottimizzate le formulazioni delle soluzioni di partenza per ottenere risultati soddisfacenti dal punto di vista morfologico.

## 0.2 Introduzione

In letteratura si considera micro-particella una particella sferica il cui diametro varia da 1 a 1000  $\mu\text{m}$ , mentre si considera nano-particella sempre una particella sferica il cui diametro però varia da 1 a 1000 nm (Campos et al., 2013). Le micro- e le nano-particelle sono presenti in varie tipologie, forme e composizioni, possono derivare da materiali naturali o sintetici e possono essere preparate secondo tecniche differenti (Kawaguchi, 2000; Arshady, 1990). I campi di applicazione sono molteplici e riguardano soprattutto le attività connesse con la medicina, come ad esempio il trasporto di medicinali e di DNA in terapia genica o il rilascio di proteine e peptidi (Liu et al., 2013; Soppimath et al., 2001).

Vari sono i metodi di preparazione delle micro-particelle. La maggior parte di essi riguarda sistemi di polimerizzazione in fase liquida, come la macro-, mini- e micro-emulsione, la precipitazione o la sospensione, solo per citarne alcuni.

In questo lavoro di tesi le micro-particelle sono state prodotte, invece, con un sistema diverso di polimerizzazione: la foto-polimerizzazione in aerosol. Questo metodo prevede l'atomizzazione delle gocce della soluzione di partenza in gocce di monomero e il successivo passaggio di queste ultime nel foto-reattore per essere convertite in particelle polimeriche.

Il metodo in aerosol presenta dei vantaggi rispetto ai metodi descritti precedentemente. Infatti il meccanismo in aerosol è un processo continuo e conduce alla produzione di particelle con maggiore purezza data l'assenza di componenti che possono contaminare il prodotto come ad esempio tensioattivi. Inoltre permette di controllare il diametro delle particelle prodotte monitorando il diametro delle gocce della soluzione di partenza (Shin and Oh, 1996).

L'atomizzazione della soluzione di partenza può avvenire secondo diversi metodi che considerano il tipo di forza che viene applicata alla soluzione. I metodi più diffusi sono il metodo pneumatico, ultrasonico ed elettro-spray. Nella tesi la formazione di gocce primarie è avvenuta attraverso un'atomizzazione pneumatica.

La polimerizzazione può avvenire secondo diversi meccanismi di reazione. Quello cationico e radicalico acrilico sono tipi di polimerizzazione a catena che inglobano una fase di iniziazione, una di propagazione e una di terminazione per costituire la catena polimerica. La polimerizzazione che avviene, invece, attraverso il meccanismo radicalico tiolenico coinvolge un monomero tiolico e uno vinilico che reagiscono attraverso una reazione a step.

La strumentazione che è stata utilizzata per condurre gli esperimenti di questa tesi consiste in due dispositivi, un atomizzatore e un foto-reattore.

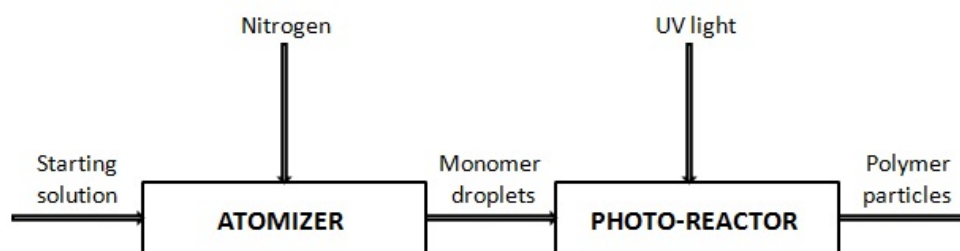


Figura 1: Processo schematico della foto-polimerizzazione in aerosol.

La soluzione di partenza contenuta in un recipiente è spruzzata dall'atomizzatore. L'atomizzazione da gocce di soluzione a gocce di aerosol avviene grazie alla presenza di un nozzle a due componenti dell'atomizzatore e di un flusso di azoto che crea un effetto Venturi. Le gocce di aerosol vengono trasportate via dalla corrente stessa di azoto e vengono convogliate nel reattore. Il reattore è formato da un cilindro di quarzo circondato da 6 tubi UV fluorescenti. La radiazione policromatica UV emessa da queste lampade varia tra i 270 e i 360 nm con un massimo ai 312 nm. Il materiale in uscita dal reattore è raccolto in un contenitore di alluminio oppure in un filtro in relazione al tipo di esperimento condotto. La durata di ogni prova varia dai 30 minuti, se il materiale viene raccolto nel recipiente di alluminio, alle 2 ore, se viene raccolto nel filtro.



Figura 2: Strumentazione completa: atomizzatore, foto-reattore, filtro.

I campioni prodotti sono stati sottoposti ad analisi tecniche. La microscopia elettronica a scansione

ad emissione di campo, FE-SEM, è una tecnica di analisi che ha permesso di valutare la dimensione e la morfologia delle particelle prodotte. La spettroscopia infrarossa a trasformata di Fourier, FT-IR, invece, è un'altra metodologia che ha permesso di analizzare la conversione dei legami reattivi del monomero dopo il passaggio nel reattore.

## 0.3 Risultati

Il lavoro sperimentale può essere suddiviso in tre parti. La prima parte della tesi riguarda gli esperimenti condotti per la produzione di micro-particelle attraverso un meccanismo di polimerizzazione cationica. La seconda parte tratta la polimerizzazione attraverso un meccanismo radicalico e la terza tramite uno tiolenico. Per ogni meccanismo di reazione si è cercato di produrre micro-particelle con un diverso grado di strutturazione. piene, porose, caps o capsule.

### 0.3.1 Polimerizzazione cationica

La prima parte della tesi concerne esperimenti condotti attraverso un meccanismo di polimerizzazione cationica.

La produzione di particelle piene è stata ottenuta utilizzando una soluzione di partenza composta da solo monomero e foto-inziatore. Il monomero impiegato è stato il trietilenglicole divinil etere (DVE-3), mentre il foto-inziatore è stato il sale di triarilsolfonio esafluoroantimoniato (TAS-HFA). Il parametro che è stato variato è stato la pressione. La variazione di questo parametro ha avuto come obiettivo lo studio della distribuzione della dimensione delle particelle. In questo caso la variazione del parametro pressione non ha avuto influenza sulla strutturazione delle micro-particelle. Tutte le particelle prodotte sono state particelle sferiche e piene.

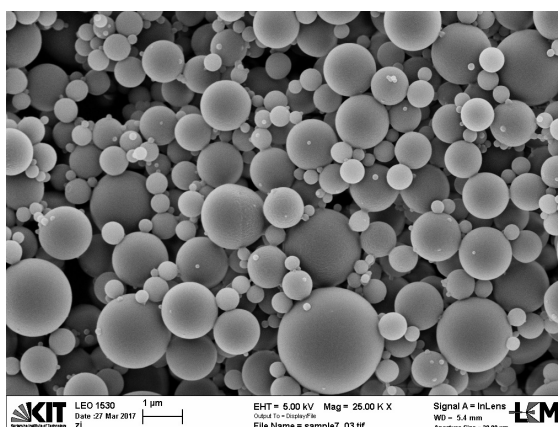


Figura 3: Immagine al FE-SEM di micro-particelle piene, meccanismo cationico.

La distribuzione della dimensione delle particelle, invece, ha mostrato che a pressioni alte, la popolazione di particelle è stata distribuita su una scala ampia di dimensioni, mentre a pressioni basse su una scala minore.

La produzione di particelle porose è stata realizzata aggiungendo alla soluzione precedentemente illustrata dei solventi. L'esadecano (HD) è stato introdotto per agire nella polimerizzazione come separatore di fase. E' stato nominato 'cattivo' solvente per la sua natura non polare e non affine né al monomero né al polimero. L'altro solvente che è stato utilizzato è il 2-ottanone. E' stato nominato 'buon' solvente perchè affine al monomero, al polimero e, in parte, all'HD. Lo scopo di questo agente è stato rendere omogenea la soluzione di partenza.

Le soluzioni sono state preparate impiegando il 70% in peso di monomero e il 30% in peso di solventi. Le prove sono state eseguite variando il rapporto tra le concentrazioni in peso dei solventi e la pressione.

Il quantitativo di HD è stato variato dal 17.5 al 10%, mentre quello di 2-ottanone è stato aumentato dal 12.5 al 20%. La formulazione che ha dato i migliori risultati in termini di porosità ben definita e di particelle separate tra loro è stata quella con rapporto in peso tra 2-ottanone ed HD di 0.71. Il quantitativo di HD è stato mantenuto il più alto possibile (incipiente separazione di fase) per consentire una separazione di fase nei primi stadi della polimerizzazione ed evitare che avvenisse quando le particelle erano del tutto polimerizzate.

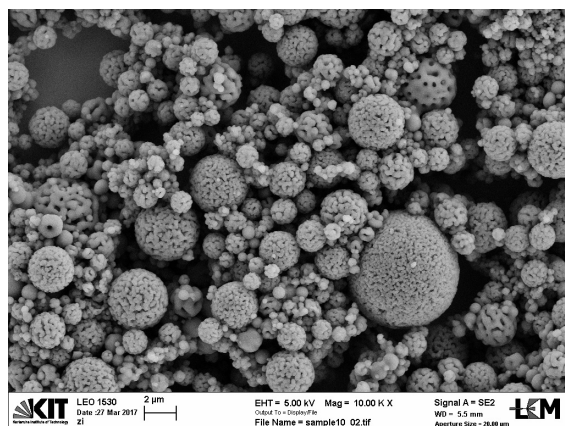


Figura 4: Immagine al FE-SEM di micro-particelle porose, meccanismo cationico.

Per quanto riguarda l'influenza della pressione, sono state eseguite prove sulla formulazione precedentemente citata. I risultati hanno mostrato che alte pressioni hanno consentito una strutturazione più definita delle particelle, mentre a basse pressioni erano presenti, oltre a particelle porose, anche particelle disintegrate e capsule.

Due diverse strategie sono state condotte per produrre le micro-capsule.

La prima strategia ha coinvolto l'aggiunta di un alcol alla soluzione composta da DVE-3, fotoiniziatore e solventi. La funzione dell'alcol è stata quella di ritardare la gelificazione dando alle particelle più tempo per strutturarsi e raggiungere la morfologia desiderata. L'alcol utilizzato è 2-etil-1-esanolo, commercialmente chiamato iso-ottanolo. Gli esperimenti sono stati condotti variando il rapporto in peso tra monomero e solventi, lasciando invariato il rapporto in peso ottimale tra monomero ed alcol di 12:1. Le formulazioni che hanno dato risultati più promettenti hanno considerato il 60% in peso del monomero e il 40% in peso dei solventi e il 56% in peso del monomero e il 44% in peso dei solventi. Per quanto riguarda la formulazione che ha inglobato il 60% in peso del monomero, varie prove sono state condotte per testare il giusto rapporto tra i solventi e anche in questo caso è stato necessario un quantitativo alto di HD per ottenere particelle ben definite. La formulazione migliore ha considerato il 27.5% di HD, il 7.5% di 2-ottanone e il 5% di iso-ottanolo. Allo stesso modo, la formula che ha considerato il 56% in peso di monomero, ha richiesto il 30.9% in peso di HD, l'8.4% in peso di 2-ottanone e il 4.7% di iso-ottanolo.

Molti esperimenti sono stati condotti impiegando il 50% di monomero e il 50% di solventi e variando diversi parametri, quali il quantitativo di iso-ottanolo, il rapporto tra le concentrazioni dei solventi e il quantitativo di foto-iniziatore. Le particelle risultanti, tuttavia, sono apparse non strutturate, talvolta di forma non identificata come se potessero derivare dal collasso di una struttura più grande oppure interconnesse come se derivassero da una polimerizzazione secondaria.

L'altra strategia per la produzione di micro-capsule ha considerato la presenza di co-monomeri mono-funzionali, quindi meno reattivi. Anche in questo caso l'uso di tali monomeri ha avuto

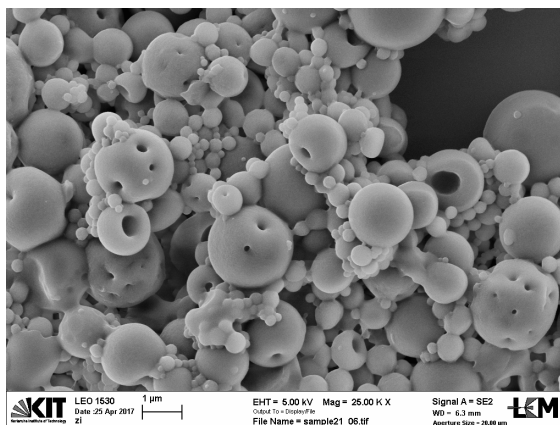


Figura 5: Immagine al FE-SEM di micro-capsule, meccanismo cationico.

come scopo il ritardo nella velocità di gelificazione. I co-monomeri che sono stati impiegati sono stati il 2-etilesil vinil etere e il dietilenglicole vinil etere. Il primo reagente ha dato problemi per quanto riguarda l'omogeneità della soluzione iniziale, quindi gli esperimenti sono stati focalizzati sull'impiego dell'altro co-monomero. Le prove condotte impiegando solo DVE-3 e dietilenglicole vinil etere hanno prodotto particelle sferiche e piene, quelle realizzate impiegando solventi, quali HD e 2-ottanone hanno condotto a produrre particelle strutturate, ma non nella forma desiderata. Vari esperimenti sono stati condotti variando il rapporto tra le concentrazioni in peso di monomeri e solventi, tuttavia senza raggiungere risultati sperati poiché, probabilmente, la velocità di reazione diminuisce troppo.

### 0.3.2 Polimerizzazione radicalica

La seconda parte della tesi è stata incentrata sulla produzione di micro-particelle attraverso il meccanismo di polimerizzazione radicalico.

La produzione di particelle piene è stata investigata utilizzando una soluzione composta da monomero, foto-iniziatore (Irgacure 907) e cross-linker. Diversi tipi di monomeri e cross-linkers sono stati provati. I due tipi di monomeri impiegati sono stati butil acrilato (BA) e metil metacrilato (MMA). L'uso di MMA non ha portato a produrre particelle piene e definite, ma queste sono apparse dal FE-SEM non completamente separate e tendenti ad attaccarsi l'una con l'altra. Ciò è stato causato dalla bassa densità di reticolazione delle particelle che conseguentemente hanno mostrato bassa resistenza meccanica. Il BA, invece, è risultato un buon monomero impiegato insieme a vari tipi di cross-linkers, quali 1,6-esandiolo diacrilato (HDDA), trimetilolpropano triacrilato (TPT) o trimetilolpropano etossilato triacrilato (TPET). Durante gli esperimenti sono stati variati i rapporti in peso tra il monomero e il cross-linker, ma le immagini della FE-SEM non hanno mostrato rilevanti differenze morfologiche, come ci si aspettava senza l'aggiunta di solventi responsabili della strutturazione delle particelle.

Le particelle porose sono state prodotte, come nel meccanismo di polimerizzazione cationico, da una soluzione di partenza composta da monomero, foto-iniziatore (Irgacure 907), cross-linker e solvente. I monomeri utilizzati sono stati BA e MMA, i cross-linkers HDDA, TPT o TPET e i solventi HD o iso-ottanolo. Sono stati effettuati molteplici esperimenti.

La prima fase di prove è stata condotta impiegando HDDA come cross-linker, BA come monomero e HD o iso-ottanolo come solvente. Sono state condotte analisi sui rapporti tra le concentrazioni in peso di monomeri e solvente. Il quantitativo di monomero è stato variato dal 70% al 60% e poi al 50%, mentre quello del solvente in maniera complementare. I risultati migliori sono stati ottenuti con un rapporto monomeri-solvente del 70%-30% e 60%-40%. Sono state prodotte micro-particelle con struttura a mosaico, mentre con la formulazione 50%-50% le particelle sono apparse

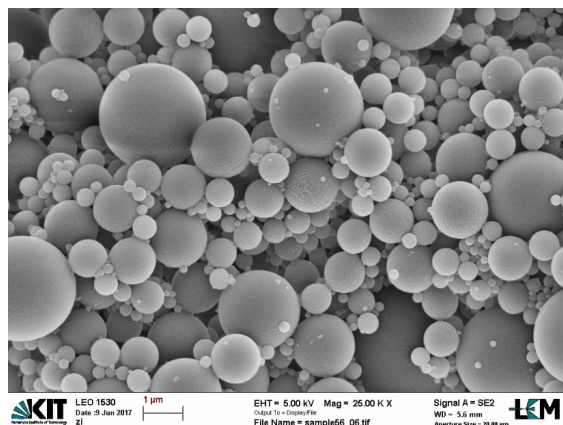


Figura 6: Immagine al FE-SEM di micro-particelle piene, meccanismo radicalico.

discretate in domini polimerici di piccole dimensioni, probabilmente a causa di un ritardo della fase di separazione.

Impiegando invece come cross-linker TPT, i monomeri impiegati sono stati BA o MMA insieme a HD o iso-ottanolo come solventi. Gli esperimenti sono stati condotti impiegando il 70% in peso di monomeri e il 30% in peso di solventi, variando il rapporto tra monomero e cross-linker. L'uso del cross-linker tri-funzionale TPT piuttosto che di HDDA, bi-funzionale, ha portato a migliori risultati grazie alla maggiore reattività e a produrre particelle definite, separate, sferiche e con una strutturazione a mosaico.

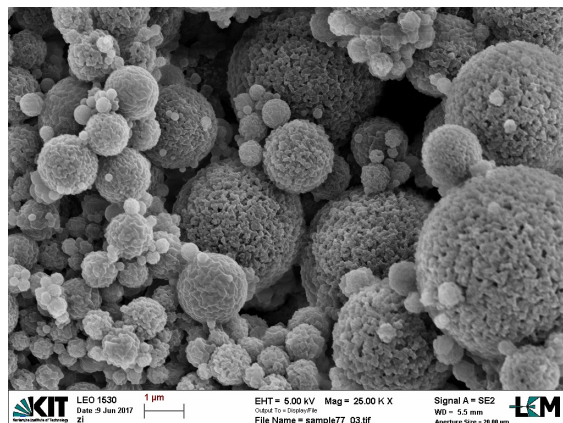


Figura 7: Immagine al FE-SEM di micro-particelle porose, meccanismo radicalico.

L'uso, invece, di TPET come cross-linker, insieme a BA come monomero e a HD o iso-ottanolo come solvente, ha portato a produrre micro-particelle con struttura 'gel', dove dal punto di vista microscopico il solvente era ancora presente all'interno della struttura e la separazione di fase non era realmente avvenuta. L'uso di MMA come monomero insieme a TPET come cross-linker e ai solventi precedentemente citati ha condotto alla produzione di particelle differenziate, quali porose, disintegrate e caps. Ciò evidenzia la migliore compatibilità del sistema co-monomerico BA-TPET. Quest'ultimo ha dato migliori risultati con l'iso-ottanolo rispetto all'HD data la sua maggiore solubilità in questo solvente. Le prove sono state per la maggior parte condotte con un rapporto monomeri-solvente 70%-30% dato che il rapporto 50%-50% ha prodotto particelle disintegrate.

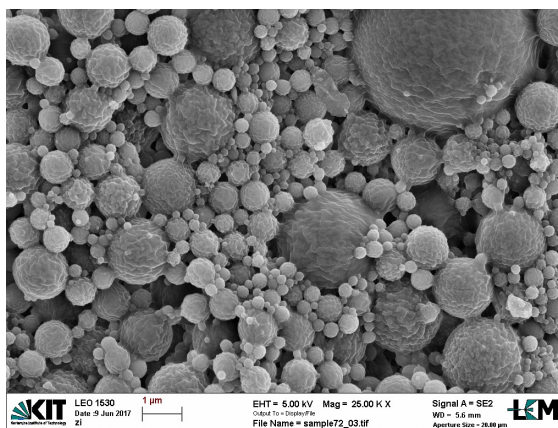


Figura 8: Immagine al FE-SEM di micro-particelle porose, meccanismo radicalico.

Per produrre micro-capsule e micro-caps è stato necessario aggiungere alla soluzione di partenza, formata da monomero, cross-linker, foto-iniziatore e solventi, glicerolo. Il glicerolo è indispensabile per ottenere questo grado di strutturazione delle particelle. Per ottenere una soluzione di partenza omogenea sono stati aggiunti etanolo o 1-propanolo. La loro evaporazione ha permesso il collasso della struttura e il raggiungimento della morfologia desiderata delle particelle.

Gli esperimenti hanno riguardato due tipi di soluzioni. La prima soluzione di partenza è stata costituita da BA come monomero, HDDA come cross-linker, foto-iniziatore, HD o iso-ottanolo come solvente, glicerolo e co-solvente. Il rapporto in peso tra monomeri e solventi è stato variato da 70%-30% a 60%-40% a 50%-50%.

Le prove con il 50% in totale di monomero e cross-linker sono state condotte variando il quantitativo di glicerolo e il rapporto in peso tra monomero e cross-linker. Le particelle prodotte sono apparse dal FE-SEM non separate e disintegrate probabilmente a causa di un quantitativo troppo basso di monomero. Inoltre il quantitativo di cross-linker è stato mantenuto basso per evitare che la separazione di fase avvenisse durante l'atomizzazione; ciò ha portato ad una maggiore debolezza delle interconnessioni.

Le prove con il 60% in peso della miscela monomero-cross-linker hanno condotto all'ottenimento di micro-caps. l'HD è stato utilizzato come unico solvente e il maggior quantitativo di monomero ha permesso alle micro-caps di essere più definite e con un involucro uniforme.

Gli esperimenti in cui il quantitativo di monomero è stato del 70% hanno prodotto micro-caps e micro-capsule definite, separate e della conformazione desiderata. Questo è stato reso possibile grazie ad un delicato equilibrio tra la densità di cross-linking e l'attività plasticizzante del glicerolo. Quest'ultimo è stato indispensabile per la strutturazione delle micro-particelle e il suo quantitativo è stato incrementato notevolmente fino ad arrivare al 20% in peso. Anche il quantitativo di cross-linker è stato aumentato per incrementare la produzione di queste micro-particelle. Tuttavia non è stato possibile decifrare con precisione quale fattore influenzasse la formazione di micro-capsule o micro-caps.

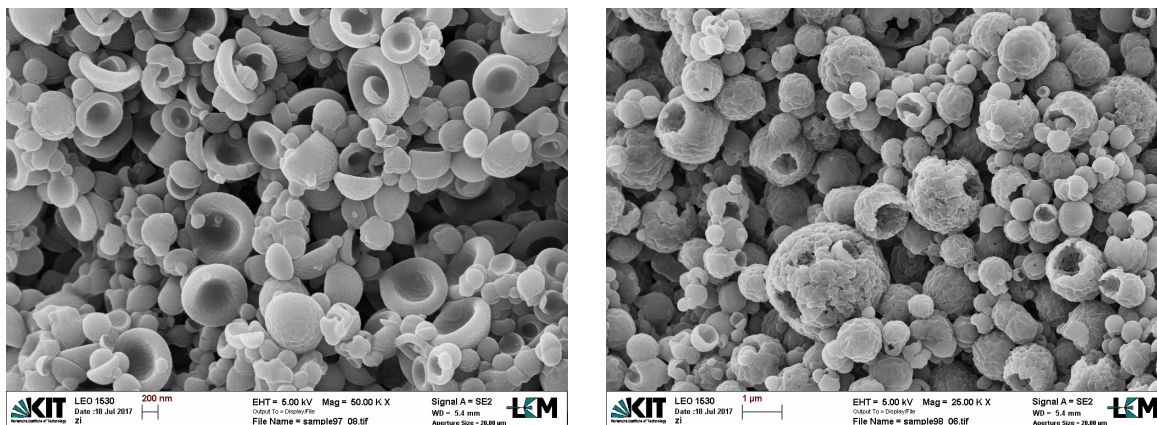


Figura 9: Immagine al FE-SEM di micro-caps e micro-capsule, meccanismo radicalico.

La seconda soluzione che è stata investigata ha coinvolto il BA come monomero, il TPT come cross-linker, Irgacure 907 come foto-iniziatore, i solventi HD o isottanololo, il glicerolo e i co-solventi etanolo o 1-propanolo. Gli esperimenti sono stati condotti con una concentrazione in peso di monomero e cross-linker del 70% e di solventi del 30%. Sono stati variati i rapporti in peso tra monomero e cross-linker, il quantitativo di glicerolo e di foto-iniziatore. Anche in questo caso, il miglior solvente è stato l'iso-ottanololo data la natura polare del TPT; infatti con l'HD sono state ottenute particelle disintegrate. Le micro-capsule che sono state ottenute hanno presentato un guscio poroso, tenuto unito da domini di materiale polimerico. Aumentando il quantitativo di foto-iniziatore, invece, il guscio è diventato liscio e uniforme. Probabilmente il quantitativo di foto-iniziatore ha avuto influenza nella strutturazione delle particelle. Anche per questo sistema co-monomerico è stato difficile identificare quale agente influenzasse la produzione di una o dell'altra struttura.

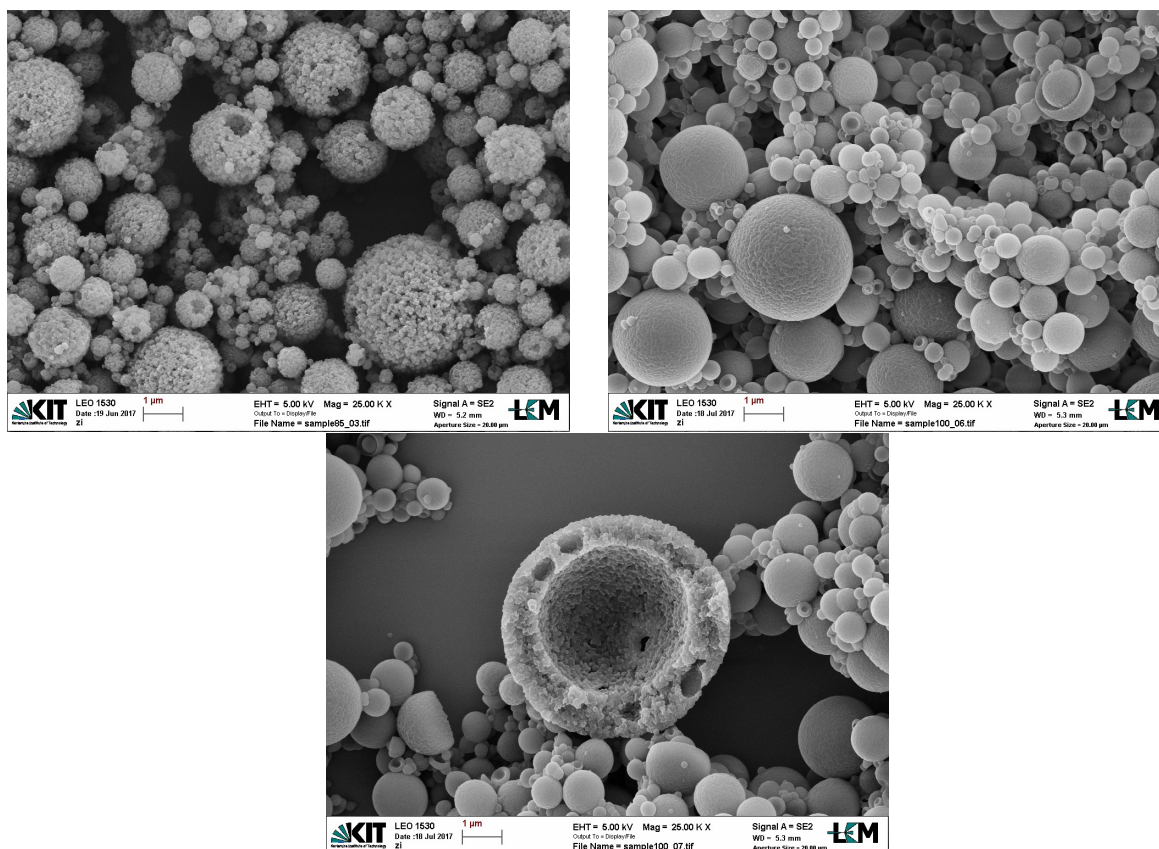


Figura 10: Immagine al FE-SEM di micro-caps e micro-capsule, meccanismo radicalico.

### 0.3.3 Polimerizzazione tiolenica

L'ultima parte della tesi ha riguardato lo studio del meccanismo di polimerizzazione tiolenica per la produzione di micro-particelle per la prima volta investigato tramite una foto-polimerizzazione in aerosol.

Le particelle piene sono state realizzate utilizzando una soluzione di partenza costituita da un monomero vinilico, un monomero tiolenico, il foto-iniziatore e i solventi. L'uso dei solventi è stato necessario per ottenere particelle piene, al contrario dei meccanismi di polimerizzazione precedentemente descritti. Infatti, sono stati aggiunti per evitare problemi alle attrezzature causati da una soluzione di partenza troppo viscosa. Irgacure 907 è stato utilizzato come foto-iniziatore, mentre come solventi sono stati usati HD, 2-ottanone o etanolo. Neopentil glicol diacrilato, dialile adipato o trietilenglicole etere divinilico sono stati impiegati come monomeri vinilici, come monomero tiolenici invece trimetilolpropano tris 3-mercaptopropionato o pentaeritritolo tetrakis 3-mercaptopropionato. Le soluzioni di partenza sono state formulate con il 70% in peso di monomeri e il 30% in peso di solventi, 60%-40% e 50%-50%. In questo caso, però, il rapporto significativo è stato quello riguardante il quantitativo in peso di monomero tiolenico e vinilico. Normalmente questo tipo di reazione funziona bene con un rapporto unitario tra i due monomeri che impedisce la formazione di oligomeri. In questo caso gli esperimenti hanno portato a risultati soddisfacenti con un rapporto in peso tra monomero tiolenico e vinilico di 1.5:1. Dalle immagini del FE-SEM non è stato possibile identificare differenze importanti tra i vari rapporti in peso monomeri-solventi. Gli esperimenti con un rapporto monomero tiolenico-vinilico 1.5:1 hanno prodotto particelle piene, meno viscosi e più separate di quelle prodotte con un rapporto unitario.

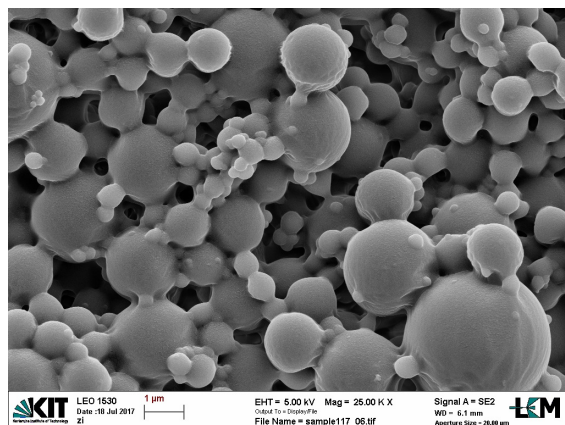


Figura 11: Immagine al FE-SEM di micro-particelle piene, meccanismo tiolenico.

Le particelle porose sono state realizzate aggiungendo alla soluzione precedentemente descritta un alcol, quale l'iso-ottanolo. Gli esperimenti sono stati condotti con un rapporto in peso monomeri-solventi del 70%-30% e 60%-40% e con un rapporto in peso monomero tiolenico-monomero vinilico dell'1.5:1. Dal FE-SEM le particelle di grandi dimensioni sono apparse con una struttura dotata di pori, mentre quelle di dimensioni inferiori sembravano piene e senza una differenziazione strutturale.

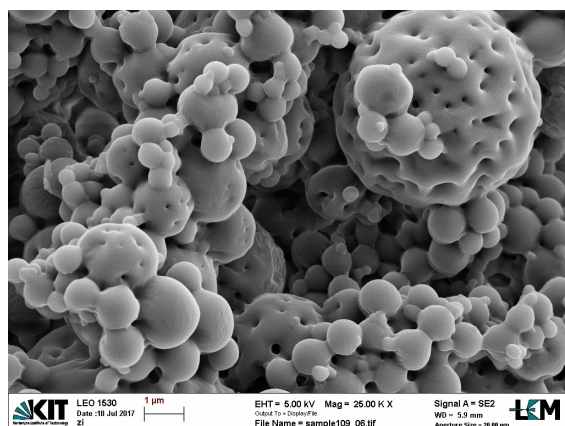


Figura 12: Immagine al FE-SEM di micro-particelle porose, meccanismo tiolenico.

## 0.4 Conclusioni

Questa tesi ha dimostrato nuovamente la possibilità di produrre micro-particelle piene e strutturate con il metodo aerosol accoppiato alla foto-polimerizzazione.

Ha avuto come obiettivo l'ottimizzazione delle formulazioni delle soluzioni di partenza per ottenere micro-particelle con i meccanismi di polimerizzazione cationico e radicalico acrilico.

Per quanto riguarda, invece, il meccanismo di polimerizzazione radicalico tiolenico è stata dimostrata per la prima volta la possibilità di produrre particelle piene e porose con il meccanismo di aerosol-foto-polimerizzazione.

Gli sviluppi di questo argomento nel futuro potranno considerare l'ottimizzazione delle formulazioni delle soluzioni di partenza in modo da ottenere strutture sempre più definite e conformi alle applicazioni scelte. Gli studi riguarderanno soprattutto il meccanismo di reazione tiolenico per cercare

di produrre particelle strutturate e ricercare reagenti idonei. Potranno, inoltre, essere migliorati i tempi necessari al completamento della reazione e i meccanismi di raccolta del polimero prodotto.



# Chapter 1

## Introduction

### 1.1 Micro-particles and Nano-particles

In literature, micro-particle is considered as a spherical particle whose diameter varies from 1 to 1000  $\mu\text{m}$ . Usually polymeric micro-particles are encapsulated systems: an active compound is immobilized within a polymeric matrix. As to the distribution of the active compound, micro-particles can be divided into micro-spheres and micro-capsules. If the active compound is homogeneously mixed with the raw material the micro-particle is considered a micro-sphere, on the other hand, if the active compound is placed within the core and surrounded by the polymeric shell the micro-particle is considered a micro-capsule (Campos et al., 2013).

Micro-particles are employed in many fields regarding composites, paints, coatings, oil and gas exploration, adhesives, cosmetics, personal grooming products, life sciences, biotechnology, medicine and medical devices. Micro-particles are available in different types, divided in terms of size, size distribution, composition, surface chemistry, topography and morphology (Kawaguchi, 2000) thanks to the many starting materials used for their production, that can be natural or synthetic, and the different preparation techniques (Arshady, 1990).

In 1953 the chemists L. Schleicher and B. Green for the first time produced an industrial product using micro-particles (Green and Schleicher, 1957). They developed an improved copying paper by undercoating sheets of paper with micro-capsules containing a colorless dye precursor (Campos et al., 2013). In the pharmaceutical field, in 1970, W.M. Holliday and collaborators used for the first time micro-particles (Bell et al., 1970), as an orally administered. Acetylsalicylic acid was encapsulated within micro-capsule made of ethyl cellulose.

In literature, nano-particle is considered as a solid colloidal particle whose size varies from 1 to 1000 nm. It contains a number of atoms that varies from 20 to 15.000 and exists in a realm that straddles the quantum and Newtonian scales (Liu, 2006; Soppimath et al., 2001; Mora-Huertas et al., 2010). Similarly to micro-particles, nano-particles can be divided into nano-capsules or nano-spheres based upon the distribution of the active compound and upon the method of preparation. If the active compound is surrounded by a sole polymeric membrane the nano-particle is considered a nano-capsule, on the other hand, if the active ingredient is uniformly dispersed in the matrix the nano-particle is considered a nano-sphere (Soppimath et al., 2001).

Different materials in different shapes such as spheres, rods, wires and tubes are used to produce nano-particles. The fields of application of these particles include advanced materials, electronic, magnetic and optoelectronic, biomedicine, pharmaceutical, cosmetic, energy, catalytic and environmental detection and monitoring. In the last years, the attention is reserved to their use as carrier of drugs and DNA in gene therapy, to target particular organs and tissues and to deliver proteins, peptides and genes (Liu, 2006; Soppimath et al., 2001).

## 1.2 Polymerization Techniques

Different types of techniques are available for production of micro- and nano-particles.

*Macro-emulsion polymerization* is performed in a heterogeneous system and allows the production of rather mono-disperse particles whose size varies in the micro-scale. Components involved in this mechanism are monomers, water, water-soluble initiator and surfactants. This polymerization allows to attain both high molecular weights and high reaction rates. The process can be divided into three intervals (Fig. 1.1). In the first phase particle nucleation occurs, it is conducted in a homogeneous phase or in micelles and the percentage of conversion is the lowest, around 2-15%. This nucleation happens when radicals, shaped in the aqueous phase, propagate and come into micelles or grow to precipitate and create primary particles. All surfactants are adsorbed to the particles at the end of this phase. Number of particles increases as rate of polymerization. The second phase involves polymerization within the monomer swollen polymer particles, the monomer diffuses from droplets. Number of particles is constant, as the rate. The last phase of the process starts when droplets disappear and stops at the end of the reaction. The number of particles is constant, but the rate decreases. (Schork et al., 2005)

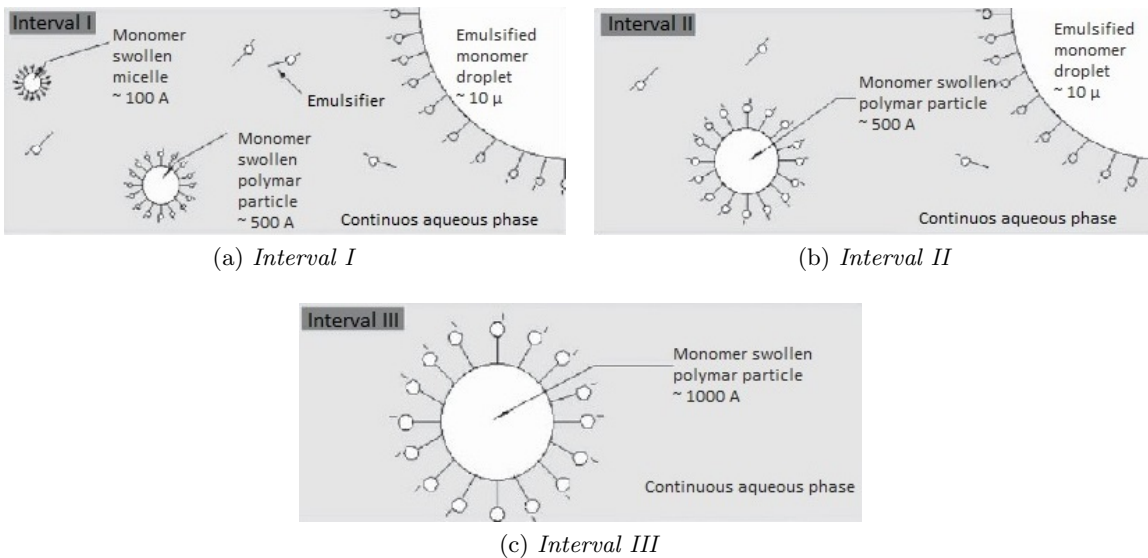


Figure 1.1: Macro-emulsion polymerization. Figure adapted from (Schork et al., 2005) with modification.

*Mini-emulsion polymerization* is performed in a heterogeneous system and allows the production of quite mono-disperse particles, whose diameter ranges from 50 to 500 nm. The feature of this technique is the use of an effective surfactant/costabilizer system that permits to produce very small (0.01–0.5 μm) monomer droplets. Nucleation takes place within droplets, initiation is performed by a radial entry of pre-polymeric or oligomeric material.

The difference from macro-emulsion is the absence of the second phase of polymerization since the reaction takes place in monomer droplets (Fig. 1.2). The process involves the presence of monomers, water, water-soluble initiator, surfactant and costabilizer, which is highly insoluble in water and slows down the diffusion of the monomer from the smaller droplets to the bigger ones. Mini-emulsion process can be carried out for other types of polymerizations, not only radical (Landfester, 2009; Schork et al., 2005).

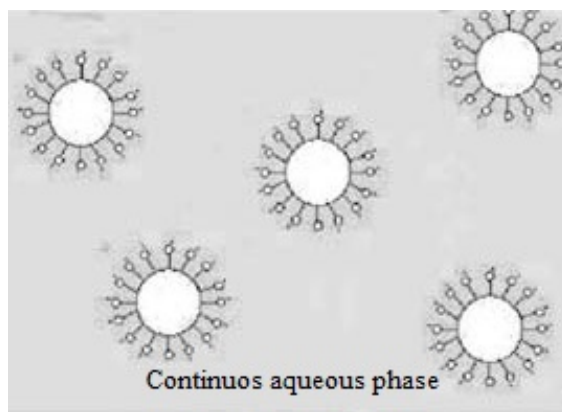


Figure 1.2: Mini-emulsion polymerization. Figure adapted from (Schork et al., 2005) with modification.

*Micro-emulsion polymerization* is executed in a homogeneous system through micelles dispersion, whose diameter is inferior to 20 nm. It is executed when surfactant concentration in a macro-emulsion is really increased above critical micellar concentration (CMC) or when monomer concentration is greatly decreased. It is a spontaneous process. It allows the production of really small particles, ranging from 10 to 100 nm (Schork et al., 2005).

*Precipitation polymerization* is carried out in a system which is homogeneous at the beginning and becomes heterogeneous during the process. It leads to the production of particles whose size varies from one hundred of nanometers to few micrometers, with a highly mono-disperse distribution. Monomers soluble in water, water, water-soluble initiator and, if needed, surfactant are involved into the reaction. Nucleation site is water and polymerization needs several hours.

*Dispersion polymerization* is performed in a heterogeneous system composed of the dispersion of the liquid monomer in a continuous phase, usually water. It allows the production of particles whose distribution is really mono-disperse, from 1 to 15 micrometers. Nucleation site is the media and polymerization time is long, more than 24 hours. Compounds used are medium-soluble monomers, alcohol, water-insoluble initiator and a stabilizer. Advantages of this kind of polymerization are: low viscosity of the medium during polymerization and, if the dispersed phase is water, a very effective heat transfer medium, due to the high thermal conductivity, and a large safety margin in the event of a runaway polymerization, thanks to the high specific heat and large latent heat of vaporization of water (Schork et al., 2005).

*Suspension polymerization* is executed in a heterogeneous system: an oil-soluble monomer dispersed in a continuous aqueous phase without the use of surfactants. Particles created are really poly-disperse, their size varies in a range from 1 to thousands of micrometers. Nucleation site is the droplet, polymer beads of the same size of monomer droplets are formed. Time necessary to polymerization is long, more than 10 hours. Oil-soluble initiators are employed. Viscosity remains constant during the process.

Other techniques, as *solution polymerization* and *bulk or mass polymerization*, are available but not used to produce nano-particles, thus they are not deepened in this thesis. Recently, innovative processes have been developed for the synthesis of polymeric particles. They are based on template-based printing, mold stretching, photo-lithographic fabrication and several microfluidics-based processes (Eerikäinen and Kauppinen, 2009). But, on this thesis the attention is focused on an other technique of polymerization: the aerosol combined with photo-initiated polymerization.

## 1.3 Aerosol Photo-Polymerization

Aerosol photo-polymerization is an alternative process to liquid-based methods. It involves two equipments: a sprayer and a reactor. The starting solution, made of a monomer and a photo-initiator, is sprinkled through the sprayer producing monomer droplets. These droplets are converted into polymer particles during the passage through the reactor. This is irradiated by UV light which allows the reaction to start.

Two different methods based on aerosol are employed to produce nano-particles. One of them provides atomization of the solution to form droplets and conversion of these droplets to solid particles. Solids can be produced via crystallization and evaporation of the solvent or via photo-polymerization. The other method provides, however, gas-to-particle conversion via nucleation and growth by condensation and coagulation.

In this thesis production of nano-particles was performed using aerosol photo-polymerization. Advantages of aerosol method are several. The process does not involve additional compounds which can contaminate the product, consequently produced nano-particles are extremely pure. Diameters of nano-particles can be determined by diameter of droplets contained in the spray solution. Furthermore, it is a continuous process and allows the production of fine disperse particles by rapid process (Shin and Oh, 1996).

Aerosol method provides a powerful way of manufacturing nano-structured materials of well-defined morphology and chemical composition. It is being used in the fabrication of opto- and nano-electronic devices and of medical applications. Furthermore, nano-particles synthesized by aerosol technique have shown increased catalytic and gas sensing properties (Biskos et al., 2008).

However, this method presents some drawbacks. First of all, it allows the production of spherical particles, but with a wide size distribution which depends to nozzle characteristics. Then, components used are limited since components which show a direct interaction with UV light can not be used. Rate of polymerization can decrease due to an interaction between UV and components in the starting solution. Finally, the not defined time of polymerization can cause problems if some droplets need more residence time and damage UV sensible components.

The other method to produce nano-particles, gas-to-particle conversion, is not developed in this work. It consists of evaporation of the material, nucleation and condensation in an inert gas. It allows the production of particles of uniform chemical composition, high purity and handled morphology and size. Cooling of the gas-vapor system is well controlled and production rates are high. Methods used for synthesizing particles in the gas phase are furnace reactors, glowing wires, spark discharges, flame, plasma, laser (Biskos et al., 2008).

### 1.3.1 Atomization of liquid solutions

Liquid solutions are atomized applying forces which aim is to split the liquid within small airborne droplets. Depending on the kind of applied force, different kinds of atomization are categorized. The most used techniques to produce small primary droplets are pneumatic, ultrasonic and electro-spray atomization.

*Pneumatic atomization* provides a flow of pressurized air through an orifice and expansion of this stream perpendicularly to the end of a tube connected to the liquid tank. Interaction between the two phases, air and liquid, is achieved thanks to Bernoulli effect. In fact, the liquid is dragged from the vessel to the air flow due to low pressure at the end of the tube. Forces playing in the interaction of the phases cause the rupture of the liquid into small droplets. These droplets become airborne and are carried away by the air flow. This last one comes to an impactor plate to divide droplets from the stream. Bigger droplets, deposited on the plate, can go back to the liquid tank or can split into smaller droplets and get out of the atomizer into the outlet stream (Biskos et al., 2008). Primary droplets produced in this atomization are in the size range of 1-10  $\mu\text{m}$  and concentrations

from 5 to 50  $gm^{-3}$ . In literature and in commerce, different types of pneumatic aerosol atomizers are analyzed and available (Biskos et al., 2008).

In *ultrasonic atomization* a piezoelectric crystal is used to agitate the surface of the solution. Formation of droplets is caused by creation of capillary waves and by break-up of cavitation bubbles. Finally droplets are carried away by an air stream. Primary droplets produced in this atomization are function of the frequency of vibration and the physical properties of the solution. Nano-particles generated are highly mono-disperse. Disadvantages of this technique are the instability of atomizers and the really low particle number concentration (Biskos et al., 2008).

*Electro-hydrodynamic atomization (EHDA) or electro-spraying* is a method that requires the presence of electrical forces. Droplets, whose diameter varies in a range from nanometers up to several micrometers, are produced monitoring the liquid flow rate and the electrostatic potential between the liquid and the counter electrode. Particles produced are really finely mono-disperse (Biskos et al., 2008). Depending on the intensity of electrical forces, different spraying modes can be obtained. As an example, production of nano-particles is preferentially performed using the 'cone-jet' mode. Disadvantage of EHDA technique is the low production rate which prevents an industrial implementation (Biskos et al., 2008).

### 1.3.2 Formation of solid particles

After atomization of the solution, monomer droplets are converted into polymer particles. This conversion can take place in two different ways, already mentioned: evaporation of the solvent and crystallization of the solute or photo-polymerization method.

When solvent evaporates and consequently solute crystallizes in order to create solid particles, three different kinds of processes can be applied: freeze drying, spray drying and spray pyrolysis. The processes are very similar, but are based on different temperatures used for conditioning the droplets. Spray pyrolysis is the most applied process since the other two processes need too low temperature. The high temperature used in spray pyrolysis allows a rapid evaporation of the solvent and the production of nano-particles. In fact, the temperature causes fragmentation of particles and production of smaller ones, favored also by low pressure. Produced particles are of a uniform composition and size. Advantages of this technique are the purity of synthesized particles and the easy handling on the stoichiometry of the precursor solution to produce multicomponent materials (Biskos et al., 2008).

Regarding photo-polymerization, monomer droplets are dispersed in a gas and polymerize to polymer particles. UV radiation initiates polymerization reaction. This method presents several advantages. Polymerization does not involve surfactants and it is restricted to the volume of each droplet. Furthermore, the system is simple, multi-components materials can be produced and size of polymeric particles can be predetermined by the diameter of monomer droplets (Esen and Schweiger, 1996).

In literature, significant works which deal with aerosol photo-polymerization are available. Esen and Schweiger in one of their works aimed to produce highly mono-disperse polymer particles whose diameter ranged from 5 to 50  $\mu m$  by photo-polymerization of aerosol droplets (Esen and Schweiger, 1996). After dispersion of the droplets and evaporation of the solvent, droplets were exposed to the radiation of eight 36 W black light fluorescent strip lamps (Fig. 1.3). Reactions were carried out in a nitrogen atmosphere (Esen and Schweiger, 1996).

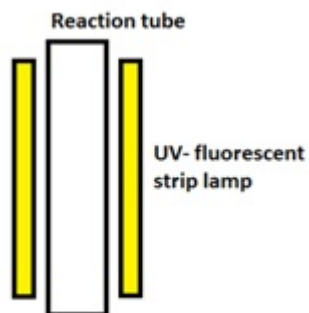


Figure 1.3: Reactor for aerosol photo-polymerization. Figure adapted from (Esen and Schweiger, 1996) with modification.

An other important work, presented by Akgün and his team, is about photo-initiated free radical polymerization of sub-micron monomer droplets for the generation of spherical polymer nanoparticles. After spraying the solution in an aerosol generator, droplets passed through the photo-reactor. This was composed of concentric quartz glass tubes. In the center was placed XeCl excimer irradiation source which emitted quasi-mono-chromatic at 308 nm (Fig. 1.4). Nitrogen, as coolant and carrier gas, passed in the annular gap in between (Akgün et al., 2013).

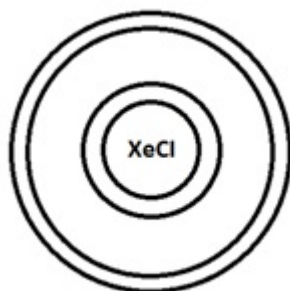


Figure 1.4: Reactor for aerosol photo-polymerization. Figure adapted from (Akgün et al., 2013) with modification.

## 1.4 Mechanisms of reaction

Two different mechanisms of reaction can be distinguished for polymerization systems: step polymerization and chain polymerization.

In the first mechanism, functional groups of monomers react to form first dimers, then trimers and oligomers. Consequently, polymer molecular weight increases at low conversion slowly. The reaction can be performed by any species.

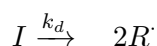
On the other hand, chain-growth polymerization needs an initiator as starter of the reaction. The initiator, which can be a free radical, a cation or an anion, produces a species with a reactive center. Monomers are added through the active center, it moves to the end of the chain and propagation phase continues. As a result, polymer molecular weight increases at relatively fast rates. The feature of this polymerization is that a monomer can react with a reactive center only.

Acrylic radical and cationic polymerizations, two of the mechanism treated in this thesis, belong to chain-growth polymerization. Thiol-ene radical polymerization, on the contrary, is based on step-growth polymerization.

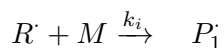
### 1.4.1 Acrylic radical chain polymerization

Acrylic radical chain polymerization can be studied in three steps.

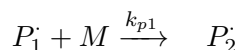
In the *initiation step* are involved two reactions. The first one includes the homolytic scission of the initiator (I) to free primary radicals ( $R^\cdot$ ) with  $k_d$  as dissociation rate coefficient. The scission of the initiator is, usually, performed by thermal, photochemical or redox methods.



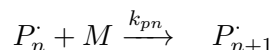
In the second reaction the primary radical reacts with the monomer (M) creating a primary monomer radical ( $P_1^\cdot$ ) where  $k_i$  is the initiation rate coefficient.



In the *propagation step* monomer adds to the primary monomer radical creating a radical chain ( $P_2^\cdot$ ) containing the active center at its end where  $k_{p1}$  is the propagation rate coefficient.



The radical chain grows to larger polymer chains adding monomers. The general propagation step can be simplified as below:



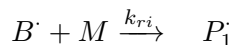
where  $k_{pn}$  is the general propagation rate coefficient.

*Termination step* occurs after a certain time of polymerization. By mechanisms, as combination with a primary radical, chain transfer reaction or disproportionation, polymer stops growing up. Termination by combination of the radical chain with a primary radical ( $P_m^\cdot$ ) allows the formation of a sole polymeric molecule ( $P_{n+m}$ ) of high molecular weight where  $k_{acc}$  is the combination rate coefficient.



Likewise, if transfer agents are not present in the system, chain transfer reaction is improbable. It takes place through chain transfer agents, which contain at least one weak bond, to monomer, polymer or solvent (AB). This mechanism allows termination of the growing polymer chain ( $P_nA$ ) and formation of another radical species ( $B^\cdot$ ) since the radical reactive center is transferred to the transfer agent.  $k_{tr}$  is considered the transfer rate coefficient. The radical can, in turn, react

with the monomer and form a new radical propagating chain ( $P_1$ ) where  $k_{tr}$  is considered as the re-beginning rate coefficient.



Termination by disproportionation, on the other hand, is not so improbable and leads to formation of two polymer molecules of low molecular weights ( $P_n$ ) and ( $P_m$ ) where  $k_{dis}$  is the disproportionation rate coefficient.



In literature different works dealing with aerosol photo-polymerization by acrylic radicalic mechanism are available.

Studies accomplished by Akgün and his team are the most suitable to this thesis (Akgün et al., 2013). Production of sub-micron polymer particles of polymethyl methacrylate (PMMA) was performed by free radical polymerization of aerosol monomer solution droplets. Chemicals used were methyl methacrylate (MMA) and butyl acrylate (BA), as monomers, Irgacure 907, as photo-initiator (PI), 1,6-hexanedioldiacrylate (HDDA), as cross-linker (Fig. 1.5).

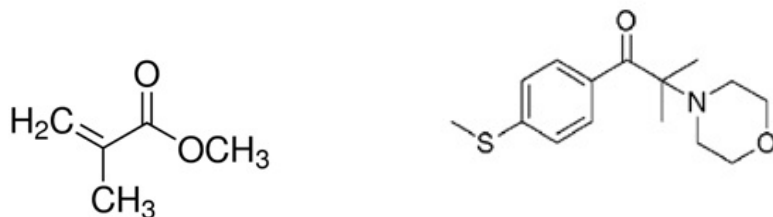


Figure 1.5: MMA and Irgacure

In the following section radical mechanism of polymerization of PMMA is explained in detail. In the initiation step scission of the initiator was achieved by ultraviolet (UV) irradiation. Below, reactions involved in the initiation step are reported (Fig. 1.6, 1.7).

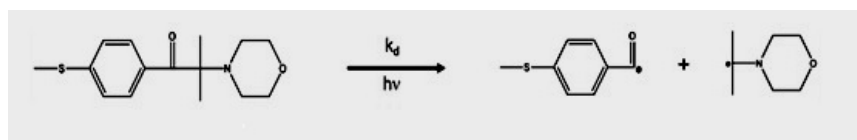


Figure 1.6: Decomposition of the initiator.

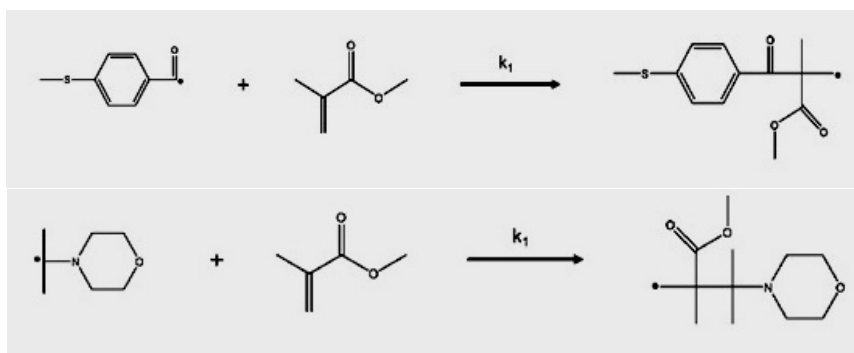


Figure 1.7: Reactions of monomer with primary radicals.

Both reaction rate coefficients of the reactions of the initiation step were assumed as  $k_1$ . In reality, they differed to some orders of magnitude.

Propagation step was generalized as (Fig. 1.8):

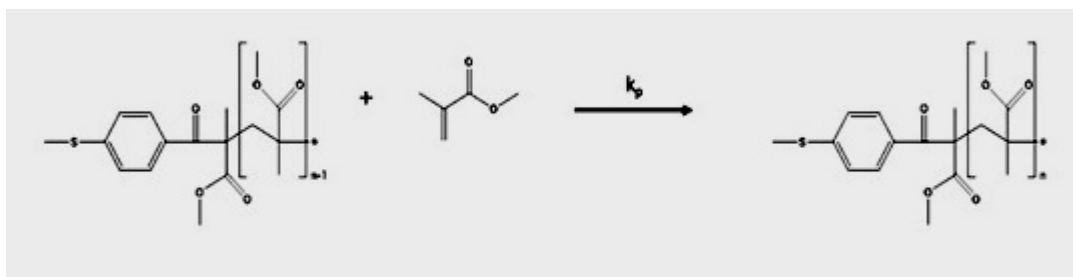


Figure 1.8: Generalized propagation step.

Mechanisms most used to terminate the polymerization were combination between two radical polymer chains and chain transfer reaction. They are reported below (Fig. 1.9, 1.10).

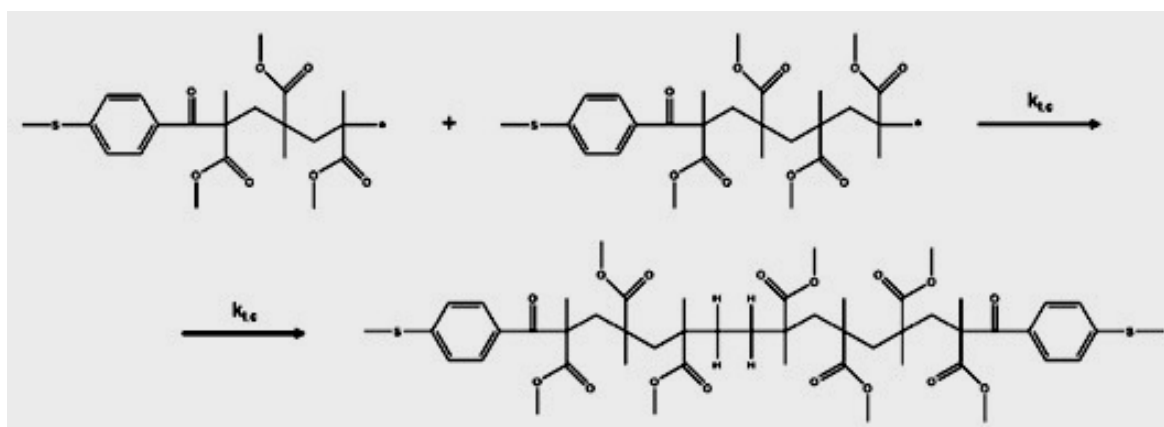


Figure 1.9: Termination by combination between two radical polymer chains.

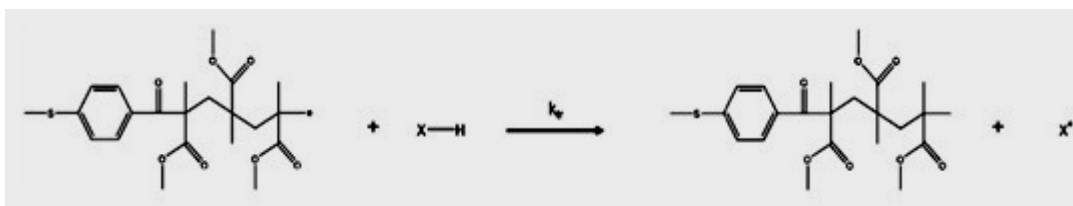


Figure 1.10: Chain transfer reaction.

Formation of aerosol droplets was achieved by spraying the starting solution with nitrogen in an atomizer. Aerosol droplets, after that, passed through a photo-reactor which, using UV irradiation, generated free radicals. The reactor used was the same described in Fig. 1.4 composed of concentric quartz glass tubes and irradiation source in the center.

The use of the sole monomer MMA with PI did not lead to a successful polymerization since polymerization rate was too slow. Nano-particles were obtained adding HDDA as cross-linker or BA as co-monomer. Specifically, using HDDA polymerization was completed and produced particles were spherical and nano-sized (Fig. 1.11 (a)). In Fig. 1.11 is also shown size distribution of HDDA-cross-linked PMMA (b) and comparison between droplets size distribution before polymerization and particles size distribution after polymerization (c). Correspondence between the two distributions shows no significant droplets evaporation (Akgün et al., 2013).

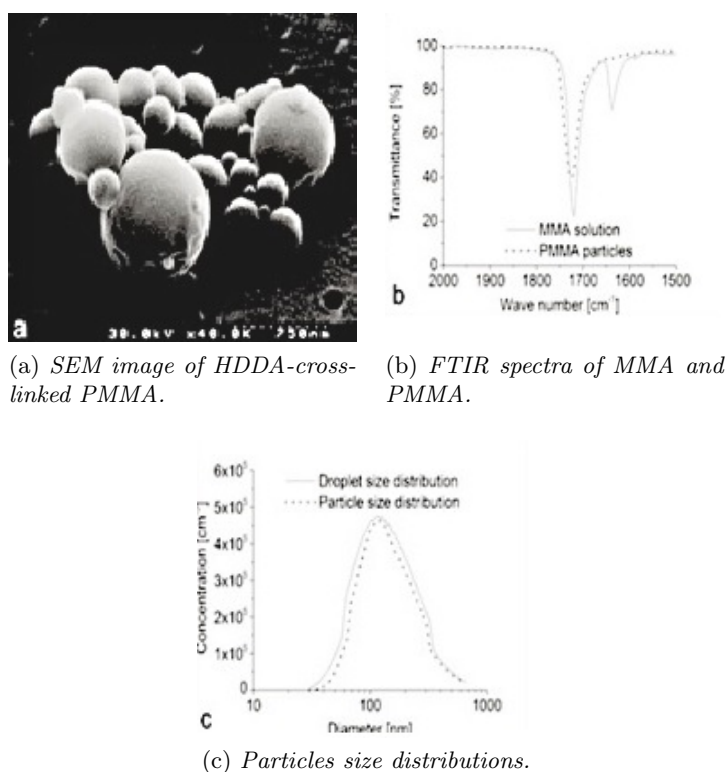


Figure 1.11: SEM images. Figure adapted from (Akgün et al., 2013) with modification.

Akgün and his team worked also on the production of organic-inorganic spherical polymer-matrix nano-composites (PMNCs) using the same technique of aerosol photo-polymerization (Akgün et al., 2014b). Through the aerosol generator and the photo-reactor, mentioned and explained above, they produced well-distributed zinc oxide (ZnO) nanoparticles in polymer networks. Chemicals employed were the same of the precedent article: MMA and BA as monomers, Irgacure 907 as photo-initiator, HDDA as cross-linker. In addition, zinc oxide nano-particles were used as source of inorganic component of hybrid nano-particles. The starting solution was composed of the monomer MMA, HDDA, Irgacure 907 and zinc oxide nano-particles. After spraying and photo-polymerizing, zinc oxide nano-particles incorporated within the polymer matrices were produced (Fig. 1.12).

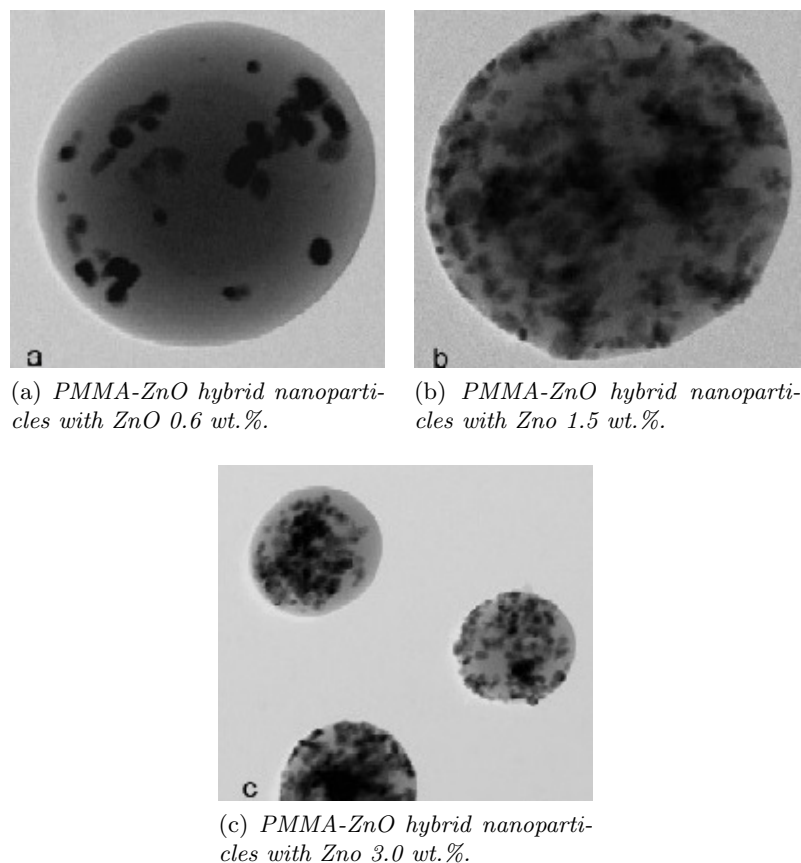


Figure 1.12: TEM images. Figure adapted from (Akgün et al., 2014b) with modification.

While ZnO nano-particles were well distributed, some agglomerates were present. The creation of these agglomerates could be caused by secondary agglomeration, which took place during formation of droplets through aerosol, or could be formed into the solution before spraying it.

In addition, using HDDA as monomer, PMNCs were produced. They contained a big amount of ZnO nano-particles that did not agglomerate, maybe due to the different surface functionalization of ZnO nano-particle dispersions in HDDA and ethanol. Consequently, solutions prepared using ethanol led to less stable dispersions and more agglomerates in the hybrid particles (Akgün et al., 2014b).

Akgün and his team investigated also in the production of nano-caps, nanostructured non-spherical particles, and mosaic nano-particles, spherical porous particles. They were generated employing the mechanism of aerosol-photo-polymerization, specifically free radical polymerization. In order to create nano-caps a volatile solvent combined with a soft-maker was utilized. On the other hand, the production of mosaic nano-particles was performed with a porogen, non-solvent, whose feature was its non-volatility (Akgün et al., 2014a).

Production of nano-caps could be described as an interplay between kinetic and thermodynamic properties. Aerosol allowed a rapid creation of spherical droplets through a fast kinetic. Each droplet was made of monomers, ethanol, solvent with high evaporative features and dissolved components, photo-initiator and glycerol. The droplet was considered homogeneous below the solubility limit of glycerol. When droplets passed through the reactor, solvent evaporated, it was in over-saturation of glycerol. Phase separation was achieved by photo-polymerization: polymer-rich phase was concentrated in the outer part of the droplets, instead, ethanol-rich phase was focused in the inner part. The function of glycerol was checking the proper collapse of droplets, acting as a softening agent, delaying gelation during ethanol evaporation.

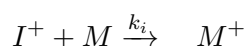
Mosaic particles were generated by aerosol-photo-polymerization as well, adding to monomer and

photo-initiator, a non-volatile solvent. The feature of this last one was the miscibility with the starting monomer solution and the immiscibility with the produced polymer. Thus, the importance of the non-volatile solvent for phase separation (Akgün et al., 2014a).

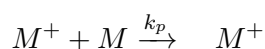
### 1.4.2 Cationic polymerization

Cationic polymerization is an other type of polymerization treated in this thesis. Since it is based on a chain growth mechanism to produce polymer, it can be divided into three steps: initiation, propagation and termination.

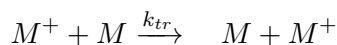
In the *initiation step*, a cationic initiator ( $I^+$ ) transfers charge to the monomer (M), which becomes a reactive species ( $M^+$ ).  $k_i$  represents the initiation rate coefficient. Electrophilic agents, Lewis acids and compounds capable of generating carbonium ions can be considered cationic initiators.



In the *propagation step*, monomers consequently add to the carbonium ion at the growing chain end.  $k_p$  represents the propagation rate coefficient.



In the *termination step*, two methods are employed. The first one provides the rearrangement of molecules in order to recreate the original monomer and to produce a polymer with an unsaturated terminal unit where  $k_t$  represents the termination rate coefficient. The second one involves, instead, chain transfer to a monomer and  $k_{tr}$  represents its transfer rate coefficient.



Solvents used in this polymerization have an important function. An increase in their dielectric strength influences a linear increase in polymer chain length and an exponential increase in reaction rate (Ebewele, 2000). Propagating cationic species, participant to the cationic polymerization, do not react among themselves. For this reason, polymerization goes on in the dark for a little time (Decker et al., 2001).

Photo-initiated polymerization of vinyl ethers (VEs) was investigated in this thesis. VEs are very reactive monomers that polymerize quickly using the cationic mechanism. Employing di-functional VEs a cross-linked polymer network is made in a short time, only seconds.

Different factors control the polymerization kinetics, as the chemical structure of the oligomer, the type of photo-initiator employed, the presence of labile hydrogens and of aromatic groups, the viscosity of the starting solution and the hardness of the polymer (Decker et al., 2001).

In literature, some works treated the theme of cationic photo-polymerization. Decker and his team investigated on the influence of VE structure on chemical structure of oligomer chain end-capped. Particularly, he studied the reactivity of five VE functionalized oligomers photo-irradiated in presence of triarylsulfonium hexafluorophosphate (TAS-PF6) as photo-initiator. In Fig. 1.13 reactivity of these VEs is shown. It increases in the following order: aromatic ether < aliphatic ester < aliphatic urethane < aromatic ester < aliphatic ether (Decker et al., 2001).

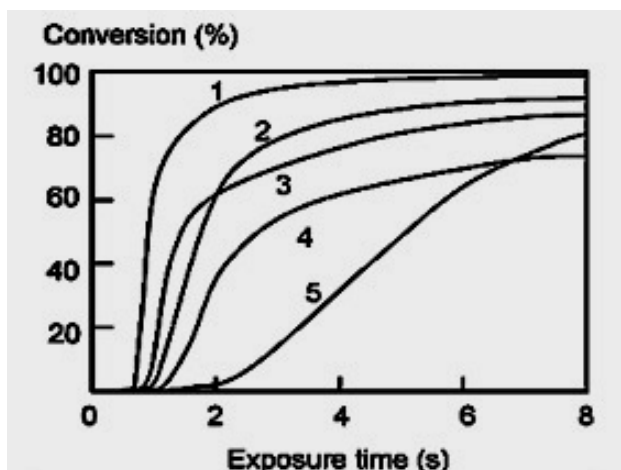


Figure 1.13: Reactivity of VE functionalized oligomers: 1. aliphatic ether, 2. aromatic ester, 3. Aliphatic urethane, 4. aliphatic ester, 5. Aromatic ether. Figure adapted from (Decker et al., 2001) with modification.

The initiation process controlled the kinetics of the cationic polymerization of VEs regarding the type of onium salt used and the light intensity. A scheme of the photolysis process for diaryliodonium salts is represented below.



Decker used three photo-initiators in his study, but the most efficient to initiate the polymerization of the monofunctional vinyl ether was SbF<sub>6</sub> iodonium salt (OPPI), as shown in Fig. 1.14.

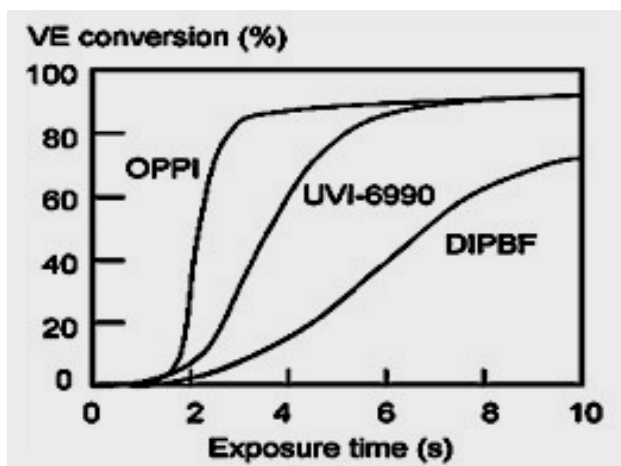


Figure 1.14: Influence of the iodonium photo-initiator (2 wt.%) on the polymerization. Figure adapted from (Decker et al., 2001) with modification.

The figure shows an initial and short induction period caused by the presence of a nucleophilic stabilizer, a fast increase arriving to 80% of conversion and finally a slowdown due to gelation and related molecular mobility restrictions. Differences in the rate of production of protonic acid from the photo-initiator excited states are responsible for differences related to initiation efficiency shown in the figure (Decker et al., 2001).

Also Akgün and his team performed studies on cationic polymerization. He investigated the reactivity of epoxy monomer and vinyl ether in cationic processes. He succeeded in producing spherical polymer particles (Fig. 1.15) using only a starting solution made of liquid monomer and dissolved cationic photo-initiator (Akgün et al., 2015).

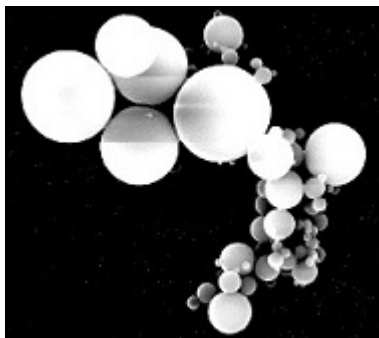


Figure 1.15: SEM image of crosslinked poly(DVE2) particles produced by cationic aerosol-photopolymerization. Figure adapted from (Akgün et al., 2015) with modification.

### 1.4.3 Thiol-ene radical polymerization

The last part of this work treats an other kind of polymerization: thiol-ene polymerization. It involves a reaction between multi-functional thiol and ene (vinyl) monomers based on a step-growth radical addition mechanism.

In the last few decades academic interest in this polymerization has been increased. Thiol-ene polymerization was discovered by Posner in 1905. In 1938 Kharasch proposed the thiol-ene polymerization mechanism which is still accepted (Fig. 1.16).

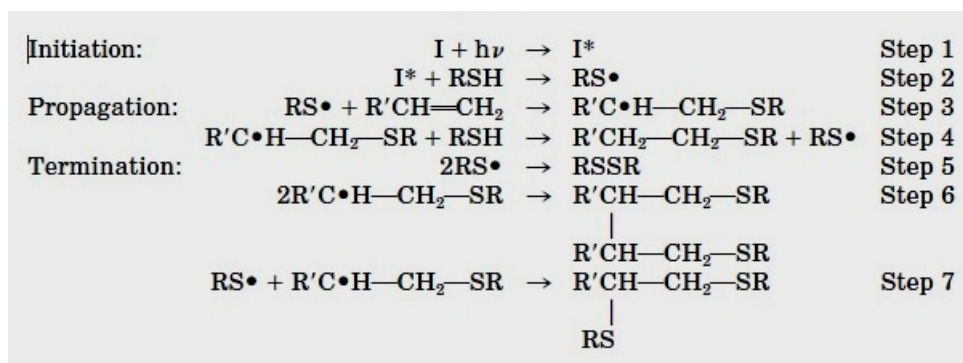


Figure 1.16: Thiol-ene polymerization mechanism. Figure adapted from (Cramer and Bowman, 2001) with modification.

*Initiation step* is composed of two reactions. In the first reaction a photon is absorbed by benzophenone (I), which becomes excited ( $I^*$ ). In the second reaction a hydrogen is extracted from a thiol monomer (RSH) by benzophenone creating a thiyl radical thiol monomer ( $RS\bullet$ ).

The *propagation step* involves two reactions. Generally, the thiol and ene components are consumed at identical rates from an initial stoichiometric mixture of their respectively functional groups.

*Termination step* can take place by radical-radical recombination or by radical recombination with initiating species (Cramer and Bowman, 2001).

This kind of polymerization presents lots of advantages. Polymerization rate, which is always fast, is not influenced by the presence-absence of hydrogen. The presence of oxygen, on the other hand, involves the addition of a chain transfer to the overall reaction. Furthermore, the thiol-ene step growth radical polymerization allows the creation of a homogeneous cross-linked network with low volume shrinkage and it delays gelation. Physical and mechanical properties of these network structures can be adapted using different monomers with different terminal -ene groups.

Limited shelf-life stability and bad odor of the thiol are disadvantages of this method. To counteract the second drawback, high molecular multifunctional low-odor thiols are now commercially

available. The main problem is, thus, the instability of the system since its life can vary from few seconds to few weeks. Reaction proceeds readily in the absence of an initiator and a lot of stabilizer systems are required to increase shelf life stability, delay gelation and reduce premature polymerization at room temperature (Esfandiari et al., 2013).

In literature, works whose aim is the production of micro-particles by polymerization photo-initiated are not currently available. Several works treat the production of polymer nano-particles via thiol-ene mini-emulsion photo-polymerization.

One of these works, executed by Amato and his team, dealt on synthesis of small, sub-100 nm polythioether nano-particles using miniemulsion thiol-ene photopolymerization. They focused also on including a radical inhibitor, 4-Methoxyphenol (MEHQ), in the thiol-ene formulation. The aim was to prevent premature polymerization during ultrasonic emulsification before exposition to UV light. The MEHQ concentration was varied and the minimum concentration which avoided the formation of solid particles on the surface of the ultrasonic horn was 55.7 mM.

MEHQ (mM)*	Solids present
111.2	NO
55.68	NO
27.93	YES
13.66	YES
7.16	YES
0	YES

Table 1.1: MEHQ concentration and relatively formation of solids.

They prepared, in addition, thiol-ene mini-emulsions with and without inhibitor using a deuterium oxide/sodium dodecyl sulfate (SDS) solution as the continuous phase. They analyzed via proton nuclear magnetic resonance (H-NMR) a fraction of samples, upon ultra-sonification and after photo-polymerization. From results, they proved the necessity of an inhibitor to prevent premature polymerization (Amato et al., 2014).

Other studies, as the one executed by Liu and his team produced hybrid micro-capsules through the one-step thiol-ene photo-polymerization at the interface between toluene and water (Liu et al., 2013). An other interesting work, carried out by Byeon and his team achieved the production of zwitterionic chitosan nano-particles (ZCNPs) by a one-step aerosol method (Hoon Byeon et al., 2014).

#### 1.4.4 Aim of the thesis

This thesis can be divided into three parts.

In the first part the purpose of the work was the production of micro-particles employing the mechanism of cationic aerosol photo-polymerization. First of all the production of spherical full micro-particles was performed employing a starting solution made of monomer and photo-initiator. Then, adding solvents porous micro-particles were obtained. Finally, using an alcohol micro-particles similar to micro-capsules were produced. Influence of pressure on size distribution of polymeric particles was investigated. Effects on gelation rate and separation rate on the production of particles were analyzed. Co-monomers systems were studied and implemented.

The second part of the thesis aimed to produce micro-particles using the mechanism of radical aerosol photo-polymerization. Also in this part, first, spherical full micro-particles were created using a mixture of monomer and photo-initiator. Then porous and chill particles were produced employing a solvent and at the end the use of an alcohol allowed the production of micro-capsules. Studies on the influence of solution composition on gelation rate and phase separation were done.

Co-monomers systems were used.

The last part of the thesis had the purpose to produce micro-particles employing the mechanism of thiol-ene aerosol photo-polymerization. Production of full spherical and porous micro-particles was achieved.

## Chapter 2

# Experimental section

### 2.1 Materials

Nitrogen, which was used to produce aerosol in all the experiments performed in this thesis, was purchased from Air Liquide (Paris, France). Its purity was higher than 99,999%.

#### 2.1.1 Cationic polymerization

The monomer which was used in all the experiments performed by cationic mechanism was tri(ethylene glycol) divinyl ether 98% (DVE-3). It had a density of 0.99 g/mL at 25 °C (Fig. 2.1).

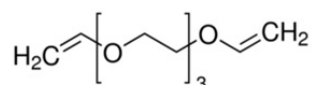


Figure 2.1: Tri(ethylene glycol) divinyl ether 98%

Co-monomers employed were di(ethylene glycol) vinyl ether 98% (Fig. 2.2 (a)), which had a density of 0.968 g/mL at 25 °C, and 2-ethylhexyl vinyl ether 98% with a density of 0.816 g/mL at 25 °C (Fig. 2.2 (b)).

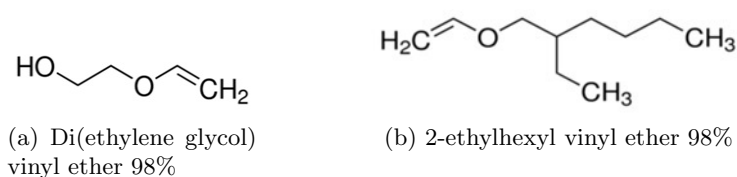


Figure 2.2: Comonomers for cationic polymerization.

The photo-initiator used was triarylsulfonium hexafluoroantimonate salts (TAS-HFA) in solution at 50 wt.% in propylene carbonate (Fig. 2.3). It had a density of 1.410 g/mL at 25 °C.

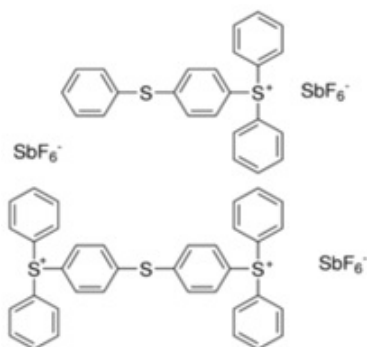


Figure 2.3: Triarylsulfonium hexafluoroantimonate salts

Solvents added to the monomer solution were hexadecane (HD) anhydrous  $\geq 99\%$ , 2-octanone  $\geq 98\%$  and 2-ethyl-1-hexanol, commercially called iso-octanol,  $\geq 99.6\%$ .

Hexadecane (Fig. 2.4), a non polar solvent, was considered the *bad* solvent since it was not affine to the monomer and the polymer.

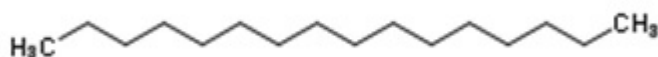


Figure 2.4: Hexadecane anhydrous  $\geq 99\%$

2-octanone  $\geq 98\%$  (Fig. 2.5), the co-solvent, was considered the *good* solvent since it was more affine to the monomer and it led to obtain a homogeneous starting solution.

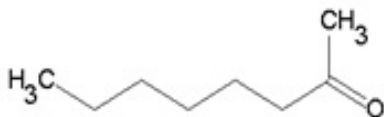


Figure 2.5: 2-octanone  $\geq 98\%$

Iso-octanol  $\geq 99.6\%$  (Fig. 2.6) was used in many experiments to control gelation rate.

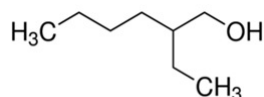


Figure 2.6: 2-ethyl-1-hexanol  $\geq 99.6\%$

All chemicals, above mentioned, used in the cationic polymerization were purchased from Sigma-Aldrich (Taufkirchen, Germany).

Polymeric material was collected using different types of filtering membranes or aluminum binders. Whatman nuclepore track-etched polycarbonate (PC) membranes, whose diameter was 47 mm and pore size was  $0.2 \mu\text{m}$ , purchased from Sigma-Aldrich (Taufkirchen, Germany) was a kind of membrane used. Then, polytetrafluoroethylene (PTFE) membranes of two different types were employed. PTFE membrane whose diameter was 47 mm and pore size was  $0.05 \mu\text{m}$  and PTFE membranes of 47 mm of diameter and  $0.2 \mu\text{m}$  of pore size which were purchased from Bola (Grünsfeld, Germany).

## 2.1.2 Acrylic radical polymerization

Monomers employed in the experiments based on acrylic radical mechanism were butyl acrylate (BA)  $\geq 99\%$  (Fig. 2.7 (a)) and methyl methacrylate (MMA) containing  $\leq 30$  ppm 4-methoxyphenol (MEHQ) as inhibitor, whose purity was 99% (Fig. 2.7 (b)).

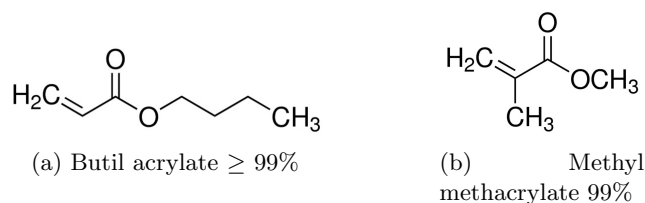


Figure 2.7: Monomers for acrylic radical polymerization.

Trimethylolpropane triacrylate (Fig. 2.8), trimethylolpropane ethoxylate triacrylate (Fig. 2.9) with an average molar weight  $M_n \sim 428$ , 1,6-hexanediol diacrylate (Fig. 2.10), 99% (reactive esters), stabilized with 90 ppm hydroquinone were employed as cross-linkers.

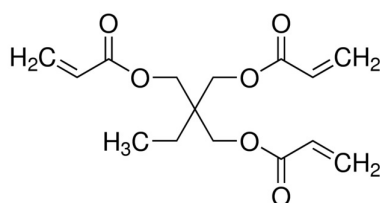


Figure 2.8: Trimethylolpropane triacrylate

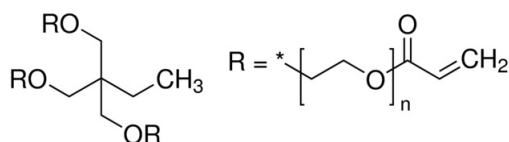


Figure 2.9: Trimethylolpropane ethoxylate triacrylate

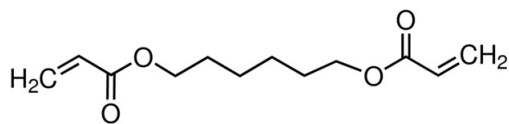


Figure 2.10: 1,6-Hexanediol diacrylate

The photo-initiator was Irgacure 907 (methyl-1[4-(methylthio)phenyl]-2-morpholinopropan-1-one) (Fig. 2.11), whose purity was 98%.

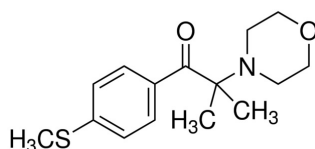


Figure 2.11: Irgacure 907 98%

Solvents used were hexadecane (HD) reagentplus, whose purity was 99%, and 2-ethyl-1-hexanol (iso-octanol) with a purity  $\geq 99.6\%$ . Chemical structures were already mentioned in the precedent section.

Glycerol  $\geq 99.5\%$  (Fig. 2.12), which acted as soft-maker, was employed in order to delay gelation.

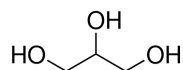


Figure 2.12: Glycerol  $\geq 99.5\%$

Ethanol Rotipuran  $\geq 99.8\%$  and 1-propanol  $\geq 99.9\%$  were employed as co-solvents in order to make the starting solution homogeneous. Their use was necessary to obtain both micro-capsules and micro-caps.

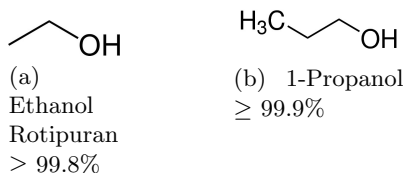


Figure 2.13: Co-solvents for acrylic radical polymerization.

All chemicals above described were purchased from Sigma-Aldrich (Taufkirchen, Germany), excepted 1,6-hexanediol diacrylate which was purchased from Alfa Aesar (Karlsruhe, Germany) and ethanol Rotipuran  $\geq 99.8\%$  which was purchased from Roth (Karlsruhe, Germany).

Polymeric material was collected into aluminum binders.

### 2.1.3 Thiol-ene radical polymerization

Monomers which were employed for thiol-ene radical polymerization were trimethylolpropane tris(3-mercaptopropionate) (Fig. 2.14 (a)) with a purity  $\geq 95.0\%$  and a density of 1.21 g/mL at 25 °C, pentaerythritol tetrakis(3-mercaptopropionate)  $\geq 95.0\%$  (Fig. 2.14 (b)) and with a density of 1.28 g/mL at 25 °C, neopentyl glycol diacrylate (Fig. 2.14 (c)) which contained 225 ppm monomethyl ether hydroquinone as inhibitor, diallyl adipate (Fig. 2.14 (d)) with a minimum purity of 98%, tri(ethylene glycol) divinyl ether 98% and trimethylolpropane triacrylate.

The photo-initiator was the same used for radical polymerization, Irgacure 907 (methyl-1[4-(methylthio)phenyl]-2-morpholinopropan-1-one) 98%.

As solvents were used hexadecane (HD) reagentplus, whose purity was 99%, 2-octanone  $\geq 98\%$  and 2-ethyl-1-hexanol (iso-octanol)  $\geq 99.6\%$ . Some monomers, the photo-initiator and solvents structures were described in precedent sections.

All chemicals were purchased from Sigma-Aldrich (Taufkirchen, Germany), excepted diallyl adipate which was purchased from TCI (Eschborn, Germany).

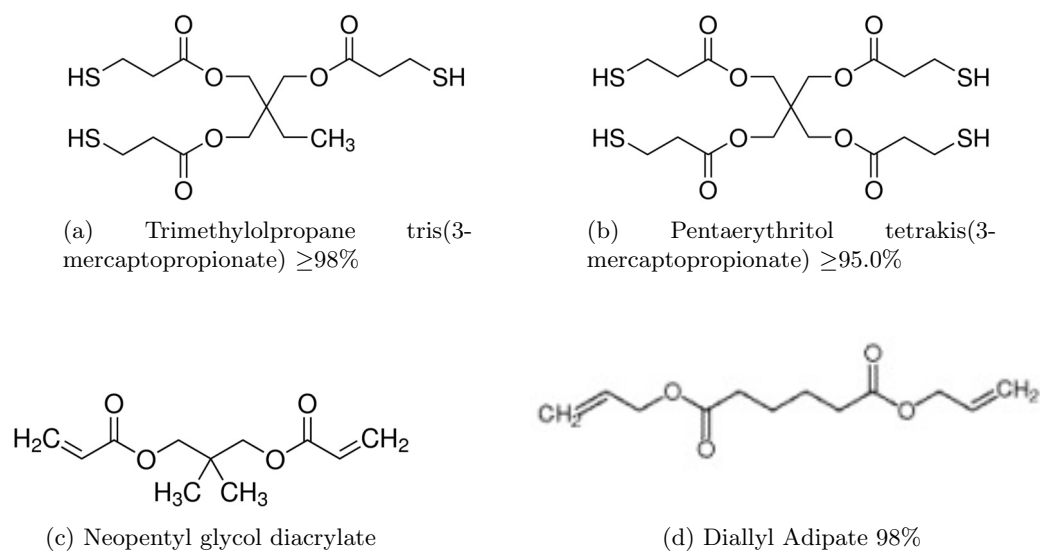


Figure 2.14: Monomers for thiol-ene radical polymerization.

## 2.2 Equipment and Instrumentation

The aerosol photo-polymerization setup consists of two main devices: an atomizer and a photo-reactor. The complete process is schematized in the following figure (Fig. 2.15).

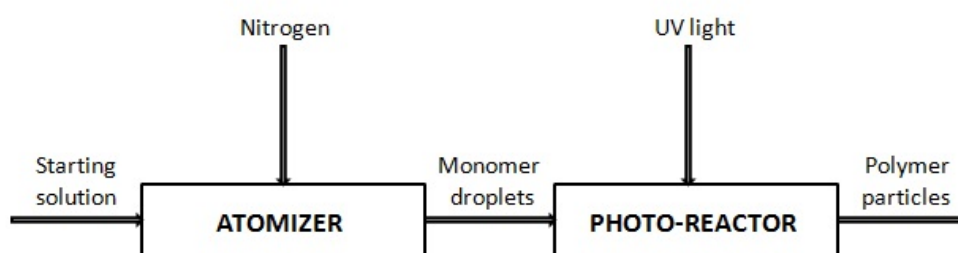


Figure 2.15: Schematic process of aerosol photo-polymerization.



Figure 2.16: Complete equipment: atomizer, photo-reactor, filter.

Pneumatic atomization was performed in this thesis. The starting solution, which is contained in a glass flask, is sprayed through the atomizer (V3-TOPAS, ATM 220, Topas-GmbH, Dresden, Germany) (Fig. 2.17). Aerosol droplets are created spraying the solution with a nitrogen flow which withdraws the solution from the flask by the Venturi effect. Nitrogen is employed as the carrier and continuous phase and the solution represents the carried and dispersed phase.

The component of the sprayer which allows to produce aerosol is the two-component nozzle. This nozzle creates micro poly-disperse droplets with a concentration of  $10^7$ - $10^8$   $\text{cm}^{-3}$ . Droplets of higher size come back to the flask containing the solution through an orifice. In fact, the nozzle has three openings. The second orifice allows the connection between the nozzle and the flask since a tube, which is immersed in the solution, is screwed in it. The other orifice allows droplets of a defined size to leave the flask. The nozzle, furthermore, influences the residence time of droplets in the photo-reactor and the volumetric aerosol flow rate. Indeed, varying the nozzle inlet pressure of nitrogen, which ranges from 1 to 6 bars, the average residence time in the reactor varies and the flow rate can change in a range from 1 to 5  $\text{Lmin}^{-1}$ . Normally, residence time is about 1 minute or less and it depends also on photo-reactor length.



Figure 2.17: Atomizer.

After atomization of the solution, monomer droplets pass into the photo-reactor (Fig. 2.18). It is composed of a cylindrical quartz glass tube surrounded by 2 irradiation sources. The quartz tube has a length of 0.44 m and an inner diameter of 0.052 m. Each source, instead, is made of 3 fluorescent tubes of a length of 0.41 m. The poly-chromatic UV radiation is emitted by these tubes. It ranges between 270 and 360 nm, with a maximum at 312 nm. The complete radiance at the quartz tube is about  $5 \text{ mWcm}^{-2}$ . After polymerization, particles are collected into aluminum binder or filter containing membranes. Time of each experiment varies related on the collector. For aluminum binder the experiment lasts 2 hours, for the filter membrane it lasts 30 minutes.



Figure 2.18: Photo-reactor.

## 2.3 Analysis techniques

### 2.3.1 Field emission scanning electron microscopy

Scanning electron microscopy (SEM) is a microscopy technique which uses a focused beam of high-energy electrons to scan the surface of a sample and produce images of it. Field emission (FE)-SEM provides topographical and elemental information at magnifications of 10x to 300,000x, with virtually unlimited depth of field. Images are clearer, less electro-statically distorted and with a higher resolution. Samples need to be prepared before microscopy to resist to vacuum and high energy of electron beam.

The microscope which was used in this thesis was a high resolution field-emission scanning electron microscope (Leo Gemini 1530, Carl Zeiss, Oberkochen, Germany). It permitted to evaluate dimension and morphology of polymeric particles produced. Samples analyzed were prepared as suspension. A small amount of polymer was suspended into ultra-pure water for cationic polymerization and into pure ethanol for radical polymerization. Then, these containers were stirred for hours in order to break second agglomerates. Membrane (Whatman, Nucleopore Track-Etch Membrane, 200 nm pore width) or silicium wafer were used to absorb few micro-liters of suspension. After drying, particles were coated (1-2 nm) with platinum or a mixture of platinum-palladium.

### 2.3.2 Fourier transform infrared spectroscopy

Fourier transform infrared spectroscopy (FT-IR) is a technique which, in one action, sparkles a beam of several frequencies of light to the sample and measures its absorbance. This process is repeated different times changing the frequencies of light in the beam. The beam is generated by a

source containing the full spectrum of wavelengths which needs to be analyzed. The beam glitters into a Michelson interferometer, which contains a configuration of mirrors moved by a motor. Movement of this mirrors causes wave interferences responsible for block or transmission of each wavelength of light. The beam which comes out from the interferometer has a different spectrum at each moment since different wavelengths are modulated at different rates. A computer detects all these raw dates and can deduct the absorption of light at each wavelength converting them into the spectrum using the mathematical Fourier transform. This spectrum is always compared to a reference.

In this thesis FT-IR allowed to analyze the conversion of the reactive double bonds of the monomer. Fourier transform infrared spectrometry utilizing attenuated total reflectance (FTIR-ATR, Equinox 55, Bruker Optics, Ettlingen, Germany) was employed. A droplet of the starting solution and a small amount of the corresponding polymer were analyzed and corresponding spectra were obtained.

## Chapter 3

# Results and discussion: Cationic Polymerization

The first part of the thesis was focused on polymerization by cationic mechanism.

### 3.1 Production of full micro-particles

A solution composed of monomer DVE-3 (100%) and photo-initiator (2% wt. referred to the monomer) was prepared to obtain full micro-particles. The monomer was bi-functional and, thus, able to act as a cross-linker. It was a fast propagating molecule with a polyethyleneglycol-like backbone. Depending on the type of collector, time of spraying of the solution changed, as already discussed in the precedent chapter. Starting solution was sprayed for 2 hours if the produced polymer was collected on an aluminum binder, it was sprayed for an hour if the container was a membrane filter.

#### Influence of pressure

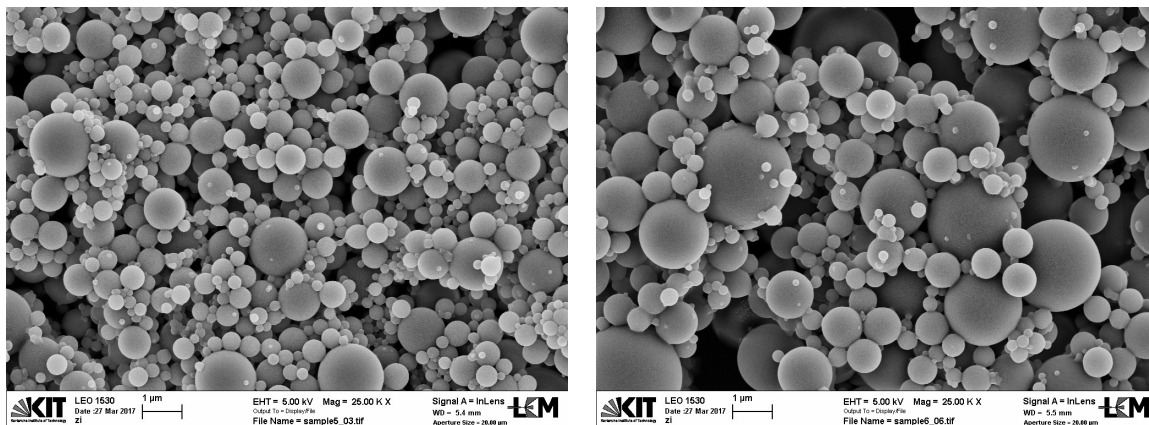
Nozzle inlet pressure of nitrogen was varied from 1 up to 2.5 bar in order to study variations in aerosol characteristics and analyze effects on particles size distribution. A change in inlet pressure influenced consequently average residence time of aerosol droplets in the photo-reactor. An increase of inlet pressure corresponded to a decrease of average residence time in the reactor, which became shorter than a minute. Even if aerosol droplets had less time to polymerize, produced particles showed the desired structure. They were completely polymerized and separated each other, thus phase separation did not take place too late.

Here is provided a list of experiments (Tab. 3.1) performed at different pressures.

Table 3.1: List of experiments performed with only monomer and photo-initiator. Use of membranes as container of the polymer.

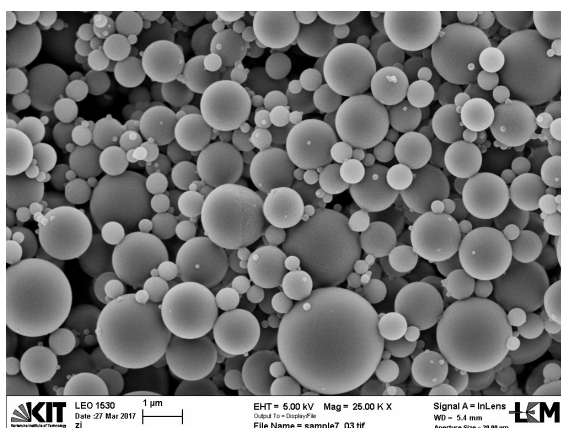
N. exp.	Composition of spray solution	Pressure [bar]
1	100% DVE-3	2
2	100% DVE-3	1
3	100% DVE-3	2.5
4	100% DVE-3	0.5

FE-SEM analyses (Fig. 3.1) confirmed the production of spherical and full sub-micron particles.



(a) FE-SEM image of experiment n. 1.

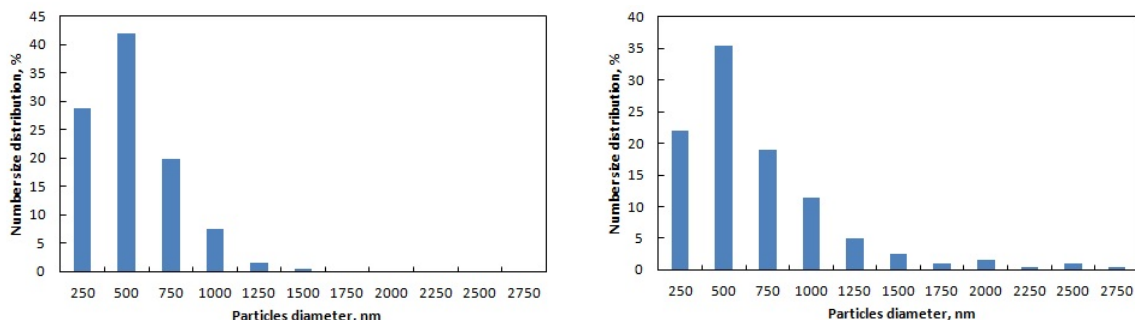
(b) FE-SEM image of experiment n. 2.



(c) FE-SEM image of experiment n. 3.

Figure 3.1: FE-SEM images of experiments described in Table 3.1.

By evaluation of particles size distribution, at higher pressure polymeric particles appeared to be smaller (Fig. 3.1 (a)), otherwise, at lower pressure particles looked larger. In fact, distribution terminated at bigger dimension (Fig. 3.1 (b)). Particles demonstrated a mono-disperse distribution with a mean diameter of approximately 500 nm.



(a) Particles size distribution of experiment n. 1.

(b) Particles size distribution of experiment n. 2.

Figure 3.2: Particles size distributions of experiments described in Table 3.1.

## 3.2 Production of porous micro-particles

Porous micro-particles were produced adding solvents to the starting solution which consisted of monomer and photo-initiator. Two different types of solvents were added. Hexadecane (HD) was introduced for its non-polar nature that was not affine to the monomer and the polymer. It was named "bad solvent" and acted as a phase separator. Otherwise, the co-solvent which was introduced to obtain a homogeneous solution was 2-octanone. It was named "good solvent" since it was affine to the monomer, the polymer and the phase separator. Solutions were prepared employing 70% wt. of monomer and 30% wt. of solvents. Influence of solvents concentration and influence of pressure were investigated.

### Influence of solvents ratio

The amount of 2-octanone was gradually increased from 12.5% to 20%, meanwhile the amount of HD was decreased from 17.5% to 10%. HD allowed phase separation in the earlier stages of polymerization. Decreasing its amount, phase separation was delayed and took place when particles were already of a big dimension. Produced particles appeared not separated and connected each other. For this reason, formulation which gave porous and separated micro-particles contained 12.5% of 2-octanone and 17.5% of HD (Fig. 3.3).

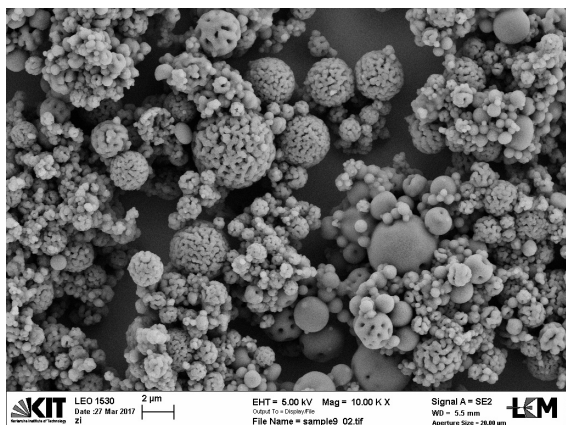
### Influence of pressure

In some experiments pressure was varied in order to evaluate effects on particles structure and particles size distribution. Particularly, here are provided results obtained starting from recipe discussed before (Tab. 3.2).

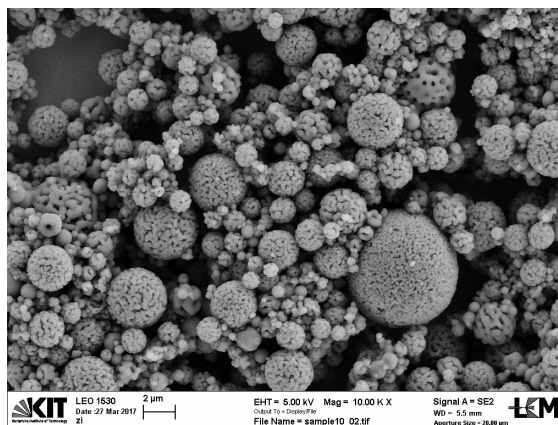
Table 3.2: List of experiments performed with HD and 2-octanone. Use of membranes as container of the polymer.

N. exp.	Composition of spray solution			Pressure [bar]
	DVE-3	HD	2-Octanone	
5	70%	17.5%	12.5%	1.5
6	70%	17.5%	12.5%	2
7	70%	17.5%	12.5%	2.5

Observing images by FE-SEM, nano-structured particles were produced. At higher pressure (Fig. 3.3 (b)) particles were more defined. They were mosaic-like particles, made of small domains of polymeric material strictly connected each other. At lower pressure (Fig. 3.3 (a)), instead, particles were not so defined. Some of them, mostly bigger ones, showed a mosaic structure, others looked sponges-like and caps-like and smaller ones appeared as disintegrated. Maybe particles of a small size were originated from disintegration of a bigger particle or they were going to aggregate in order to form a big mosaic particle.



(a) FE-SEM image of experiment n. 5.

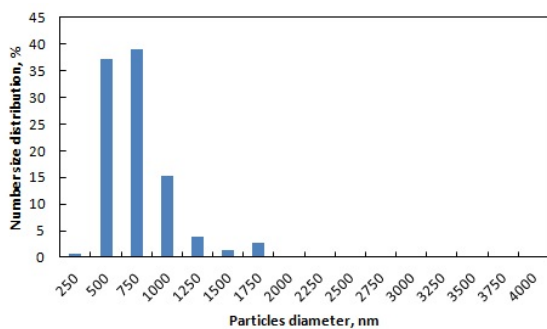


(b) FE-SEM image of experiment n. 7.

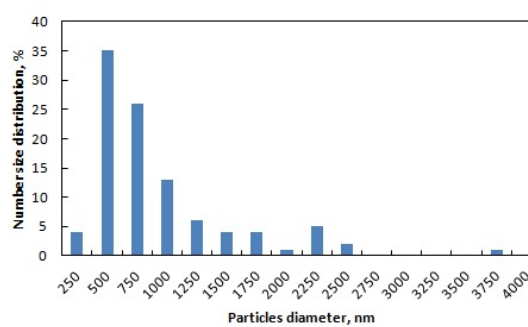
Figure 3.3: FE-SEM images of experiments described in Table 3.2.

Analyzing particles size distribution (Fig. 3.4) a shift in the diameter peak and a different size distribution could be observed in the three samples. This was not expected. Particles dimension was related on droplets dimension. Pressure influenced aerosol characteristics.

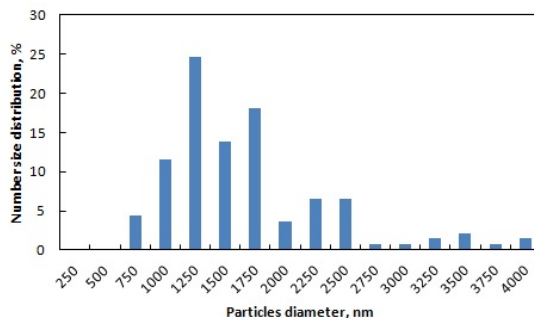
Different causes could be responsible for this atypical distribution. The nozzle could be not so efficient or not totally free from impurities or the aerosol could be not so fine. Furthermore, evaporation of solvents after a certain period of spraying could take place and consequently produce changes in the starting solution.



(a) Particles size distribution of experiment n. 5.



(b) Particles size distribution of experiment n. 6.



(c) Particles size distribution of experiment n. 7.

Figure 3.4: Particles size distributions of experiments described in Table 3.2.

### 3.3 Production of micro-capsules

#### 3.3.1 Use of Iso-Octanol

Production of micro-capsules was performed adding an alcohol to the solution, made of monomer, photo-initiator and solvents. The alcohol possessed the ability to react via chain transfer mechanism with the carbocationic growing polymer. In this way, it delayed gelation rate. Gelation prevented polymer particles to migrate across monomer droplets. Particles had more time to structure and reach the desired conformation.

The alcohol which was used in these experiments was 2-ethyl-1-hexanol, commercially called iso-octanol. Experiments were conducted varying different factors as the ratio between monomer and solvents, the amount of iso-octanol, the ratio between solvents, the amount of photo-initiator and the pressure.

First experiments were employed using 60% wt. of monomer and 40% wt. of solvents, then the amount of monomer was reduced to 56% and the amount of solvents was increased to 44% and finally the composition of the spray solution arrived to be 50% by 50%.

#### Monomer-solvents ratio: 60%-40%

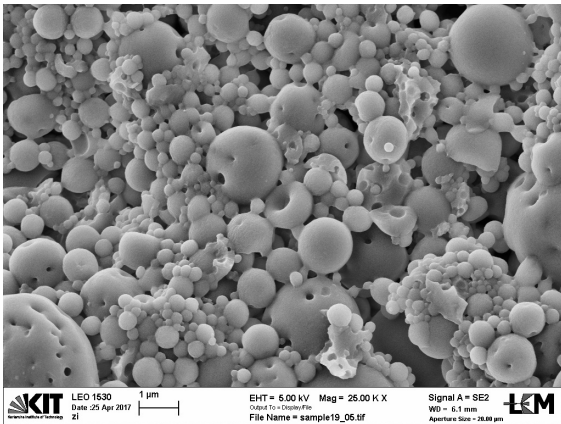
In these experiments the amount of iso-octanol was kept constant at 5% wt. referred to the monomer, instead the amount of photo-initiator was varied. In fact, first an amount of 2% wt. was employed, as reported in literature, then it was decreased to 1% wt. in order to avoid formation of solids inside the vessel during preparation of the solution itself. So, this allowed homogeneity of the solution before and after spraying. The pressure of the system was varied from 1 up to 2.5 bar and the ratio between the two solvents also was not constant. HD was increased from 23 up to 27.5% and 2-octanone was decreased from 12 to 7.5%.

Table 3.3: List of experiments performed with iso-octanol, ratio monomer-solvents 60%-40%.

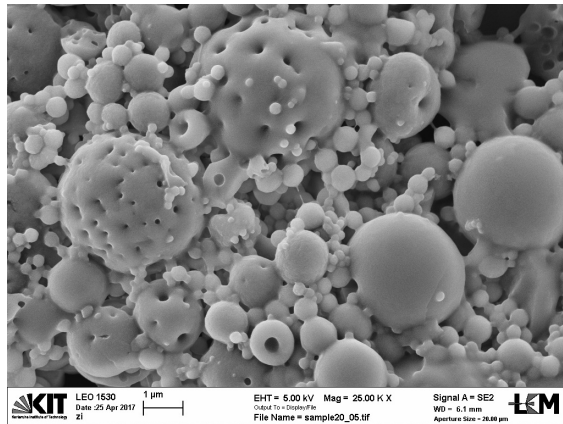
N. exp.	Composition of spray solution					Pressure [bar]
	DVE-3	PI	HD	2-Octanone	Iso-Octanol	
8	60%	2%	25%	10%	5%	2*
9	60%	2%	23%	12%	5%	2.5*
10	60%	2%	27.5%	7.5%	5%	1.5*
11	60%	1%	27.5%	7.5%	5%	1
12	60%	1%	27.5%	7.5%	5%	1.5*

\* Use of membranes as container of the polymer.

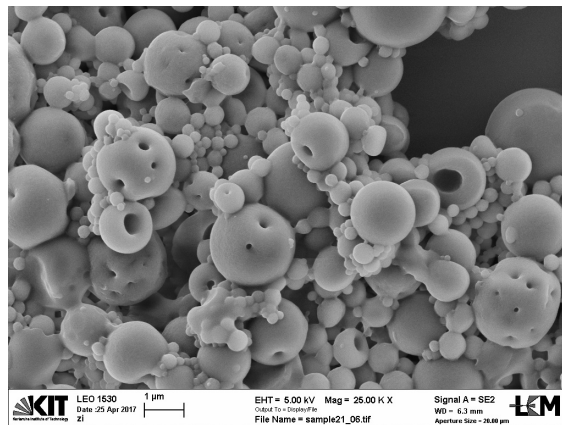
Referring to the amount of photo-initiator, experiments n. 10, 11 and 12 were analyzed. Influence of photo-initiator seemed not relevant for structuring and size distribution of micro-capsules. In fact, it was not possible to distinguish, by means of FE-SEM images (Fig. 3.5), different features between these three samples.



(a) FE-SEM images of experiment n. 10.



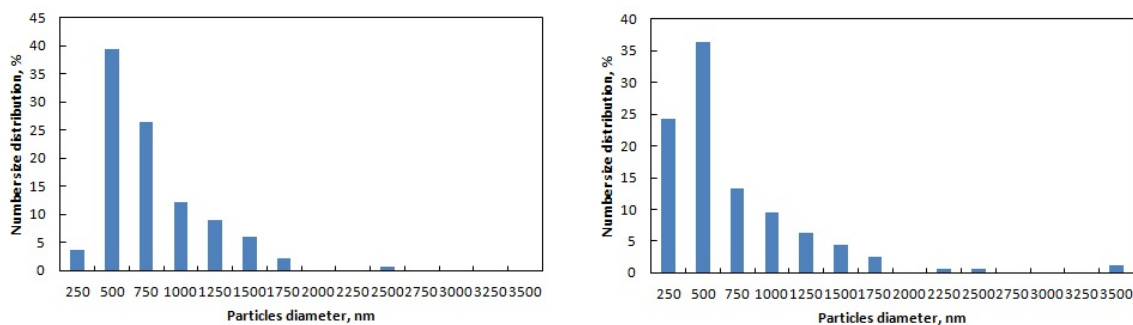
(b) FE-SEM images of experiment n. 11.



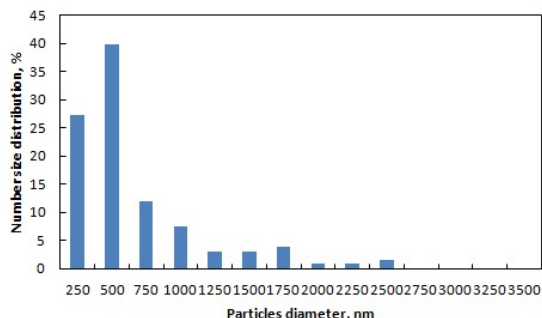
(c) FE-SEM images of experiment n. 12.

Figure 3.5: FE-SEM images of experiments described in Table 3.3.

Also analyzing particles size distributions (Fig. 3.6) were not present evident differences among the samples, which presented a mean diameter of approximately 500 nm.



(a) Particles size distribution of experiment n. 10. (b) Particles size distribution of experiment n. 11.



(c) Particles size distribution of experiment n. 12.

Figure 3.6: Particles size distributions of experiments described in Table 3.3.

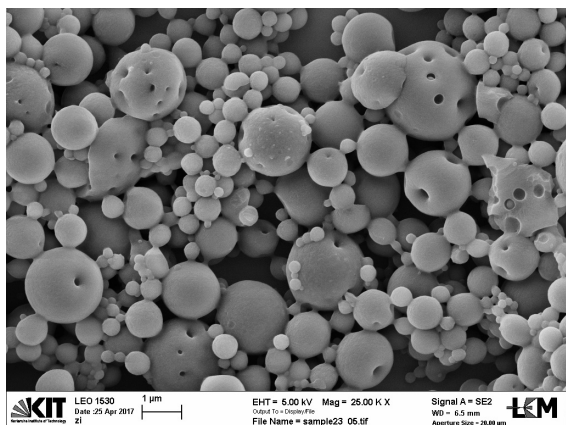
Referring to the amount of HD and 2-octanone, best results were achieved in experiments n. 10, 11 and 12, described above. Their formulation involved a high amount of HD and a correspondent low amount of 2-octanone. FE-SEM images (Fig. 3.5) showed the presence of both caps-like and sponges-like structures. Caps structures might be produced, starting from capsules particles, by evaporation of solvents and consequent collapse of their shell. It appeared, furthermore, that particles had a certain conformation depending on their size. Particles of a small dimension appeared full, of a medium size looked caps-like and of a big size seemed sponges-like. A large amount of HD allowed phase separation to take place not too late during polymerization.

#### Monomer-solvents ratio: 56%-44%

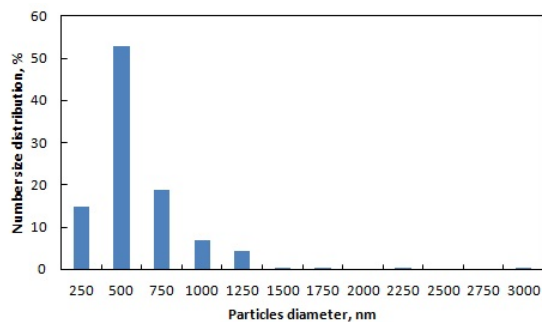
The next step of the work was to decrease the amount of monomer to 56% wt. and increase the amount of solvents to 44% wt. The experiments performed with this ratio monomer-solvents did not show, where analyzed by means of FE-SEM (Fig. 3.7 (a)), important or characteristic differences from experiments developed using a ratio monomer-solvents of 60%-40%. Micro-particles were both sponges-like and capsules-like. Also particles size distribution (Fig. 3.7 (b)) presented a peak at 500 nm, as noted for precedent experiments.

Table 3.4: List of experiments performed with iso-octanol, ratio monomer-solvents 56%-44%.

N. exp.	Composition of spray solution					Pressure [bar]
	DVE-3	PI	HD	2-Octanone	Iso-Octanol	
13	56%	1%	30.9%	8.4%	4.7%	1



(a) FE-SEM image of experiment n. 13.



(b) Particles size distribution of experiment n. 13.

Figure 3.7: FE-SEM image and particles size distribution of experiment described in Table 3.4.

FT-IR analysis were conducted to evaluate the conversion of the monomer during polymerization. For each experiment were analyzed both the starting solution and the produced polymer. Figure 3.8 showed the disappearance of double bond C=C peak at  $1600\text{ cm}^{-1}$  and of the inert group C-O at  $1100\text{-}1150\text{ cm}^{-1}$  which demonstrated the complete conversion during polymerization. The C=O bond peak at wavelength of approximately  $1700\text{ cm}^{-1}$  also disappeared. It was associated to the presence of 2-octanone which might evaporate during spraying. The last group which was visible in the figure was the group -OH at  $3400\text{ cm}^{-1}$ .

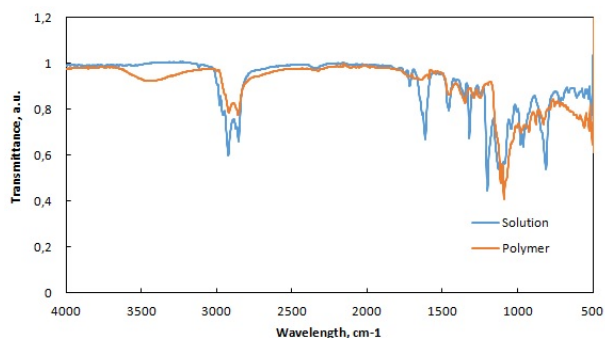


Figure 3.8: FT-IR of experiment described in Table 3.4.

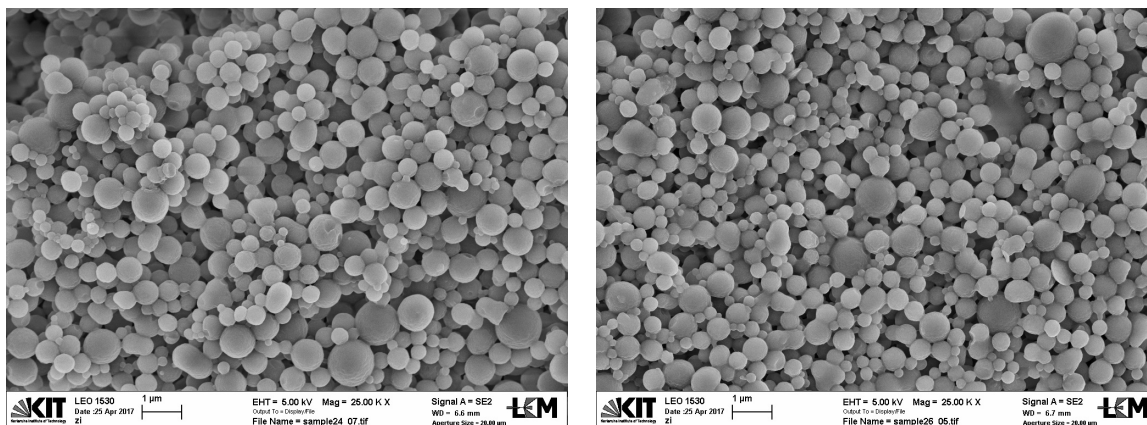
### Monomer-solvents ratio: 50%-50%

In these experiments the amount of monomer was reduced to 50% wt., instead the amount of solvents was increased to 50% wt. Tests were performed varying different factors such as the amount of photo-initiator, the ratio between solvents and the amount of iso-octanol, which ranged from 1 to 8%.

Table 3.5: List of experiments performed with iso-octanol, ratio monomer-solvents 50%-50%.

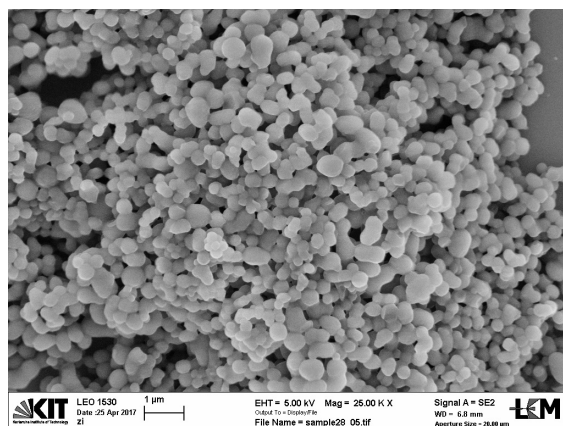
N. exp.	Composition of spray solution					Pressure [bar]
	DVE-3	PI	HD	2-Octanone	Iso-Octanol	
14	50%	1%	36%	9.8%	4.2%	1
15	50%	0.5%	36%	9.8%	4.2%	1
16	50%	0.5%	30.8%	15%	4.2%	1
17	50%	0.5%	35.8%	8.2%	6%	1
18	50%	0.5%	35.8%	6.2%	8%	1
19	50%	1%	36%	13%	1%	1
20	50%	1%	36%	12%	2%	1
21	50%	1%	36%	10.5%	3.5%	1

Experiments n. 14 and 15 were conducted employing the same recipe but decreasing the amount of photo-initiator, always referred to the monomer, from 1 to 0.5%. First of all analyzing FE-SEM images (Fig. 3.9 (a, b)), particles appeared spherical and small sized. This might confirm the hypothesis, anticipated in the precedent paragraph, that relating on size, particles assumed different conformations. Particles of a small size appeared as spherical particles, while medium sized particles appeared as caps-like and bigger sized particles showed a sponges-like structure. In these experiments the presence of so small particles might be caused by a high amount of HD or a change in spraying solution composition during time. Small particles could aggregate in order to create a bigger structure. Referring to the amount of photo-initiator, in Fig. 3.9 (b) particles conformation appeared not ideal. This could be due to a deficit in photo-initiator quantity. For this reason the suitable amount of photo-initiator referred to the monomer was 1%.



(a) FE-SEM image of experiment n. 14.

(b) FE-SEM image of experiment n. 15.

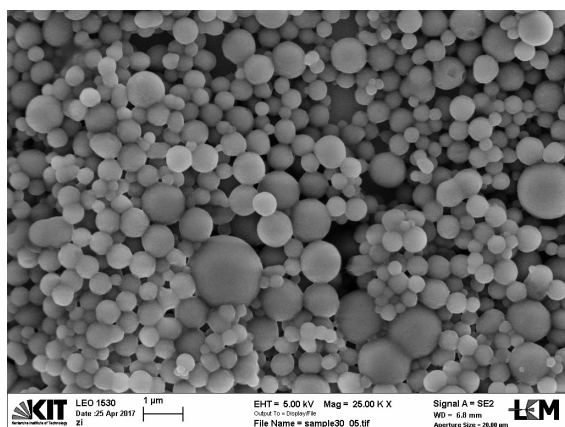


(c) FE-SEM image of experiment n. 16.

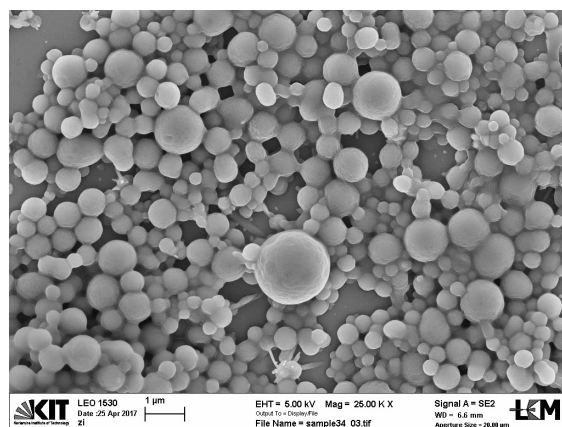
Figure 3.9: FE-SEM images of experiments described in Table 3.5.

Referring to experiments performed with a constant amount of iso-octanol, tests n. 14, 15 and 16 were considered. The alcohol amount was 4.2% in order to keep the ratio between monomer and alcohol to 1:12. The amount of HD was varied from 36 to 30.8%, consequently the amount of 2-octanone was enhanced from 9.8 to 15%. By FE-SEM images (Fig. 3.9), particles conformation did not appear as expected. The high amount of 2-octanone (Fig. 3.9 (c)) retarded phase separation and particles appeared sticky and not structured, as derived from a collapse of a bigger particle.

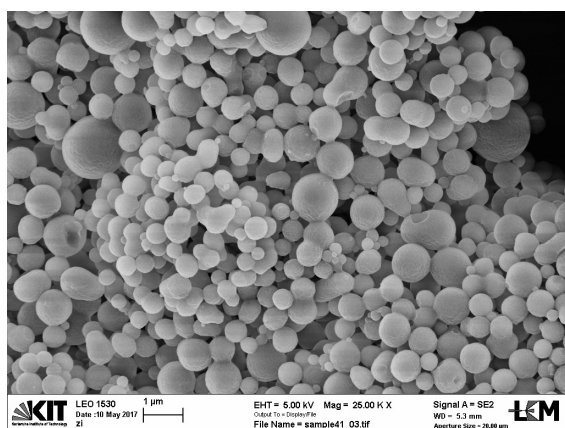
The other parameter which was varied in these experiments was the amount of iso-octanol. An increase in quantity of the alcohol caused a weak gelation due to an enhance in chain-transfer mechanism. Produced particles were sticky, as shown in figure 3.10 (a, b). In the same way, a decrease in iso-octanol amount did not produce desired particles (Fig. 3.10 (c, d)). By FE-SEM images it was not possible to confirm the real nature of these particles. They could be micro-capsules with a core shell structure or full micro-particles. They could derive from a secondary polymerization or be generated by a bigger structure.



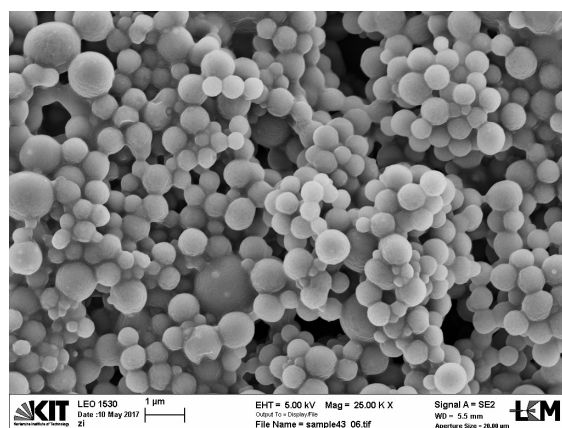
(a) FE-SEM image of experiment n. 17.



(b) FE-SEM image of experiment n. 18.



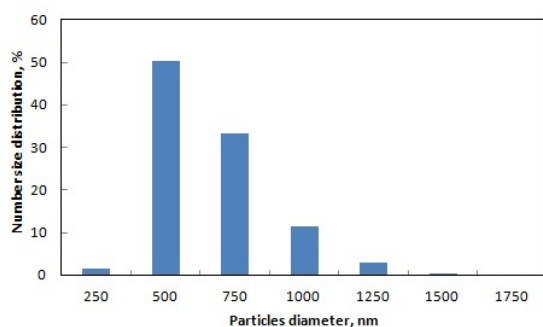
(c) FE-SEM image of experiment n. 19.



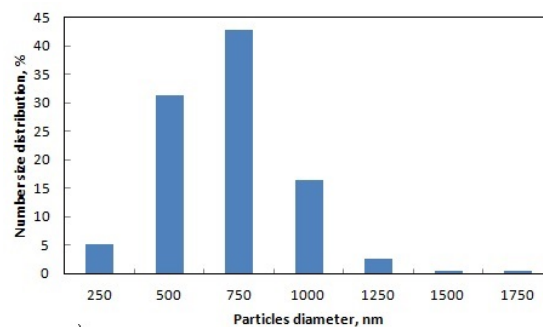
(d) FE-SEM image of experiment n. 21.

Figure 3.10: FE-SEM images of experiments described in Table 3.5.

Particles size distributions of experiments with a different amount of iso-octanol (Fig. 3.11) showed that population of particles had the same range of size. The difference was in the main diameter of particles since a low amount of iso-octanol shifted the peak from 500 (Fig. 3.11 (a)) to 750 nm (Fig. 3.11 (b)).



(a) Particles size distribution of experiment n. 18.



(b) Particles size distribution of experiment n. 19.

Figure 3.11: Particles size distributions of experiments described in Table 3.5.

FT-IR analyses (Fig. 3.12) indicated the complete conversion of double bond  $C=C$ . In fact the peak at  $1600\text{ cm}^{-1}$ , which was visible in the starting solution, was not present in the polymer. Furthermore, the group  $-OH$  was visible in the polymer at approximately  $3400\text{ cm}^{-1}$ .

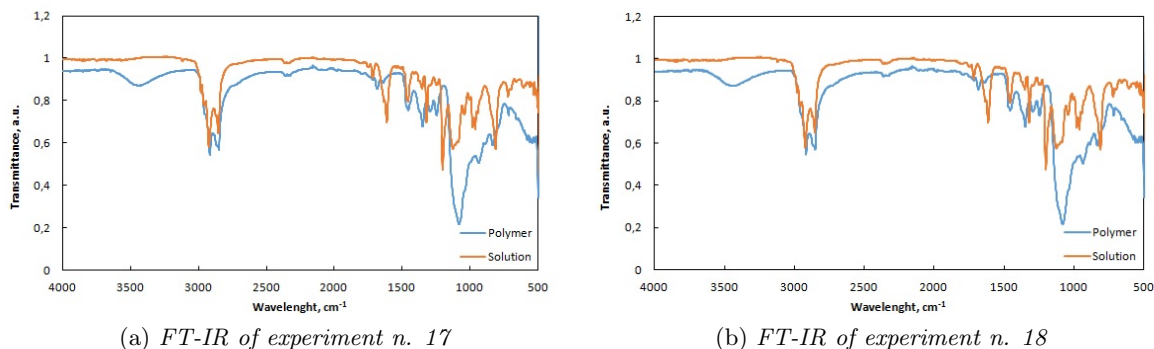


Figure 3.12: FT-IR of experiments described in Table 3.5.

The low amount of monomer might cause the production of non-structured particles. In fact monomer precipitation was too slow and did not promote the creation of a networking between particles. The reaction, in this way, could be not so fast and phase separation among particles took place too late. Particles had not time to be structured. Thus, the best ratios monomer-solvents which were investigated and implemented in this thesis were 56%-44% and 60%-40%.

### 3.3.2 Use of co-monomers

Co-polymerization was the other method used in this thesis to produce micro-capsules. A solution made of the bi-functional monomer, DVE-3, the co-monomer and solvents already mentioned, HD, 2-octanone and iso-octanol, was prepared. Two co-monomers were used: di(ethylene glycol) vinyl ether and 2-ethylhexyl vinyl ether. Both of them were mono-functional monomers. A decrease in the quantity of functional groups of monomers determined a decrease in gelation rate. Consequently, networking among particles took place slower and its density was reduced.

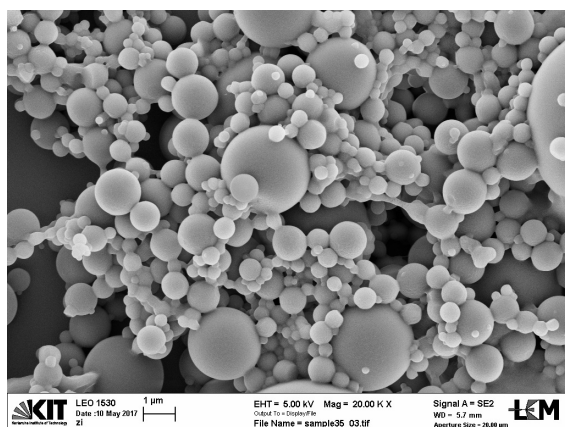
Experiments were performed using 1% of photo-initiator referred to the monomer.

Table 3.6: List of experiments performed with co-monomers.

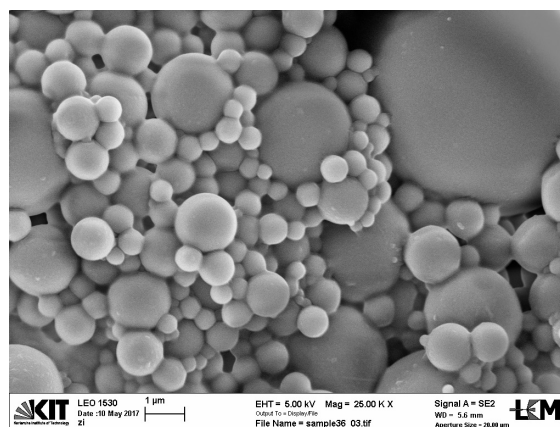
N. exp.	Composition of spray solution				Pressure [bar]
	DVE-3	Co-monomer	HD	2-Octanone	
22	79.2%	19.8% di(ethylene glycol) v. e.			1
23	79.2%	19.8% 2-ethylhexyl v. e.			1
24	55.68%	13.92% 2-ethylhexyl v. e.	17.5%	12.5%	1
25	40%	10% 2-ethylhexyl v. e.	29.2%	20.8%	1

The use of di(ethylene glycol) vinyl ether in this work was not promising. The starting solution was not completely homogeneous. Mostly of the experiments were achieved employing 2-ethylhexyl vinyl ether in combination with DVE-3. The starting solution was made of a part in weight of the co-monomer and four parts in weight of the monomer. The amount of solvents was varied. We tried to add to the solution also iso-octanol but we did not achieve good results.

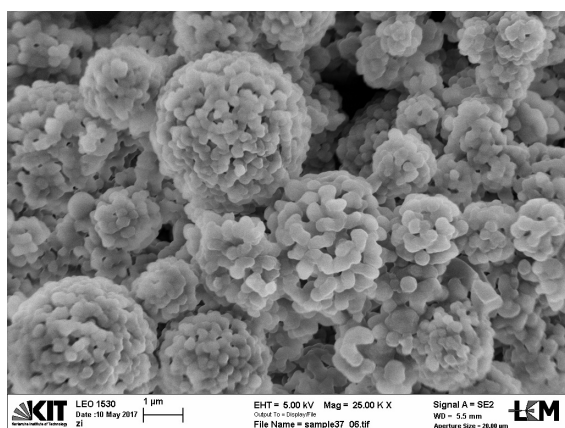
By analyzing FE-SEM images, experiments n. 22 and 23 with only monomers produced spherical and full particles, as expected (Fig. 3.13 (a, b)). Adding solvents, the recipe which employed a ratio monomers-solvents 70%-30% produced big mosaic particles not completely separated and composed of dominions of material weakly connected each other (Fig. 3.13 (c)). Ratio monomers-solvents 50%-50% generated disintegrated particles (Fig. 3.13 (d)), maybe derived from shattered bigger particles.



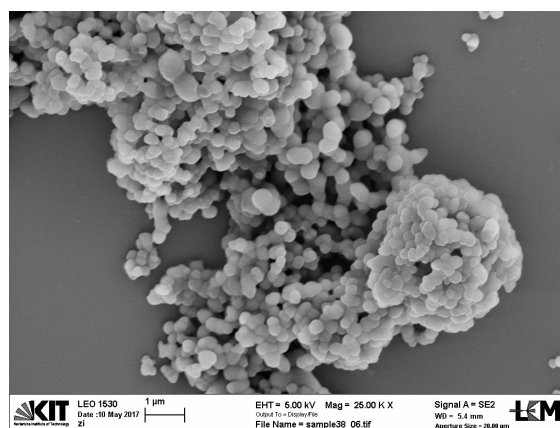
(a) FE-SEM image of experiment n. 22.



(b) FE-SEM image of experiment n. 23.



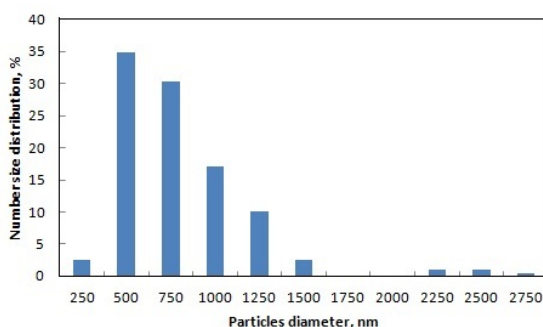
(c) FE-SEM image of experiment n. 24.



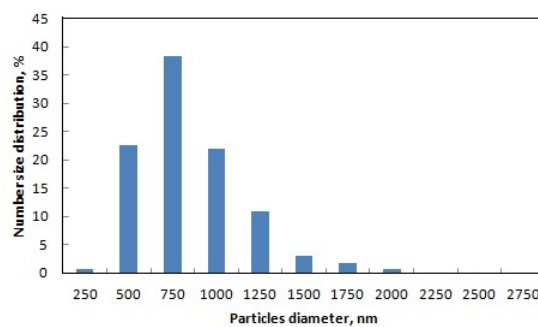
(d) FE-SEM image of experiment n. 25.

Figure 3.13: FE-SEM images of experiments described in Table 3.6.

Particles size distribution of experiment n. 22 (Fig. 3.14 (a)) showed a population of particles with a broad size diameter and a peak at 500 nm. On the other hand, experiment n. 23 (Fig. 3.14 (b)) illustrated a size distribution more concentrated in a defined range with a peak in diameter at 750 nm.



(a) Particles size distribution of experiment n. 22.



(b) Particles size distribution of experiment n. 23.

Figure 3.14: Particles size distributions of experiments described in Table 3.6.

FT-IR graphics of experiments n. 24 and 25 (Fig. 3.15) illustrated the presence of a broad -OH bond in polymers at  $3000-4000\text{ cm}^{-1}$  and the disappearances in polymers of the bond C=O at approximately  $1700\text{ cm}^{-1}$  and C=C at around  $1600\text{ cm}^{-1}$ .

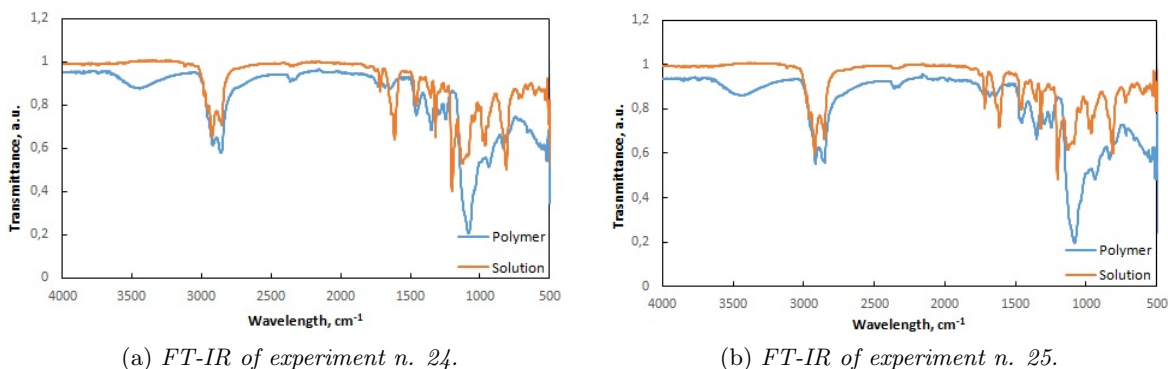


Figure 3.15: FT-IR of experiments described in Table 3.6.

### 3.4 Conclusion cationic polymerization

The first part of the thesis was focused on the production of micro-particles by photo-polymerization in aerosol employing a cationic radicalization. Full and porous particles, as well as capsules micro-particles, were successfully obtained.

Employing a solution made of DVE-3 and PI the production of full micro-particles was achieved. Pressure influenced particles size distribution since it was demonstrated that at high pressure population of particles occupied a thinner distributive scale.

To obtain porous micro-particles solvents were added to the monomer solution. The best recipe which was investigated consisted of 70% wt. of monomer and 30% wt. of solvents. Solvents used were HD and 2-octanone. Various experiments were conducted to investigate the best ratio between the solvents. HD was required in higher amount with respect to 2-octanone since it was responsible for phase separation in the earlier stages of polymerization. In fact, particles which showed desired structure were produced using 17.5% of HD and 12.5% of 2-octanone.

Micro-capsules were produced in two different ways. The first one provided the add of iso-octanol to the starting solution made of DVE-3, PI, HD and 2-octanone. The use of the alcohol was absolutely necessary to obtain capsules since it delayed gelation rate. The optimal ratio wt. between monomer and iso-octanol was 12:1. Many experiments were conducted to investigate for the best recipe. Structured micro-particles were obtained, in fact, employing 60% wt. of monomer and 40% wt. of solvents or 56% wt. of monomers and 44% wt. of solvents. A high amount of monomer was required to allow fast monomer precipitation and reaction.

The other way to obtain micro-capsules, by literature, was the use of a co-monomer in addition to the solution composed of DVE-3, PI, HD and 2-octanone. The co-monomer which showed best results was 2-ethylhexyl vinyl ether. A part wt. of this co-monomer was mixed with four parts wt. of DVE-3. Different experiments were conducted but without achieving the desired structure of micro-capsules, only porous micro-particles.

## Chapter 4

# Results and discussion: Radical Polymerization

Radical polymerization was investigated using two different mechanisms of reaction, acrylic and thiol-ene.

### 4.1 Acrylic Polymerization

#### 4.1.1 Production of full micro-particles

A co-monomeric system made of a monomer, a cross-linker and the photo-initiator was employed to produce full micro-particles. As monomers, butyl acrylate (BA) and methyl methacrylate (MMA) were used. 1,6-hexanediol diacrylate (HDDA), trimethylolpropane triacrylate (TPT) and trimethylolpropane ethoxylate triacrylate (TPET) were used as cross-linkers and Irgacure 907 (1% wt. referred to both the monomer and the co-monomer) was employed as photo-initiator.

#### Use of BA as monomer

BA was used in combination with HDDA, TPT or TPET.

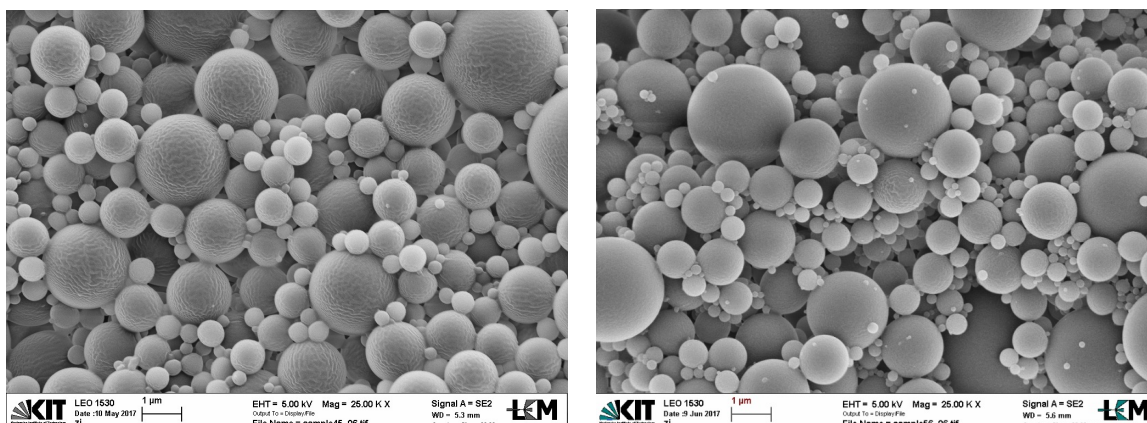
Table 4.1: List of experiments performed with BA.

N. exp.	Composition of spray solution				Ratio cross-linker-monomer
	BA	HDDA	TPT	TPET	
26	79.2%	19.8%			1:4
27	49.5%	49.5%			1:1
28	74.25%	24.75%			1:3
29	79.2%			19.8%	1:4
30	79.2%		19.8%		1:4

Referring to the solution composed of BA and HDDA, the co-monomeric system was employed in different ratios, 1:1, 3:1, 4:1. The first number was referred to the monomer and the second number to the cross-linker. For example, the ratio 1:1 represented a system made of a part in weight of BA and a part in weight of HDDA.

By analyzing FE-SEM images (Fig. 4.1), production of full and spherical micro-particles was

accomplished. It was not possible to distinguish important features relating on a different ratio between monomer and cross-linker.

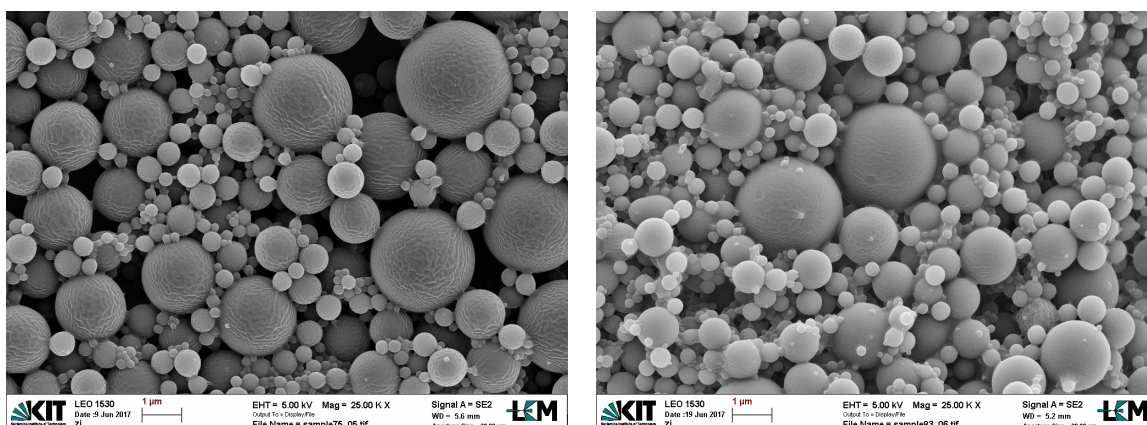


(a) FE-SEM image of experiment n. 26.

(b) FE-SEM image of experiment n. 27.

Figure 4.1: FE-SEM images of experiments described in Table 4.1.

Referring to the solution composed of BA and TPT and of BA and TPET, the co-monomeric system was employed in ratio 4:1 (four parts in weight of BA and a part in weight of co-monomer). Also in this case, spherical and full particles were produced, as visible by FE-SEM images (Fig. 4.2).

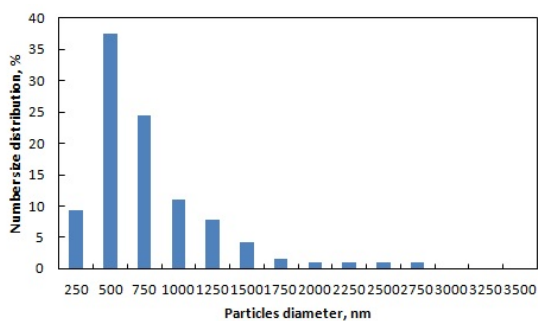


(a) FE-SEM image of experiment n. 29.

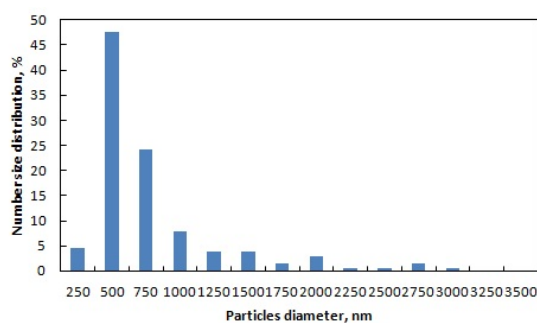
(b) FE-SEM image of experiment n. 30.

Figure 4.2: FE-SEM images of experiments described in Table 4.1.

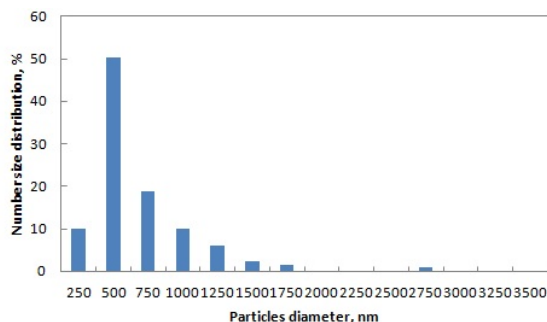
Regarding particles size distribution (Fig. 4.3), no different variations were visible. Particles occupied a broad size range with a maximum peak at 500 nm.



(a) Particles size distribution of experiment n. 27.



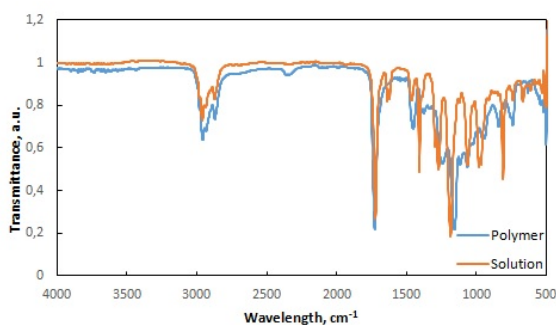
(b) Particles size distribution of experiment n. 29.



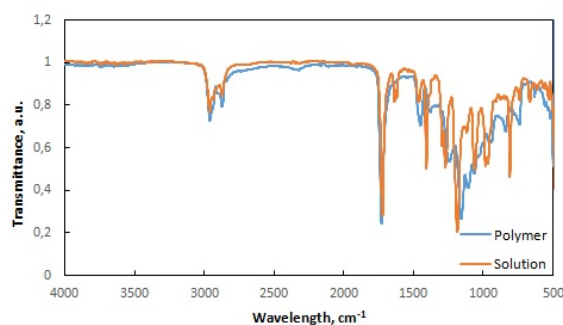
(c) Particles size distribution of experiment n. 30.

Figure 4.3: Particles size distributions of experiments described in Table 4.1.

FT-IR analyses (Fig. 4.4) showed the disappearance of double bond C=C peak at  $1600\text{ cm}^{-1}$  which demonstrated the complete conversion during polymerization. The C=O bond peak, characteristic of the monomers, at wavelength of approximately  $1700\text{ cm}^{-1}$  also disappeared. The last group which was visible in the figure was the group C-O at  $1100\text{ cm}^{-1}$  which was related on the presence of ethers.



(a) FT-IR image of experiment n. 26.



(b) FT-IR image of experiment n. 29.

Figure 4.4: FT-IR images of experiments described in Table 4.1.

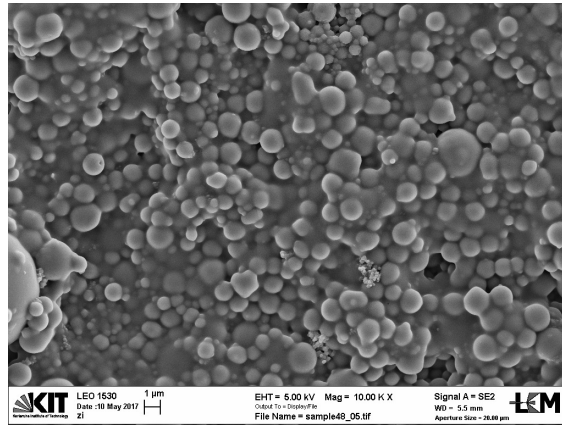
## Use of MMA as monomer

MMA was used in combination with HDDA which acted as cross-linker. Only few experiments were performed with this combination of chemicals.

Table 4.2: List of experiments performed with MMA.

N. exp.	Composition of spray solution		Ratio cross-linker-monomer
	MMA	HDDA	
31	79.2%	19.8%	1:4

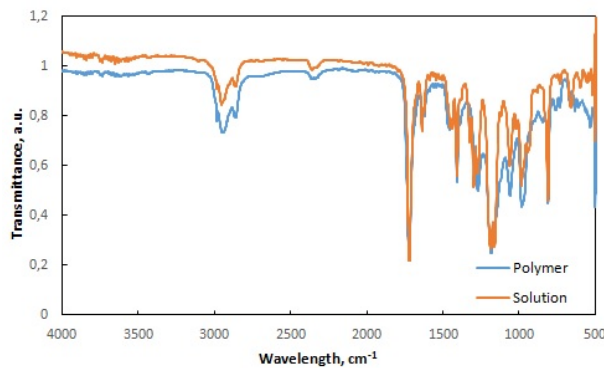
Analyzing FE-SEM images (Fig. 4.5), particles appeared sticky and not completely separated each other. For this reason, in this thesis experiments containing BA as monomer were preferred and incremented to produce polymeric material.



(a) FE-SEM image of experiment n. 31.

Figure 4.5: FE-SEM image of experiment described in Table 4.2.

FT-IR image (Fig. 4.6) showed a peak at  $1700\text{ cm}^{-1}$  which demonstrated the presence of a double bond C=O in both monomer and cross-linker. The other peak representative of the double bond C=C was present at approximately  $1600\text{ cm}^{-1}$ . The presence of this peak in the polymer indicated a bad conversion of the monomer, since this group did not disappeared after the passage in the reactor. The last peak which represented C-O bond was present at  $1100\text{ cm}^{-1}$ .



(a) FT-IR image of experiment n. 31.

Figure 4.6: FT-IR image of experiment described in Table 4.2.

### 4.1.2 Production of porous micro-particles

Porous micro-particles were produced adding a solvent to the solution made of monomer and co-monomer. Two different types of solvents were added, HD and 2-ethyl-1-hexanol (iso-octanol). Various co-monomeric systems were prepared employing different types and ratios of monomers and cross-linkers. Different ratios between the amount of monomers and solvents were implemented in order to search for the best combination to produce polymer.

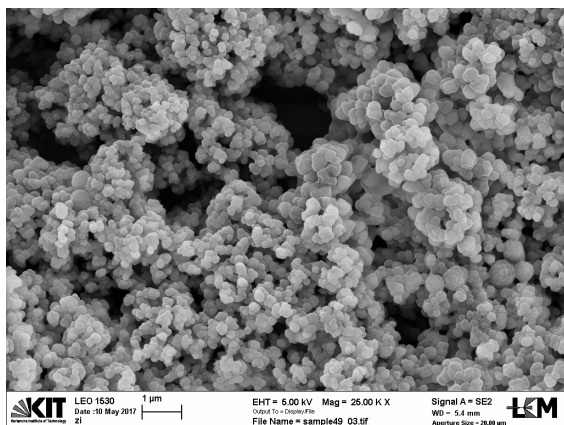
#### Co-monomeric system: BA-HDDA.

This system was implemented varying the amount of monomers from 50 to 70% and the correspondent amount of solvents from 50 to 30%. The ratio between monomer and cross-linker was varied from 1:1 to 4:1. Here is presented a list of the most important experiments (Tab. 4.3).

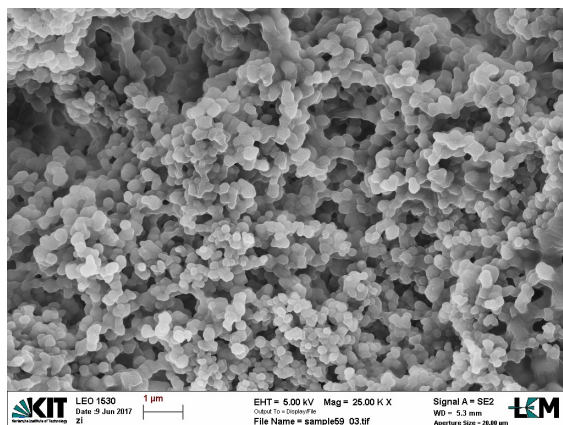
Table 4.3: List of experiments performed with BA and HDDA.

N. exp.	Composition of spray solution				Ratio mon.-solv.	Ratio c.-l.-mon.
	BA	HDDA	HD	Iso-Octanol		
32	24.75%	24.75%	50%	50%	50%-50%	1:1
33	33%	16.5%	50%		50%-50%	1:2
34	44.55%	14.85%	40%		60%-40%	1:3
35	51.98%	17.33%	30%		70%-30%	1:3
36	55.44%	13.86%	30%		70%-30%	1:3
37	39.6%	9.9%			50%-50%	1:4
38	39.6%	9.9%	50%		50%-50%	1:4
39	47.52%	11.88%	40%		60%-40%	1:4

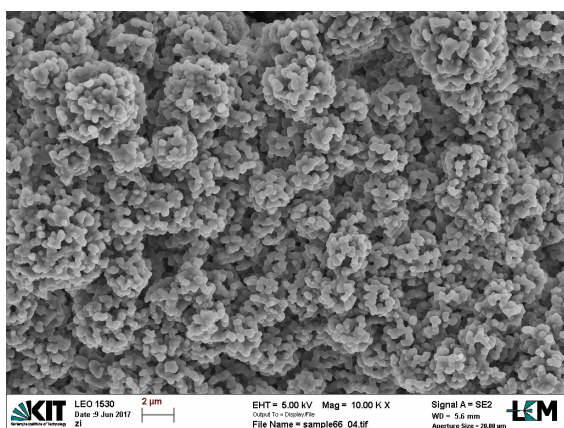
By FE-SEM images, mosaic micro-particles were obtained with a ratio monomers-solvent 60%-40% and 70%-30% (Fig. 4.7 (c, d)). In fact, all experiments performed with a ratio 50%-50% showed disintegrated particles (Fig. 4.7 (a, b)). Their formation could be caused by a delay in the separation phase which took place later. Maybe separation happened when the solution was poor of monomer and consequently polymers could not interact and aggregate among themselves. Furthermore the ratio cross-linker-monomer which permitted to obtain porous particles was 1:3. This demonstrated the necessity to employ an important amount of cross-linker to reach desired structure and desired mechanical properties.



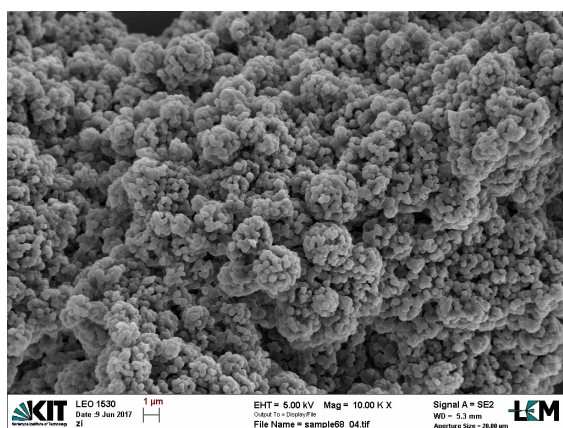
(a) FE-SEM image of experiment n. 32.



(b) FE-SEM image of experiment n. 33.



(c) FE-SEM image of experiment n. 34.



(d) FE-SEM image of experiment n. 35.

Figure 4.7: FE-SEM image of experiments described in Table 4.3.

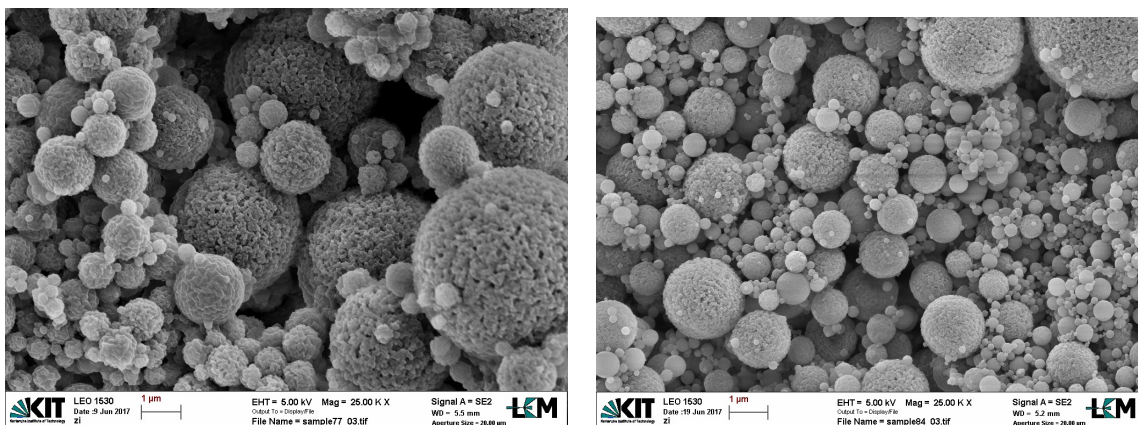
### Co-monomeric system: BA-TPT and MMA-TPT.

In this section TPT was used as cross-linker in combination with monomers, as BA and MMA. The recipe which was implemented considered 70% of monomers and 30% of solvents.

Table 4.4: List of experiments performed with BA-MMA and TPT.

N. exp.	Composition of spray solution					Ratio mon.-solv.	Ratio c.-l.-mon.
	BA	MMA	TPT	HD	Iso-Oct.		
40		46.2%	23.1%	30%		70%-30%	1:2
41	55.44%		13.86%		30%	70%-30%	1:4
42	46.2%		23.1%		30%	70%-30%	1:2

FE-SEM images (Fig. 4.8) showed the production of spherical and mosaic particles. They looked uniform, defined and completely separated each other. In this case, the ratio cross-linker-monomer which gave to particles the desired conformation was 1:2. The use of a tri-functional cross-linker (TPT) allowed the production of porous micro-particles employing both MMA and BA as monomers. The use of a bi-functional cross-linker (HDDA), instead, did not lead to successful results.

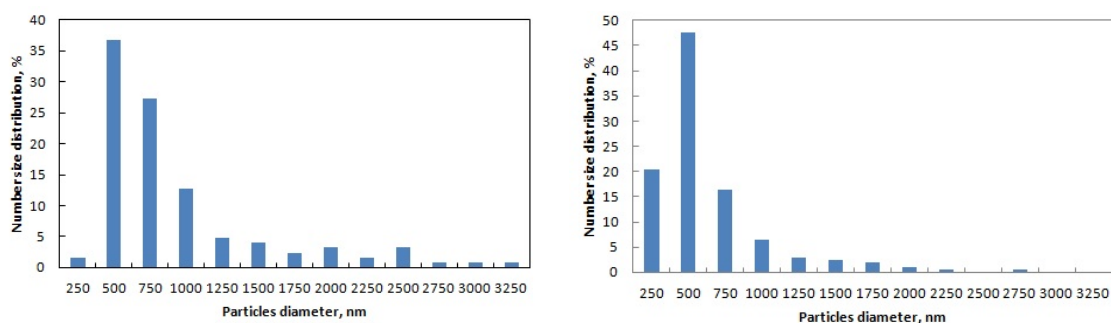


(a) FE-SEM image of experiment n. 40.

(b) FE-SEM image of experiment n. 42.

Figure 4.8: FE-SEM images of some experiments described in Table 4.4.

Particles size distributions (Fig. 4.9) did not show differences between the two monomers. In fact, particles population presented a broad diameter size with a maximum peak at approximately 500 nm.

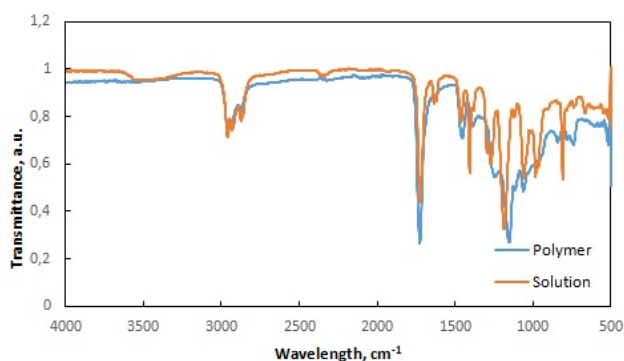


(a) Particles size distribution of experiment n. 40.

(b) Particles size distribution of experiment n. 42.

Figure 4.9: Particles size distributions of experiments described in Table 4.4.

Analyzing FT-IR image (Fig. 4.10) the group C-O, which was related on the presence of ethers, was present at  $1100\text{ cm}^{-1}$ . All the other peaks described in the precedent section were present.



(a) FT-IR of experiment n. 42.

Figure 4.10: FT-IR of experiment described in Table 4.4.

## Co-monomeric system: BA-TPET and MMA-TPET.

The last recipe which was used to produce porous micro-particles contained TPET as cross-linker and BA and MMA as monomer.

Table 4.5: List of experiments performed with BA-MMA and TPET.

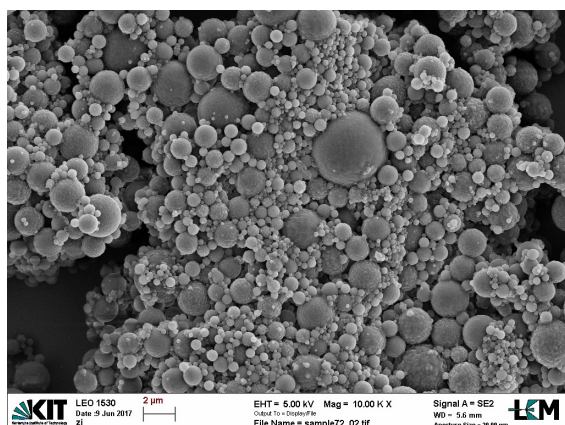
N. exp.	Composition of spray solution					Ratio mon.-solv.	Ratio c.-l.-mon.
	BA	MMA	TPET	HD	Iso-Oct.		
43	46.2%	23.1%		30%	70%-30%	1:2	
44	46.2%		23.1%		30%	70%-30%	1:2
45	55.44%		13.86%		30%	70%-30%	1:4
46	55.44%		13.86%	30%		70%-30%	1:4
47	39.5%		9.9%		50%	50%-50%	1:4

The majority of experiments was conducted employing 70% of monomers and 30% of solvent. In fact, by previous tests it was clear the necessity to employ a high amount of monomers to reach the desired structure of particles.

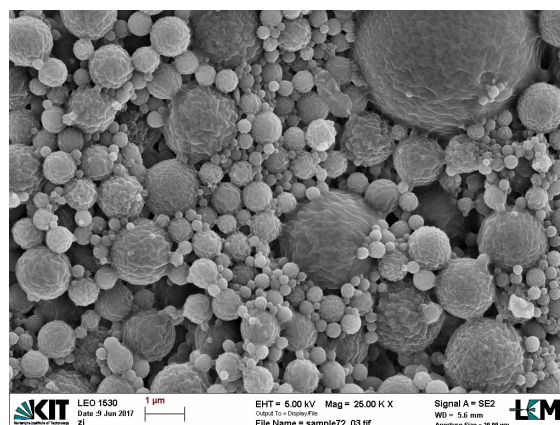
FE-SEM images of experiments performed with a ratio monomers-solvent of 70%-30% and a ratio cross-linker-monomer 1:2 with BA as monomer (Fig. 4.11 (a, b)) showed the production of gel type particles. A real phase separation did not take place since the solvent was present inside the polymeric structure.

The use of MMA, instead of BA, produced particles differently structured. Disintegrated, porous and caps-like particles were originated by the same recipe.

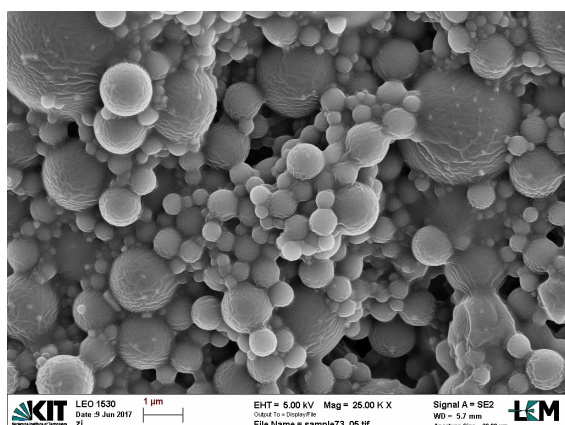
Regarding experiments n. 45 and 46 with a ratio cross-linker-monomer 1:4, was evident that TPET worked better with iso-octanol, instead of HD, since the co-monomer was much more soluble in iso-octanol. FE-SEM image 4.8 (c) showed gel-type particles, FE-SEM image 4.8 (d) presented disintegrated particles using as solvent HD. A ratio monomer-solvent 50%-50% demonstrated deficiency in monomer amount and consequently not structured particles.



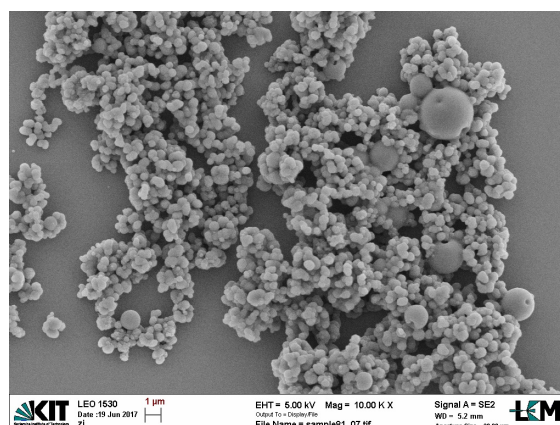
(a) FE-SEM image of experiment n. 44.



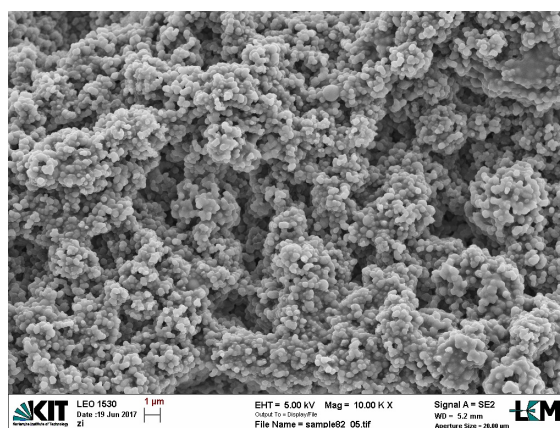
(b) FE-SEM image of experiment n. 44.



(c) FE-SEM image of experiment n. 45.



(d) FE-SEM image of experiment n. 43.



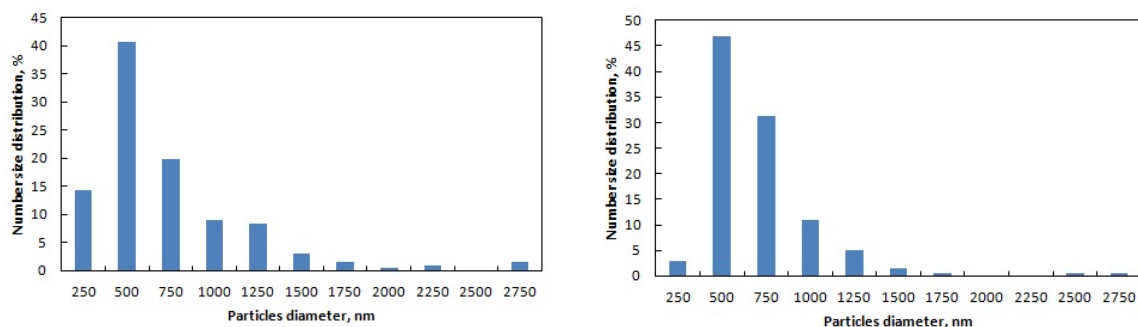
(e) FE-SEM image of experiment n. 46.

Figure 4.11: FE-SEM images of experiments described in Table 4.5.

Particles size distributions of experiments n. 45 and 46 (Fig. 4.12), the sole distributions that were possible to create, showed a similar distribution. In fact, population of particles ranged in the same scale and had a peak at approximately 500 nm.

### 4.1.3 Production of micro-capsules and micro-caps

The following section treats the production of micro-capsules and micro-caps using a solution, made of monomers and solvents previously described, plus glycerol. This chemical, in fact, was absolutely necessary to obtain these types of structures. Ethanol and 1-propanol were added to the starting



(a) Particles size distribution of experiment n. 45. (b) Particles size distribution of experiment n. 46.

Figure 4.12: Particles size distribution of experiments described in Table 4.5.

solution to make it homogeneous. Their evaporation also helped the formation of caps and capsules making possible a collapse of the structure. Experiments in this section were performed using a combination of BA with HDDA and BA with TPT. This choice derived from an analyses regarding precedent experiments for production of full and porous micro-particles. The attention was focused on FE-SEM images, yield and aspect of produced polymeric material.

### Use of BA and HDDA

Experiments were performed varying the amount of monomers from 70 to 50% and consequently the amount of solvents from 30 to 50%. The ratio between cross-linker and monomer also ranged from 1:9 to 1:1. In fact, increasing the amount of cross-linker phase separation and gelation took place earlier.

Factors which were varied were: the amount of glycerol from 5% to 20%, the alternate use of ethanol and 1-propanol and the amount of photo-initiator.

### Monomers-solvents ratio: 50%-50%

First experiments were conducted using an amount of glycerol of 5%, then glycerol was increased to 10%. Hexadecane was used as solvent.

Table 4.6: List of experiments performed with BA-HDDA 50%-50%.

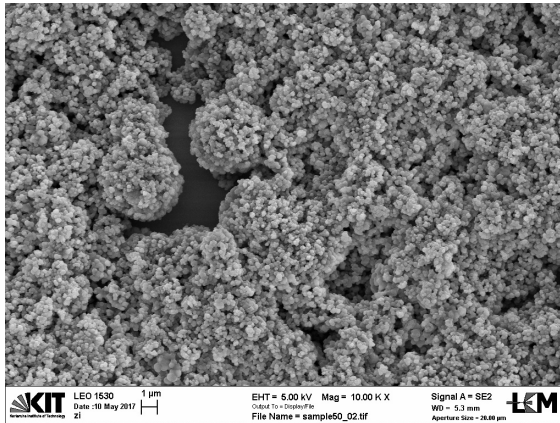
N. exp.	Composition of spray solution					Ratio cross-linker-monomer
	BA	HDDA	HD	Glycerol	Co-solvent	
48	24.75%	24.75%	45%	5%	16% Eth.	1:1
49	33%	16.5%	45%	5%	17% Eth.	1:2
50	37.13%	12.38%	45%	5%	30% Eth.	1:3
51	37.13% (4% PI)	12.38%	45%	5%	18% Eth.	1:3
52	12.38%	37.13%	40%	10%	61% 1-Prop.	1:3
53	39.6%	9.9%	40%	10%	65% 1-Prop.	1:4

The first four experiments produced only disintegrated particles, as visible in FE-SEM images (Fig. 4.13). This result was probably due to, first, a small amount of monomers whose quantity reached only 50% and, secondary, to a high amount of cross-linker. In fact, increasing the amount of cross-linker, phase separation was anticipated too much. Particles were not completely separated, but

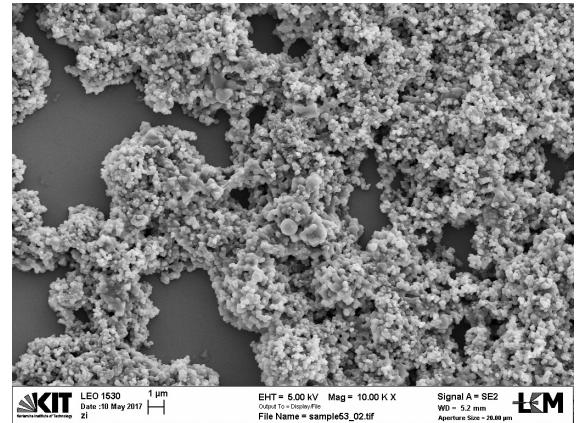
only few of them looked like porous, composed of small dominions of material. They were going to assembly in order to structure and form a bigger particle.

Regarding on the different amount of photo-initiator, experiment n. 50 was repeated increasing to 4% the quantity of PI. By FE-SEM images (Fig. 4.13 (b, c)), no differences were visible, so this factor did not influence structure of micro-capsules.

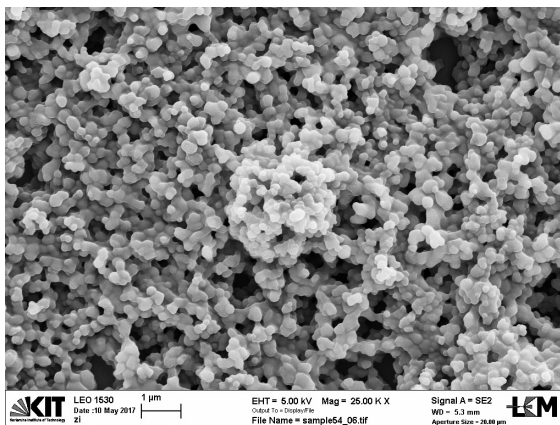
On the other hand, was evident the necessity to increase the amount of glycerol to obtain micro-caps. Images 4.13 (d, e) evidenced the presence of few micro-caps made of small dominions of polymer, as they were agglomerates of particles. Micro-caps might be created only for a determinate size.



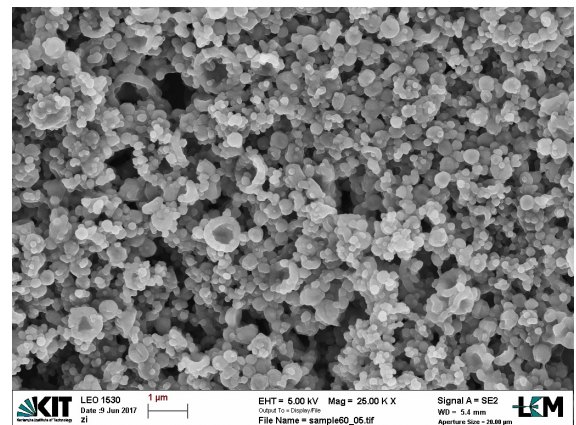
(a) FE-SEM image of experiment n. 48.



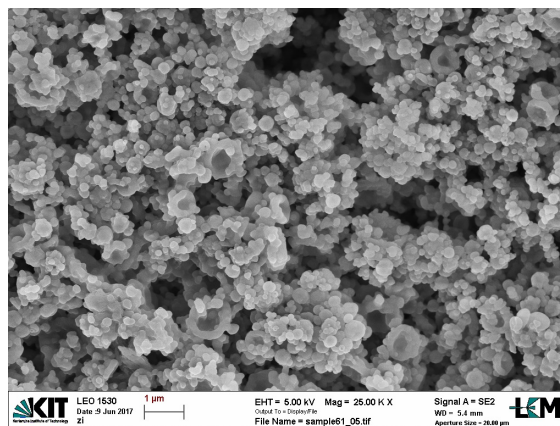
(b) FE-SEM image of experiment n. 50.



(c) FE-SEM image of experiment n. 51.



(d) FE-SEM image of experiment n. 53.



(e) FE-SEM image of experiment n. 52.

Figure 4.13: FE-SEM images of experiments described in Table 4.6.

FT-IR analyses of experiments n. 53 (Fig. 4.14) showed the presence of -OH bond in a broad range around 3500 nm. This bond was related to the presence of glycerol and co-solvents.

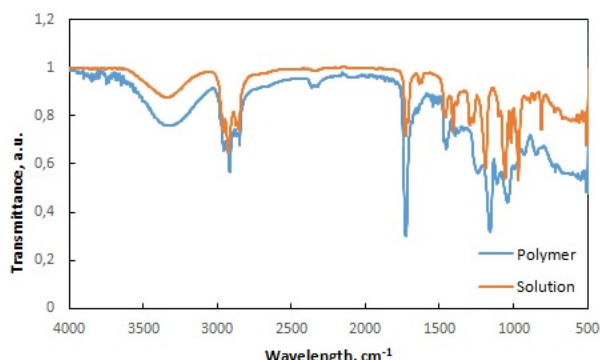


Figure 4.14: FT-IR of experiments described in Table 4.6.

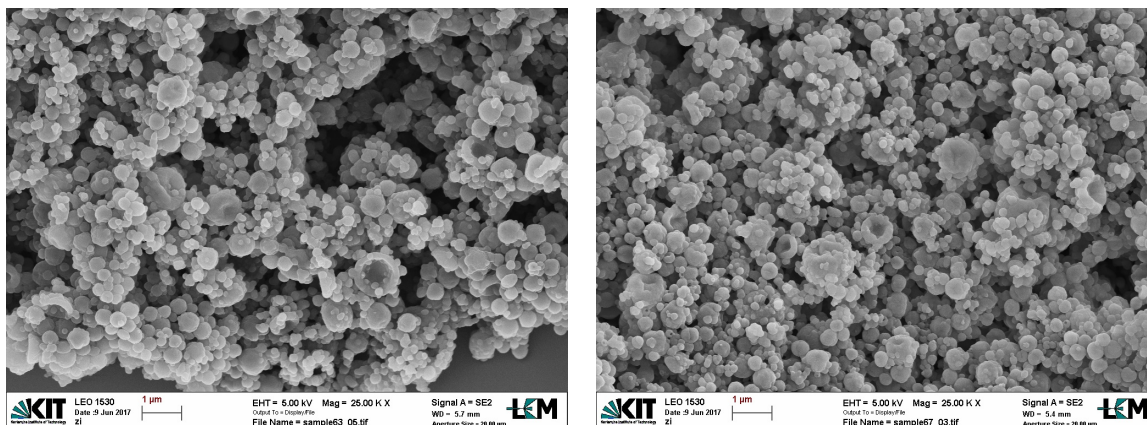
### Monomers-solvents ratio: 60%-40%

Using 60% wt. of monomers and 40% wt. of solvents, experiments were performed varying the ratio between HDDA-BA from 1:4 to 1:3. HD was used as solvent.

Table 4.7: List of experiments performed with BA-HDDA 60%-40%.

N. exp.	Composition of spray solution					Ratio cross-linker-monomer
	BA	HDDA	HD	Glycerol	Co-solvent	
54	11.88%	47.52%	32%	8%	57.29% 1-Prop.	1:4
55	14.85%	44.55%	32%	8%	71.66% 1-Prop.	1:3

Analyzing FE-SEM images (Fig. 4.15) micro-caps were produced. These micro-caps were more defined than the others precedent analyzed, shells were more complete and uniform, not made of dominions of material. The higher amount of monomers could help and improve particles to structure.



(a) FE-SEM image of experiment n. 54.

(b) FE-SEM image of experiment n. 55.

Figure 4.15: FE-SEM images of some experiments described in Table 4.7.

**Monomers-solvents ratio: 70%-30%**

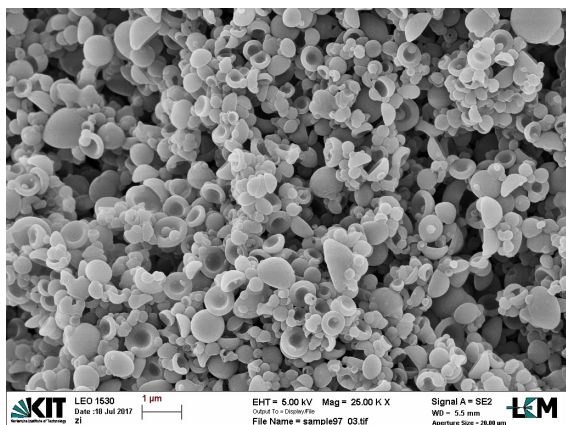
Using this ratio monomers-solvents experiments were performed varying the ratio between HDDA-BA from 1:4 to 1:3. Solvents which were used were HD and iso-octanol alone or in combination. Glycerol was increased from 3% to 20%.

Table 4.8: List of experiments performed with BA-HDDA 70%-30%.

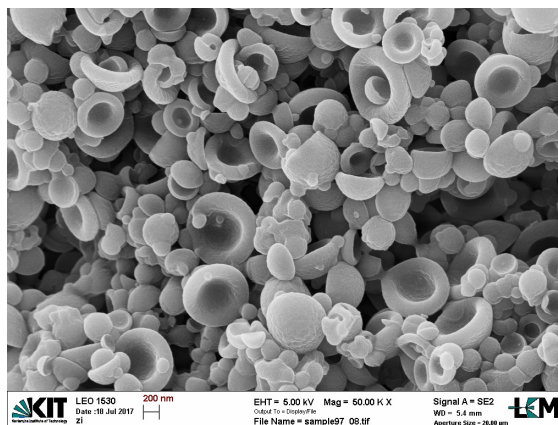
N. exp.	Composition of spray solution						Rat. c.l.-m.
	BA	HDDA	HD	Iso-Oct.	Glyc.	Co-solv.	
56	13.86%	55.44%	24%		3%	44.68% 1-Prop.	1:4
57	17.33%	51.98%	27%		3%	46.44% 1-Prop.	1:3
58	12.6%	50.4%		27%	9%	64.7% 1-Prop.	1:4
59	12.6%	50.4%	27%		9%	66.88% 1-Prop.	1:4
60	12.6% (2.8% PI)	50.4%		27%	9%	67.34% 1-Prop.	1:4
61	12.6%	50.4%		27%	9%	55.25% Eth.	1:4
62	12.45%	49.76%		17.76%	20%	81.85% 1-Prop.	1:4
63	15.55%	46.66%		17.76%	20%	77.92% 1-Prop.	1:3
64	14%	56%	15%	15%	10%	66.96% 1-Prop.	1:3
65	14%	56%	15%	15%	10%	53.05% Eth.	1:4

Production of micro-caps and micro-capsules was achieved. Glycerol acted the main role in structuring particles. Production of micro-capsules and micro-caps was influenced by an interplay between cross-linking density and glycerol soft-making. Micro-capsules were produced increasing cross-linking density, which meant increasing the amount of the cross-linker.

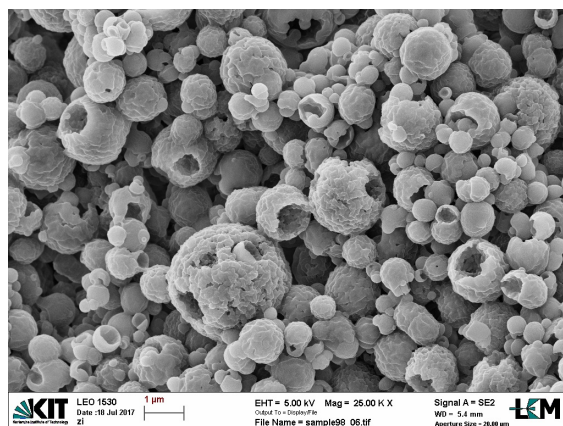
Incrementing the amount of glycerol, particles were more defined and structured. In fact, by FE-SEM images (Fig. 4.16) of experiments n. 62 and 63 with 20% of glycerol, micro-particles showed the desired structure and were totally separated. Experiment n. 62 produced micro-caps, n. 63 produced micro-capsules. In this case, the only difference in the recipe was the ratio between monomers and solvents since solvent and co-solvent used were the same.



(a) FE-SEM image of experiment n. 62.



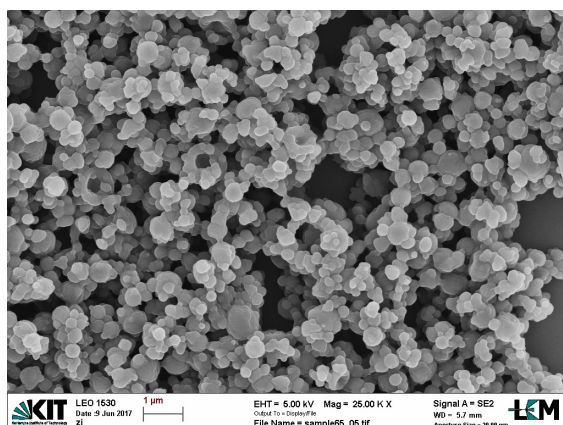
(b) FE-SEM image of experiment n. 62.



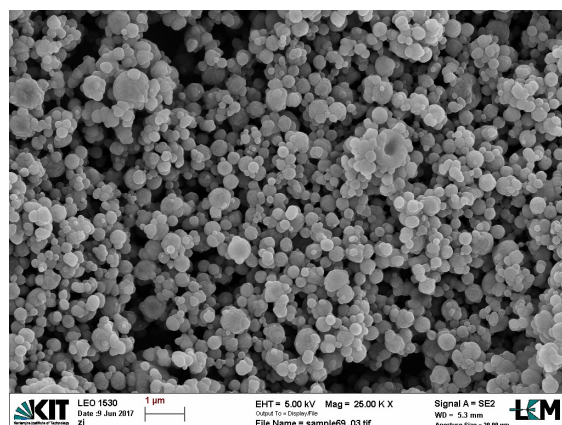
(c) FE-SEM image of experiment n. 63.

Figure 4.16: FE-SEM images of experiments described in Table 4.8.

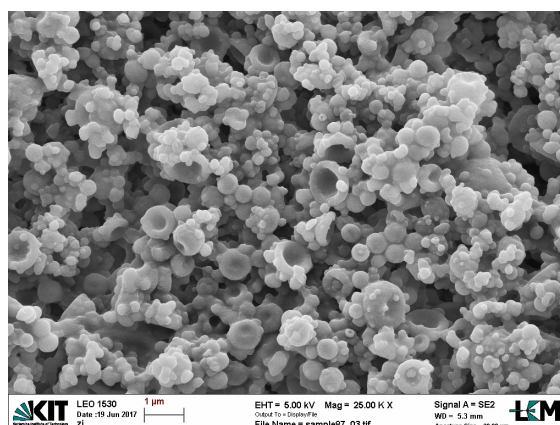
Micro-caps were produced also in experiments n. 56, 57 and 59 as shown by FE-SEM images (Fig. 4.17). Here, micro-particles assumed the conformation of caps in an early stage. In fact, they needed more glycerol and cross-linker to structure themselves and polymerize at the right time. Micro-caps were produced by a quick evaporation of the cross-linker and a collapse of the core structure.



(a) FE-SEM image of experiment n.146.



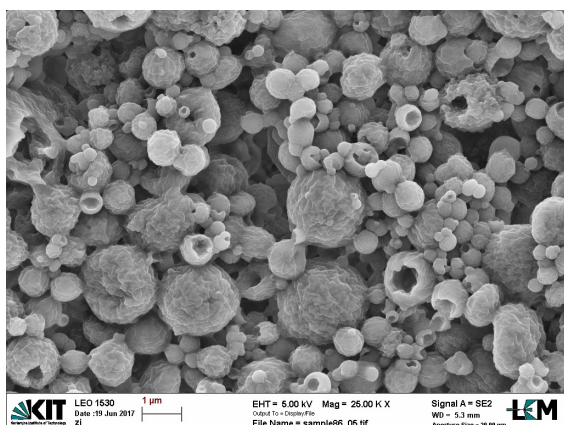
(b) FE-SEM image of experiment n.150.



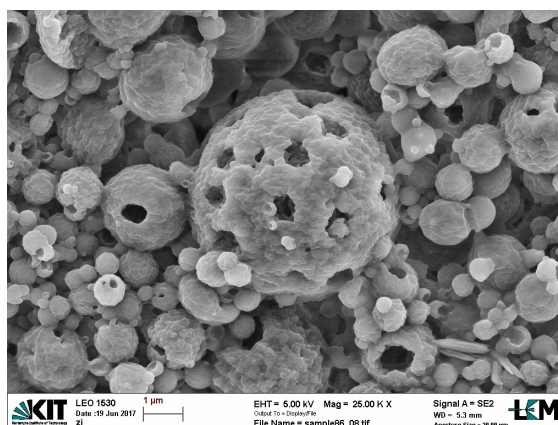
(c) FE-SEM image of experiment n.180.

Figure 4.17: FE-SEM images of experiments described in Table 4.8.

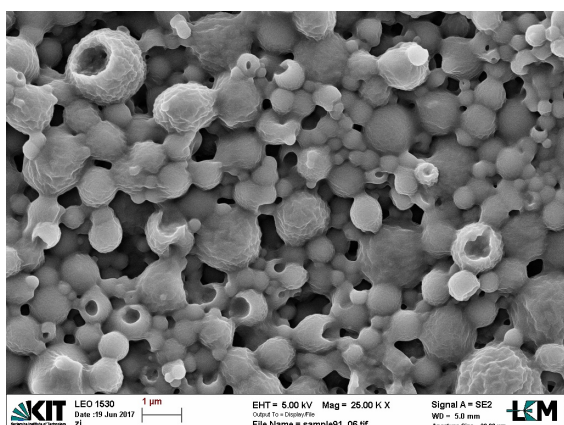
Micro-capsules were produced in experiments n. 58, 60, 61 and 64 (Fig. 4.18). In this case particles were made of small domains of material, the shell was not smooth. The amount of glycerol was 10% wt. in all experiments. Experiments n. 60 and 61 were performed using the same recipe, but with a different amount of photo-initiator. The last one had a higher amount of photo-initiator, but no differences in FE-SEM images were visible.



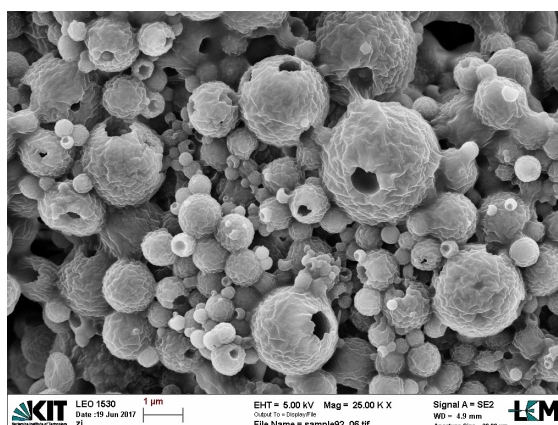
(a) FE-SEM image of experiment n. 58.



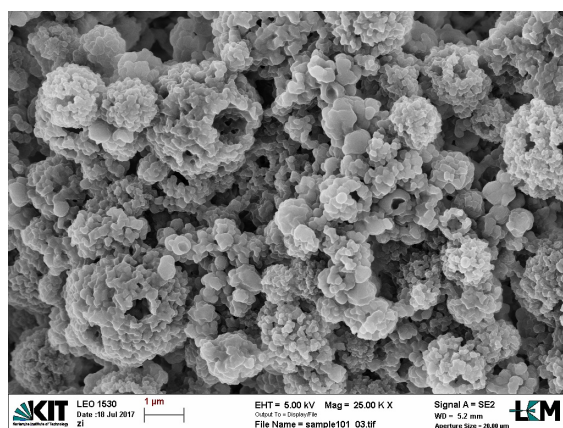
(b) FE-SEM image of experiment n. 58.



(c) FE-SEM image of experiment n. 60.



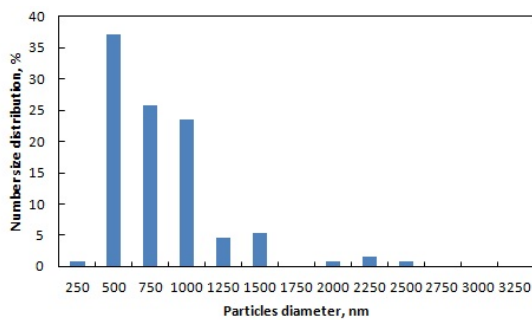
(d) FE-SEM image of experiment n. 61.



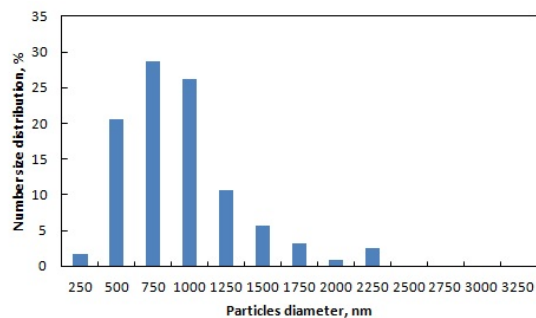
(e) FE-SEM image of experiment n. 64.

Figure 4.18: FE-SEM images of experiments described in Table 4.8.

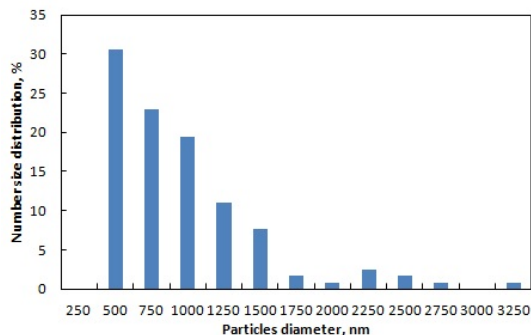
Referring to experiments conducted using the same recipe n. 58, 60 and 61 this last one showed particles population more broad until 3500 nm. Changing only the co-solvent from 1-propanol to ethanol, size distribution was similar, only wider. On the other hand, increasing the amount of PI, distribution illustrated its peak at 750 nm.



(a) Particles distribution of experiment n. 58.



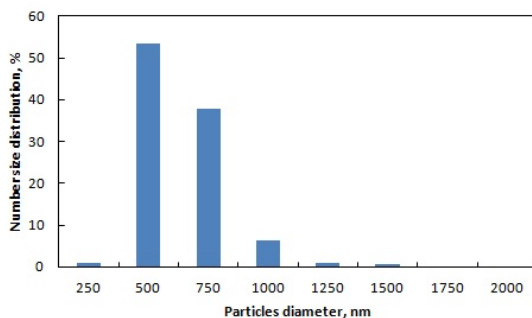
(b) Particles distribution of experiment n. 60.



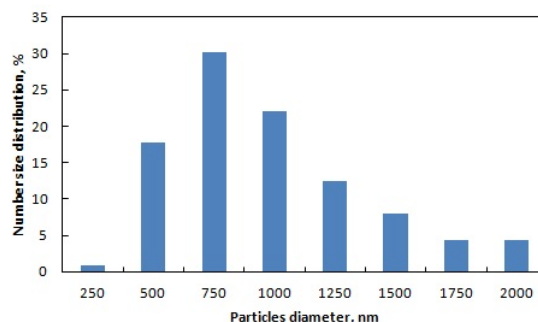
(c) Particles distribution of experiment n. 61.

Figure 4.19: Particles distributions of experiments described in Table 4.8.

Varying the ratio between monomers and solvents from 1:4 to 1:3 of experiments n. 62 and 63, particles size distributions were really different. They differed in the position of the peak which was shifted of 250 nm in experiment n. 63 and in diameters of particles which were bigger.



(a) Particles distribution of experiment n. 62.



(b) Particles distribution of experiment n. 63.

Figure 4.20: Particles distributions of experiments described in Table 4.8.

## Use of BA and TPT

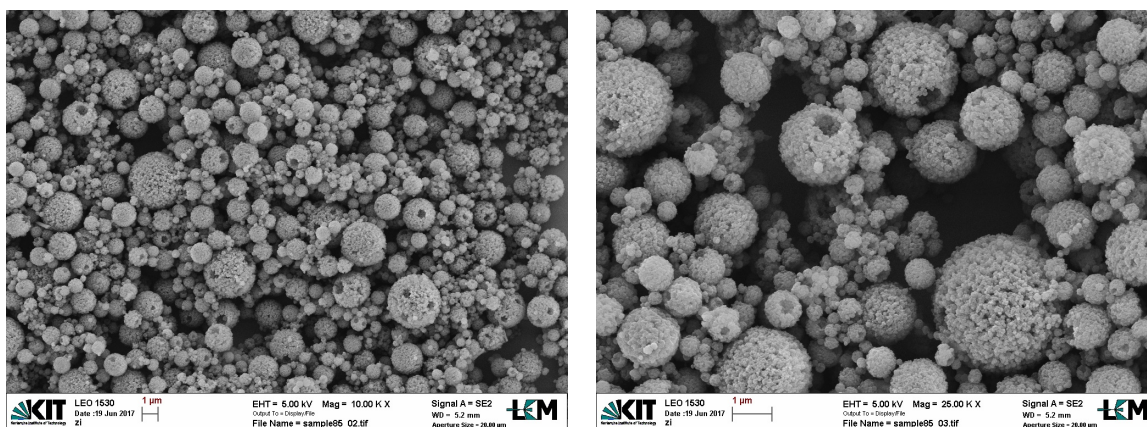
Experiments were performed using 70% wt. of monomers and 30% in wt. of solvents. The ratio between cross-linker and monomer ranged from 1:4 to 1:2. Factors which were varied were: the amount of glycerol from 6 to 20%, the alternate use of ethanol and 1-propanol and the amount of photo-initiator, as before.

Table 4.9: List of experiments performed with BA-TPT 70%-30%.

N. exp.	Composition of spray solution						Ratio c-l-mon.
	BA	TPT	HD	Iso-Oct.	Glyc.	Co-solv.	
66	51.73%	12.93%		28%	5.6%	35% Eth.	1:3
67	43.1%	21.55%		28%	5.6%	35% Eth.	1:2
68	50.4%	12.6%		27%	9%	63.15% 1-Prop.	1:4
69	50.4%	12.6%	27%		9%	66.94% 1-Prop.	1:4
70	50.4%	12.6%		27%	9%	55.25% Eth.	1:4
71	49.78%	12.45%		17.78%	20%	81.36% 1-Prop.	1:4
72	49.78%	12.45%		17.78%	20%	81.07% Eth.	1:4
73	49.78% (2.8% PI)	12.45%		17.78%	20%	80.32% 1-Prop.	1:4
74	49.78% (2.8% PI)	12.45%		17.78%	20%	80.70% Eth.	1:4

The use of TPT conducted to the production of micro-capsules made of a porous shell. Their shell was not smooth, but always made of small dominions of material. This could be caused by a fast precipitation of the structure, which presented a high networking density.

Experiments more successful employed a recipe with a ratio cross linker-monomer 1:4. This was the best compromise to obtain structured micro-particles. However also the experiment n. 67 with a ratio cross linker-monomer 1:2 gave porous micro-capsules (Fig. 4.21).

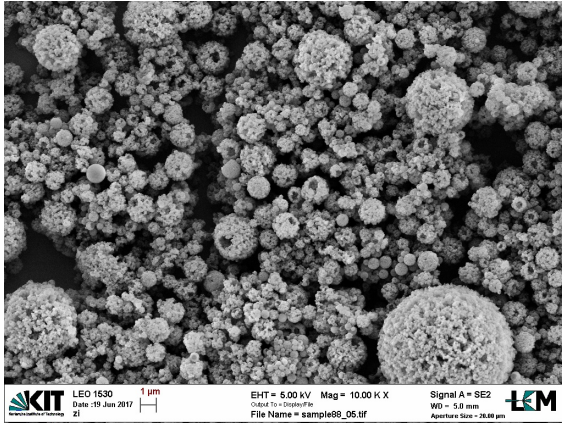


(a) FE-SEM image of experiment n. 67.

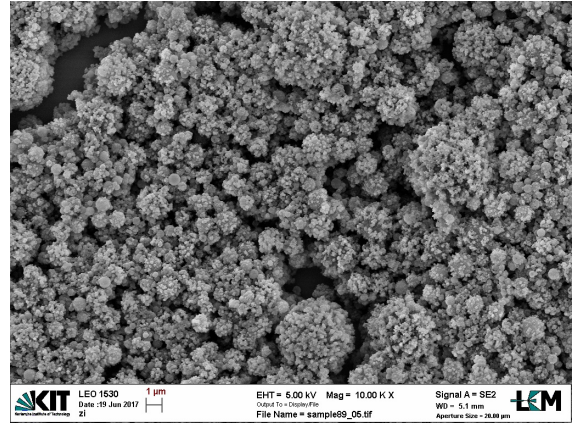
(b) FE-SEM image of experiment n. 67.

Figure 4.21: FE-SEM images of experiments described in Table 4.9.

Referring to experiments with a ratio cross linker-monomer 1:4, the best solvent which was used was iso-octanol. In fact, analyzing FE-SEM images (Fig. 4.22) of two experiments n. 68 and 69 conducted with the same recipe, but different solvent, HD and iso-octanol, HD was the more precipitating porogene. Using HD particles were disintegrated since it was a bad solvent for both TPT and TPET which were polar. On the other hand, micro-capsules produced with iso-octanol were porous as the networking occurred too quickly.



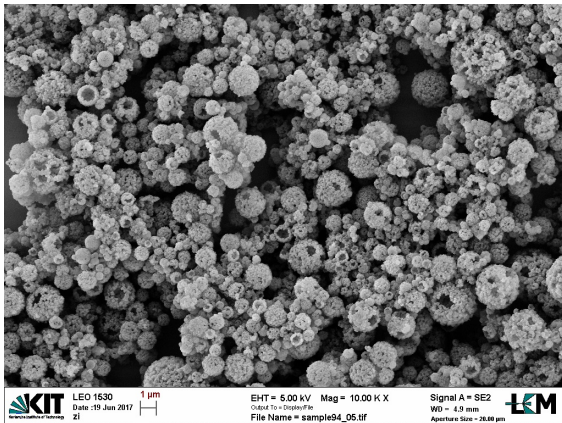
(a) FE-SEM image of experiment n. 68.



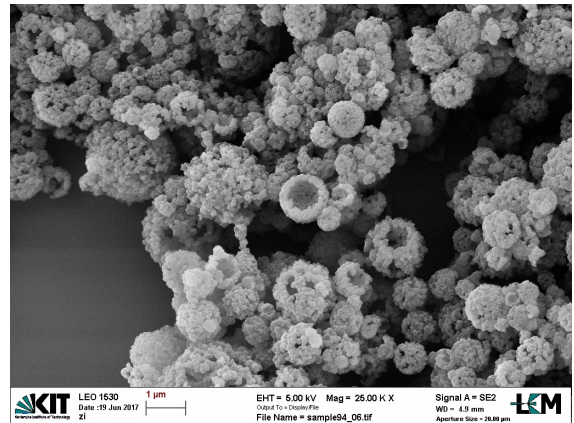
(b) FE-SEM image of experiment n. 69.

Figure 4.22: FE-SEM image of experiments described in Table 4.9.

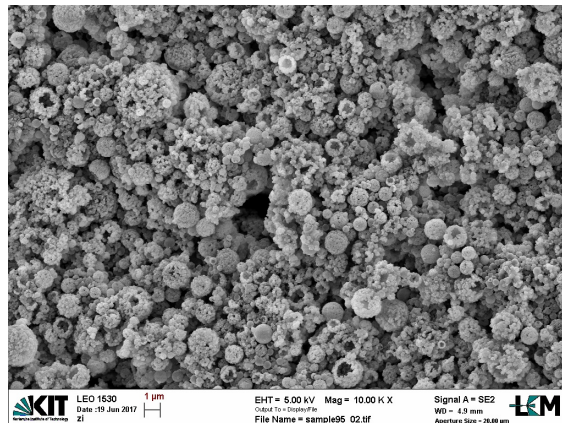
Regarding the type of co-solvent it was difficult to consider which one was the best co-solvent, if ethanol or 1-propanol. Also by FE-SEM images, there were not significant differences varying only the type of co-solvent in experiment n. 71 and 72 (Fig. 4.23).



(a) FE-SEM image of experiment n. 71.



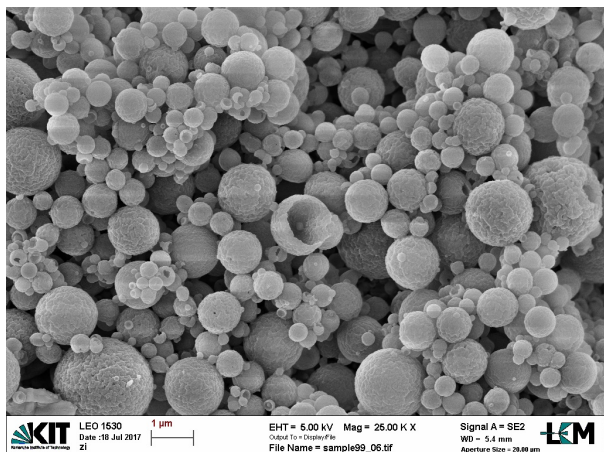
(b) FE-SEM image of experiment n. 72.



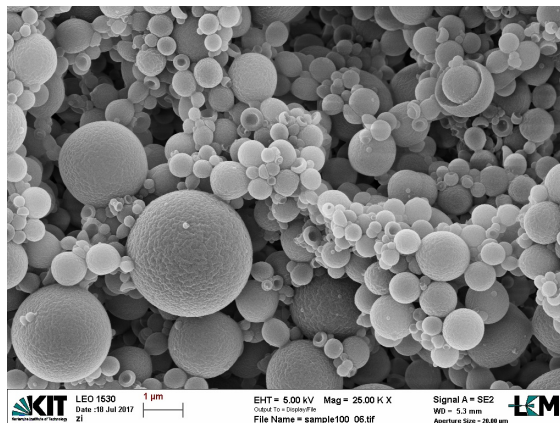
(c) FE-SEM image of experiment n. 72.

Figure 4.23: FE-SEM images of experiments described in Table 4.9.

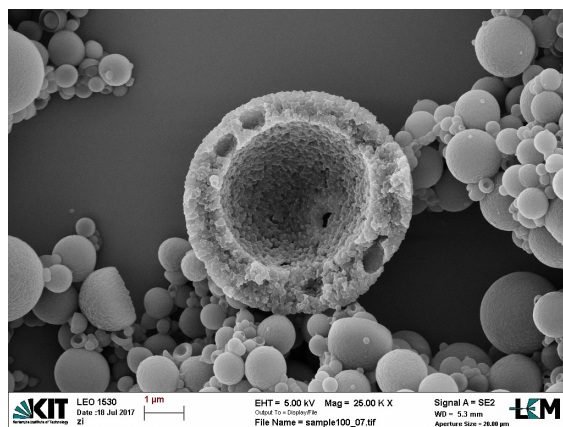
Increasing the amount of photo-initiator with the same recipe, really important changes appeared by FE-SEM images (Fig. 4.24). In fact, micro-particles looked like less porous, as gel type, made of smaller dominions of material. Their shell appeared smooth. Maybe the increase in photo-initiator quantity could help in agglomerating and structuring.



(a) FE-SEM image of experiment n. 73.



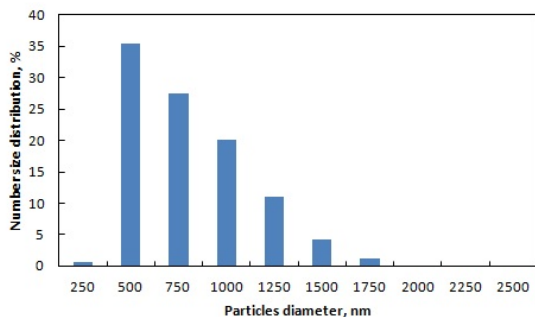
(b) FE-SEM image of experiment n. 74.



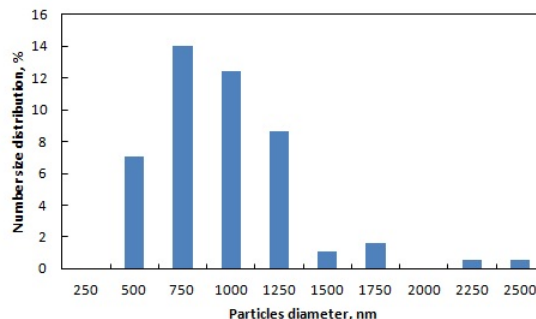
(c) FE-SEM image of experiment n. 74.

Figure 4.24: FE-SEM image of experiments described in Table 4.9.

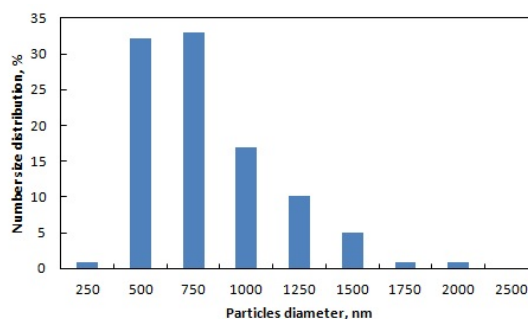
Particles size distribution of experiments n. 70, 71 and 72 (Fig. 4.25) showed that increasing the amount of glycerol from 10 up to 20% the peak shifted from 500 to 750 nm. Furthermore, particles population was wider reaching a size of 2500 nm, instead of 1750 nm. Co-solvents did not influence size distribution.



(a) *Particles size distribution of experiment n. 70.*



(b) *Particles size distribution of experiment n. 71.*



(c) *Particles size distribution of experiment n. 72.*

Figure 4.25: Particles size distributions of experiments described in Table 4.9.

FT-IR images (Fig. 4.26) illustrated the presence of C=O bond at around  $1700\text{ cm}^{-1}$ .

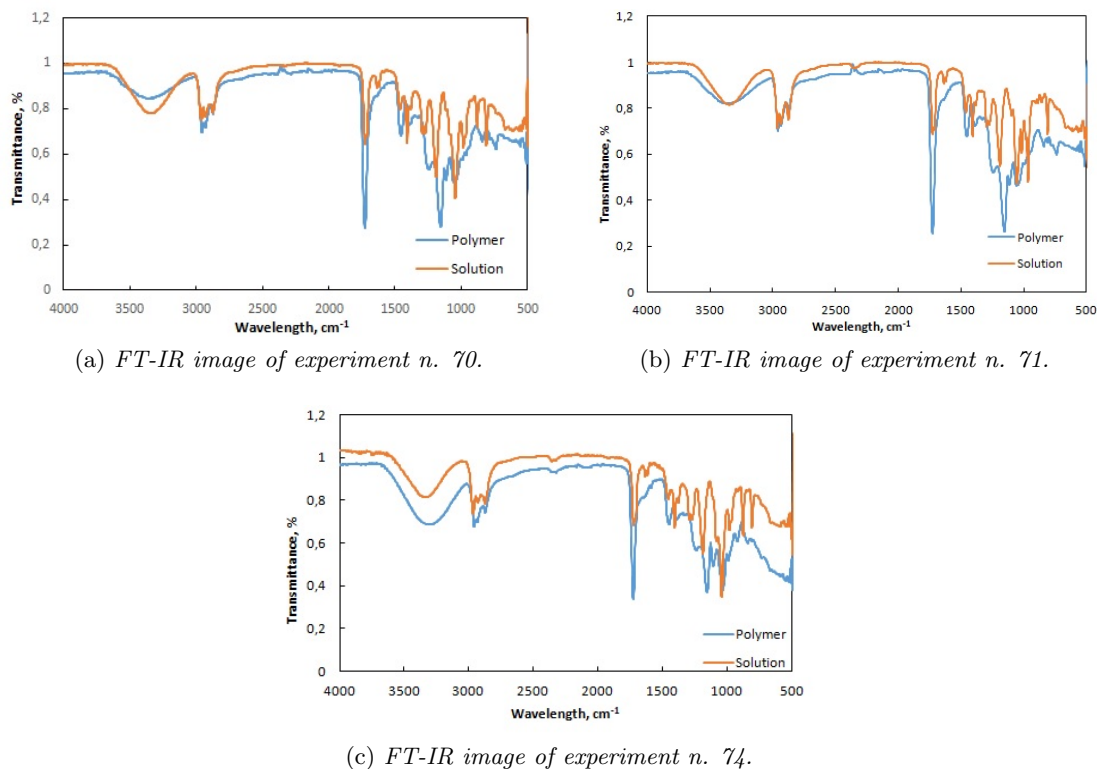


Figure 4.26: FT-IR images of experiments described in Table 4.9.

## 4.2 Conclusion acrylic polymerization

The second part of the thesis was focused on the production of micro-particles by aerosol photo-polymerization using a radicalic mechanism of polymerization.

The production of full particles was achieved employing a co-monomeric system consisting of monomer (BA), photo-initiator and alternatively co-monomer (HDDA or TPT or TPET). The use of MMA as monomer instead of BA was not promising since it led to obtain sticky and not separated particles.

Porous micro-particles were produced using different recipes. As monomers were employed BA and MMA, HDDA, TPT and TPET were used as cross-linkers, while HD and iso-octanol were used as solvents. The best recipe which led to the production of porous structures involved 70% wt. of monomers and 30% wt. of solvent and the use of the tri-functional cross-linker TPT in combination with BA or MMA. The ratio wt. between the cross-linker and the monomer was 1:2. In addition to porous micro-particles, gel type micro-particles were produced employing a co-monomeric system made of TPET and BA in ratio wt. 1:2 and 1:4. The recipe involved 70% wt. of monomers and 30% wt. of iso-octanol, as solvent.

Lots of experiments were conducted to obtain micro-caps and micro-capsules. The formulation which gave best results involved 70% wt. of monomers and 30% wt. of solvents. First of all, a high amount of glycerol was indispensable to structure micro-particles and consequently a co-solvent, ethanol or 1-propanol, was needed to homogenize the starting solution. Structured particles were produced in two ways. The first one, included BA as monomer, HDDA as cross-linker, PI, iso-octanol as solvent, glycerol as soft-maker and ethanol or 1-propanol as co-solvents. The ratio wt. between co-monomer and monomer was 1:3 or 1:4. It was not clear which agent acted in the

formulation of micro-caps or micro-capsules, but it was clear that glycerol acted the main role in structuring micro-particles. Furthermore, an increase in its amount determined an improvement in micro-particles conformation. The second way to obtain, above all, micro-capsules involved BA as monomer, TPT as cross-linker, PI, iso-octanol as solvent, glycerol as soft-maker and ethanol or 1-propanol as co-solvents. The ratio wt. 1:4 between co-monomer and monomer gave best results.

## 4.3 Thiol-ene Polymerization

### 4.3.1 Production of full micro-particles

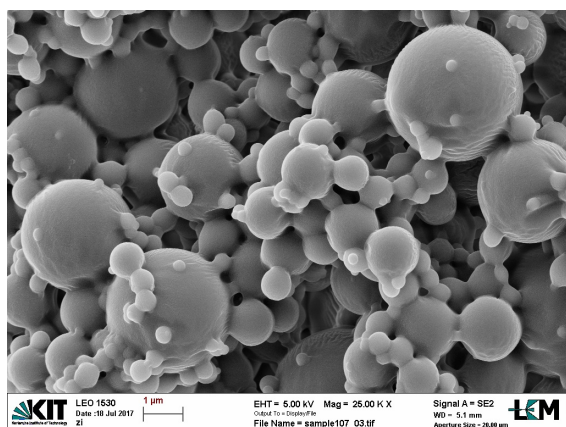
Production of full micro-particles was achieved employing a solution made of two different monomers, the photo-initiator Irgacure 907 and solvents. Reaction took place between monomers with a functional group  $-(SH)$ , trimethylolpropane tris(3-mercaptopropionate) and pentaerythritol tetrakis(3-mercaptopropionate), and monomers with a double bond  $C=C$ , neopentyl glycol diacrylate, diallyl adipate, DVE-3. Ratios wt. 1:1 and 1.5:1 between the two monomers were used. Ratios, always wt., between monomers and solvents were 70%-30%, 60%-40% and 50%-50%. Solvents used were 2-octanone, HD and ethanol. Furthermore we tried to perform experiments using as monomers 2,2'(ethylenedioxy)diethanethiol in combination with DVE-3 or TPT or diallyl adipate, but reaction took place too quickly producing heat.

In the following table (Tab. 4.10) list of the performed experiments is presented .

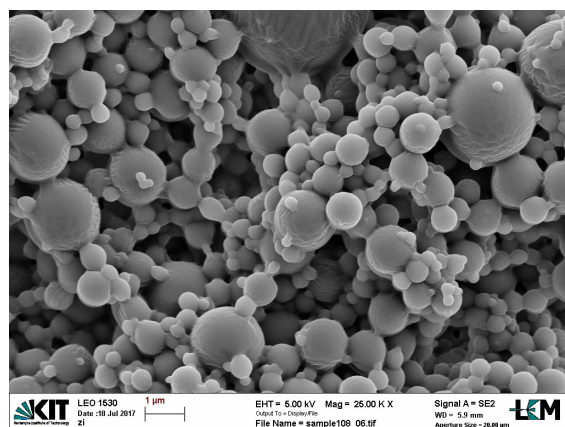
Table 4.10: List of experiments to produce full micro-particles.

N.e.	Composition of spray solution								T.-V.	S.-M.
	Neo.	Dia.	DVE-3	Tri.	Pen.	HD	2-oct.	Eth.		
75	45.42%				69.72%		25.78%		1.5:1	70%-30%
76		47.75%			68.35%		25.67%		1.5:1	70%-30%
77		31.65%			68.35%		28.7%		1:1	70%-30%
78		31.65%			68.35%		40%		1:1	60%-40%
79		31.65%			68.35%		8.31%	37.90%	1:1	50%-50%
80	52.13%			65.25%			37.21%		1.5:1	60%-40%
81	52.13%			65.25%		18.18%	28.58%		1.5:1	50%-50%
82			23.56%	46.44%			40.68%		1:1	60%-40%
83			50.9%	66.34%			39.96%		1.5:1	60%-40%

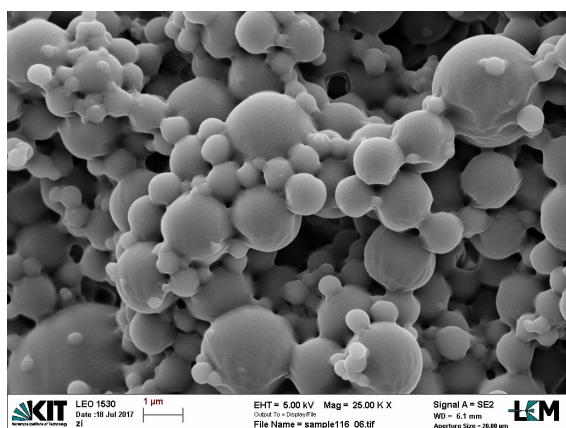
Analyzing FE-SEM images, samples with a ratio thiol-vinyl 1.5:1 (Fig. 4.27) worked better than samples with a ratio 1:1 (Fig. 4.28). This was an unusual behavior of a step reaction. In fact, normally this kind of reaction worked with an unitary ratio monomer-monomer to avoid formation of oligomers. Experiments n. 75, 76, 80, 81 and 83, whose ratio thiol-vinyl was 1.5:1, produced full micro-particles. They appeared quite sticky and not completely separated. Particles were produced with a different ratio monomers-solvents, but it was not possible to distinguish differences by FE-SEM images.



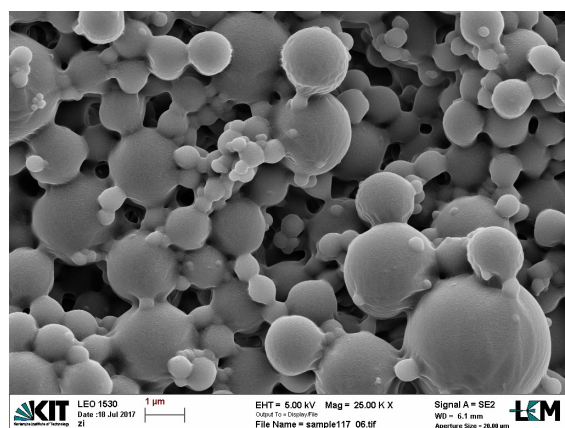
(a) FE-SEM image of experiment n. 75.



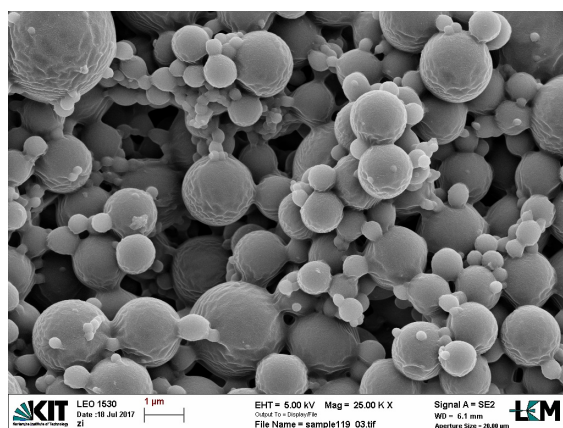
(b) FE-SEM image of experiment n. 76.



(c) FE-SEM image of experiment n. 80.



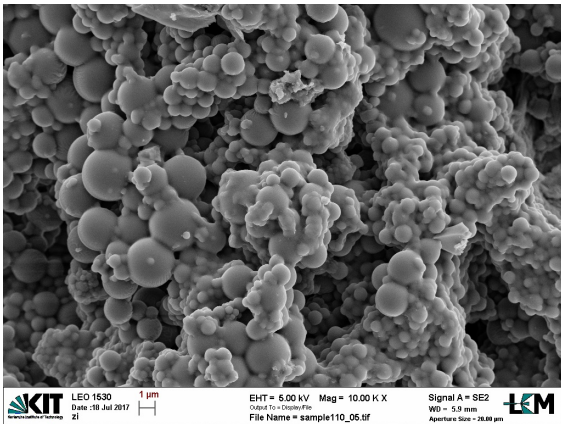
(d) FE-SEM image of experiment n. 81.



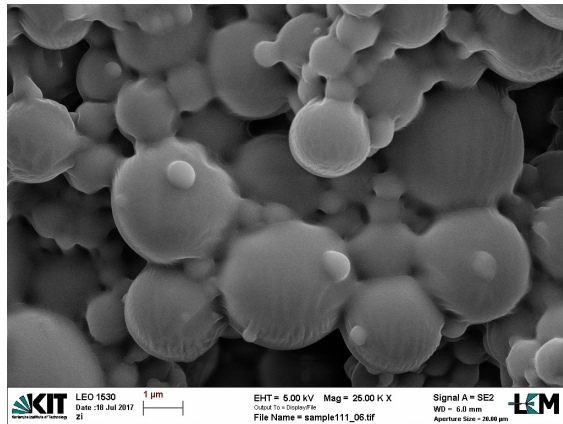
(e) FE-SEM image of experiment n. 83.

Figure 4.27: FE-SEM images of experiments described in Table 4.10.

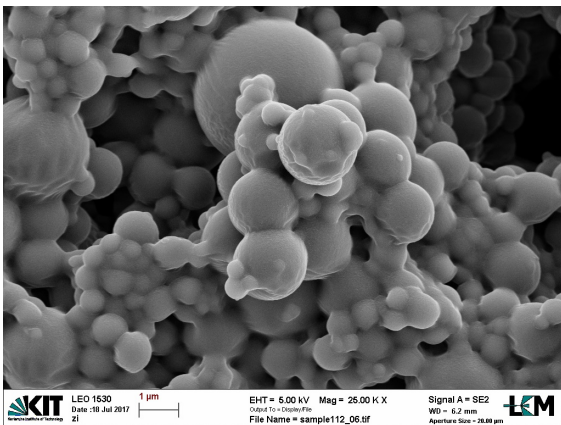
Experiments n. 68, 69, 70 and 73, whose ratio thiol-vinyl was 1:1, produced full micro-particles, but not separated. Different ratios monomers-solvents were employed. Different features were not distinguished among FE-SEM images.



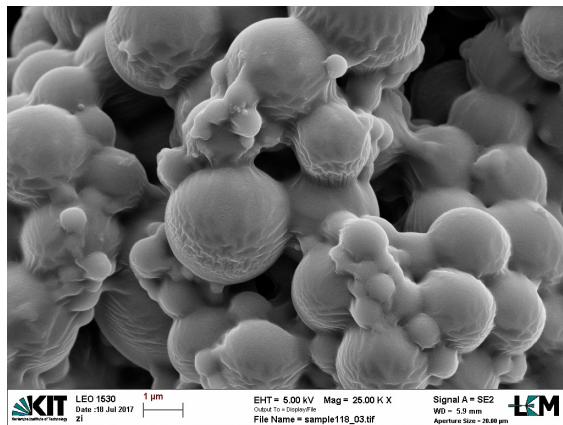
(a) FE-SEM image of experiment n. 68.



(b) FE-SEM image of experiment n. 69.



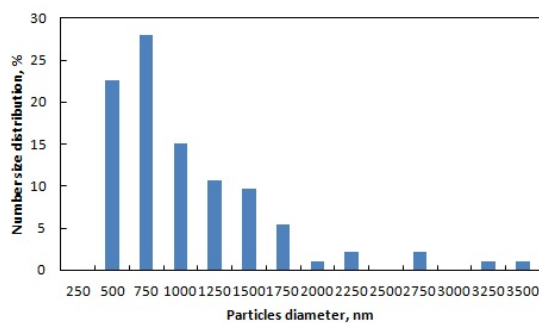
(c) FE-SEM image of experiment n. 70.



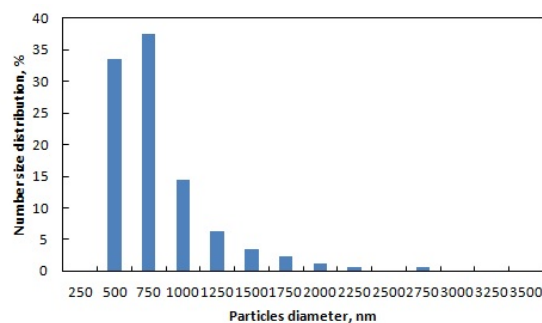
(d) FE-SEM image of experiment n. 73.

Figure 4.28: FE-SEM images of experiments described in Table 4.10.

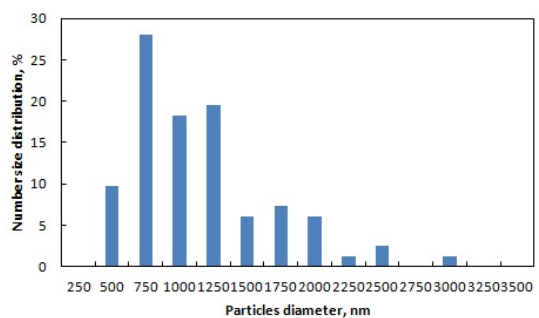
Particles size distributions of some samples previously described (Fig. 4.29) showed a broad population of particles whose diameter ranged from 250 to 3500 nm. The peak was usually at 750 nm, but images illustrated a kind of tail of particles of bigger dimensions.



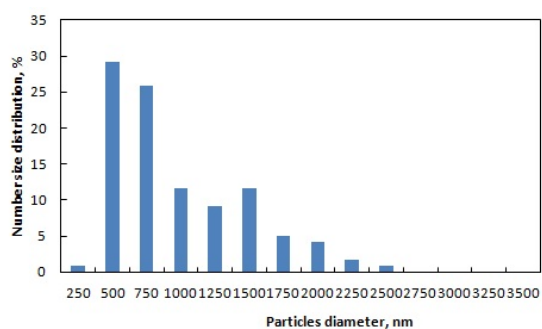
(a) Particles size distribution of experiment n. 75.



(b) Particles size distribution of experiment n. 76.



(c) Particles size distribution of experiment n. 80.



(d) Particles size distribution of experiment n. 83.

Figure 4.29: Particles size distributions of experiments described in Table 4.10.

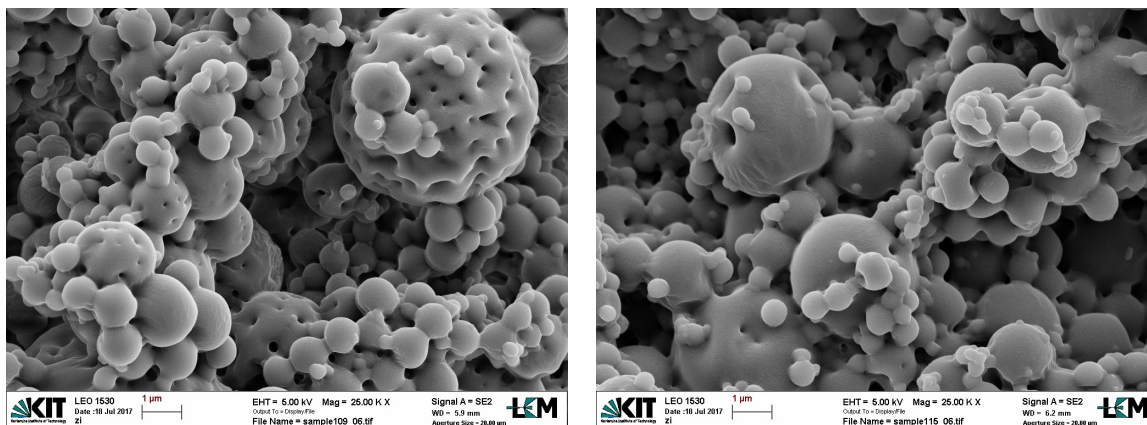
### 4.3.2 Production of porous micro-particles

Porous particles were produced adding to the recipe described in the precedent paragraph iso-octanol. In this case experiments were performed employing a ratio between thiol-vinyl 1.5:1 and between monomers-solvents 70%-30% and 60%-40%.

Table 4.11: List of experiments to produce porous micro-particles.

N. exp.	Composition of spray solution					Ratio thi-vin	Ratio solv-mon
	Neop.	Trim.	Pent.	2-oct.	Iso-Oct.		
84	45.42%		69.72%	11.41%	22.83%	1.5:1	70%-30%
85	52.13%	65.25%			37.21%	1.5:1	60%-40%

By FE-SEM images (Fig. 4.30) particles looked sponges-like. Especially particles of bigger dimensions appeared structured, particles of smaller dimensions looked like full and not structured. In this kind of reaction an alcohol was necessary to produce porous particles, while in the cationic polymerization the alcohol conducted to produce micro-capsules.

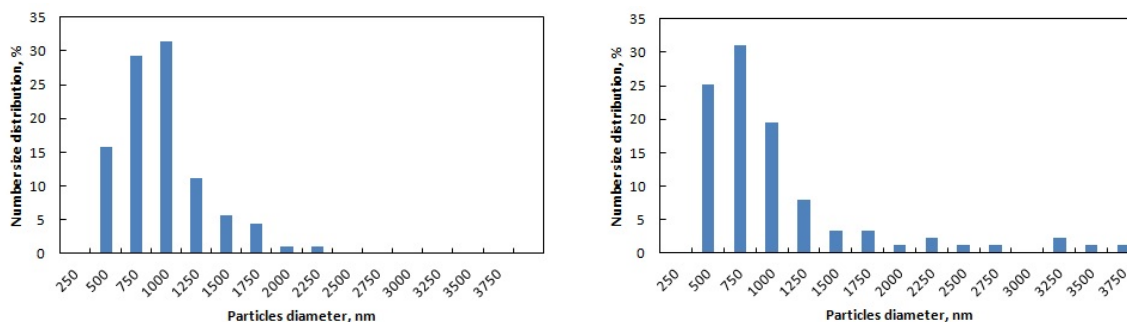


(a) FE-SEM image of experiment n. 84.

(b) FE-SEM image of experiment n. 85.

Figure 4.30: FE-SEM images of experiments described in Table 4.11.

Particles size distribution of these experiments showed a peak of distribution around 750-1000 nm and a broad population of particles which ranged from 500 to 3750 nm.



(a) Particles size distribution of experiment n. 84.

(b) Particles size distribution of experiment n. 85.

Figure 4.31: Particles size distributions of experiments described in Table 4.11.

## 4.4 Conclusion thiol-ene polymerization

The last part of this work was focused on the production of micro-particles by aerosol photo-polymerization employing the thiol-ene mechanism of reaction.

The best recipe to produce full micro-particles employed a co-monomeric system, made of a thiol-ene monomer and a vinyl monomer in ratio wt. 1.5:1, in addition to PI and solvents, HD, 2-octanone and ethanol. The ratio wt. between monomers and solvents was varied but we could not deduce how it influenced polymerization.

Sponges-like micro-particles were obtained using the precedent described co-monomeric system in ratio 1.5:1 and in addition to PI and solvents, 2-octanone and iso-octanol. Best ratios wt. between monomers and solvents were 70%-30% and 60%-40%, although no complete and homogeneous structuring of the product was visible.

Obtained results were promising and need to be improved in the future to achieve better formulations and to produce better structured micro-particles.

# List of Figures

1	Processo schematico della foto-polimerizzazione in aerosol. . . . .	ii
2	Strumentazione completa . . . . .	ii
3	Immagine al FE-SEM di micro-particelle piene, meccanismo cationico. . . . .	iii
4	Immagine al FE-SEM di micro-particelle porose, meccanismo cationico. . . . .	iv
5	Immagine al FE-SEM di micro-capsule, meccanismo cationico. . . . .	v
6	Immagine al FE-SEM di micro-particelle piene, meccanismo radicalico. . . . .	vi
7	Immagine al FE-SEM di micro-particelle porose, meccanismo radicalico. . . . .	vi
8	Immagine al FE-SEM di micro-particelle porose, meccanismo radicalico. . . . .	vii
9	Immagine al FE-SEM di micro-caps e micro-capsule, meccanismo radicalico. . . . .	viii
10	Immagine al FE-SEM di micro-caps e micro-capsule, meccanismo radicalico. . . . .	ix
11	Immagine al FE-SEM di micro-particelle piene, meccanismo tiolenico. . . . .	x
12	Immagine al FE-SEM di micro-particelle porose, meccanismo tiolenico. . . . .	x
1.1	Macro-emulsion polymerization . . . . .	2
1.2	Mini-emulsion polymerization . . . . .	3
1.3	Reactor for aerosol photo-polymerization . . . . .	6
1.4	Reactor for aerosol photo-polymerization . . . . .	6
1.5	MMA and Irgacure . . . . .	8
1.6	Decomposition of the initiator. . . . .	8
1.7	Reactions of monomer with primary radicals. . . . .	9
1.8	Generalized propagation step. . . . .	9
1.9	Termination by combination between two radical polymer chains. . . . .	9
1.10	Chain transfer reaction. . . . .	9
1.11	SEM images . . . . .	10
1.12	TEM images . . . . .	11
1.13	Reactivity of VE functionalized oligomers . . . . .	13
1.14	Influence of the iodonium photo-initiator (2 wt.%) on the polymerization . . . . .	13
1.15	SEM image of crosslinked poly(DVE2) particles produced by cationic aerosol-photopolymerization . . . . .	13
1.16	Thiol-ene polymerization mechanism . . . . .	14
2.1	Tri(ethylene glycol) divinyl ether 98% . . . . .	17
2.2	Comonomers for cationic polymerization . . . . .	17
2.3	Triarylsulfonium hexafluoroantimonate salts . . . . .	18
2.4	Hexadecane anhydrous $\geq 99\%$ . . . . .	18
2.5	2-octanone $\geq 98\%$ . . . . .	18
2.6	2-Ethyl-1-hexanol $\geq 99.6\%$ . . . . .	18
2.7	Monomers for acrylic radical polymerization . . . . .	19
2.8	Trimethylolpropane triacrylate . . . . .	19
2.9	Trimethylolpropane ethoxylate triacrylate . . . . .	19
2.10	1,6-Hexanediol diacrylate . . . . .	19
2.11	Irgacure 907 . . . . .	19
2.12	Glycerol $\geq 99.5\%$ . . . . .	20
2.13	Co-solvents for acrylic radical polymerization. . . . .	20

2.14	Monomers for thiol-ene radical polymerization . . . . .	21
2.15	Schematic process of aerosol photo-polymerization . . . . .	21
2.16	Complete equipment . . . . .	22
2.17	Atomizer . . . . .	22
2.18	Photo-reactor . . . . .	23
3.1	FE-SEM images of experiments described in Table 3.1. . . . .	26
3.2	Particles size distributions of experiments described in Table 3.1. . . . .	26
3.3	FE-SEM images of experiments described in Table 3.2. . . . .	28
3.4	Particles size distributions of experiments described in Table 3.2. . . . .	28
3.5	FE-SEM images of experiments described in Table 3.3. . . . .	30
3.6	Particles size distributions of experiments described in Table 3.3. . . . .	31
3.7	FE-SEM image and particles size distribution of experiment described in Table 3.4. . . . .	32
3.8	FT-IR of experiment described in Table 3.4. . . . .	32
3.9	FE-SEM images of experiments described in Table 3.5. . . . .	34
3.10	FE-SEM images of experiments described in Table 3.5. . . . .	35
3.11	Particles size distributions of experiments described in Table 3.5. . . . .	35
3.12	FT-IR of experiments described in Table 3.5. . . . .	36
3.13	FE-SEM images of experiments described in Table 3.6. . . . .	37
3.14	Particles size distributions of experiments described in Table 3.6. . . . .	37
3.15	FT-IR of experiments described in Table 3.6. . . . .	38
4.1	FE-SEM images of experiments described in Table 4.1. . . . .	40
4.2	FE-SEM images of experiments described in Table 4.1. . . . .	40
4.3	Particles size distributions of experiments described in Table 4.1. . . . .	41
4.4	FT-IR images of experiments described in Table 4.1. . . . .	41
4.5	FE-SEM image of experiment described in Table 4.2. . . . .	42
4.6	FT-IR image of experiment described in Table 4.2. . . . .	42
4.7	FE-SEM image of experiments described in Table 4.3. . . . .	44
4.8	FE-SEM images of some experiments described in Table 4.4. . . . .	45
4.9	Particles size distributions of experiments described in Table 4.4. . . . .	45
4.10	FT-IR of experiment described in Table 4.4. . . . .	45
4.11	FE-SEM images of experiments described in Table 4.5. . . . .	47
4.12	Particles size distribution of experiments described in Table 4.5. . . . .	48
4.13	FE-SEM images of experiments described in Table 4.6. . . . .	49
4.14	FT-IR of experiments described in Table 4.6. . . . .	50
4.15	FE-SEM images of some experiments described in Table 4.7. . . . .	50
4.16	FE-SEM images of experiments described in Table 4.8. . . . .	52
4.17	FE-SEM images of experiments described in Table 4.8. . . . .	53
4.18	FE-SEM images of experiments described in Table 4.8. . . . .	54
4.19	Particles distributions of experiments described in Table 4.8. . . . .	55
4.20	Particles distributions of experiments described in Table 4.8. . . . .	55
4.21	FE-SEM images of experiments described in Table 4.9. . . . .	56
4.22	FE-SEM image of experiments described in Table 4.9. . . . .	57
4.23	FE-SEM images of experiments described in Table 4.9. . . . .	57
4.24	FE-SEM image of experiments described in Table 4.9. . . . .	58
4.25	Particles size distributions of experiments described in Table 4.9. . . . .	59
4.26	FT-IR images of experiments described in Table 4.9. . . . .	60
4.27	FE-SEM images of experiments described in Table 4.10. . . . .	63
4.28	FE-SEM images of experiments described in Table 4.10. . . . .	64
4.29	Particles size distributions of experiments described in Table 4.10. . . . .	65
4.30	FE-SEM images of experiments described in Table 4.11. . . . .	66
4.31	Particles size distributions of experiments described in Table 4.11. . . . .	66

# List of Tables

1.1	MEHQ concentration and relatively formation of solids. . . . .	15
3.1	List of experiments performed with only monomer and photo-initiator. . . . .	25
3.2	List of experiments performed with HD and 2-octanone. . . . .	27
3.3	List of experiments performed with iso-octanol, ratio monomer-solvents 60%-40%. . . . .	29
3.4	List of experiments performed with iso-octanol, ratio monomer-solvents 56%-44%. . . . .	31
3.5	List of experiments performed with iso-octanol, ratio monomer-solvents 50%-50%. . . . .	33
3.6	List of experiments performed with co-monomers. . . . .	36
4.1	List of experiments performed with BA. . . . .	39
4.2	List of experiments performed with MMA. . . . .	42
4.3	List of experiments performed with BA and HDDA. . . . .	43
4.4	List of experiments performed with BA-MMA and TPT. . . . .	44
4.5	List of experiments performed with BA-MMA and TPET. . . . .	46
4.6	List of experiments performed with BA-HDDA 50%-50%. . . . .	48
4.7	List of experiments performed with BA-HDDA 60%-40%. . . . .	50
4.8	List of experiments performed with BA-HDDA 70%-30%. . . . .	51
4.9	List of experiments performed with BA-TPT 70%-30%. . . . .	56
4.10	List of experiments to produce full micro-particles. . . . .	62
4.11	List of experiments to produce porous micro-particles. . . . .	65



# Acronyms

<b>CMC</b>	Critical Micellar Concentration
<b>HD</b>	Hexadecane
<b>MMA</b>	Methyl Methacrylate
<b>PMMA</b>	Polymethyl Methacrylate
<b>UV</b>	Ultraviolet
<b>BA</b>	Butyl Acrylate
<b>HDDA</b>	1,6-hexanedioldiacrylate
<b>PI</b>	Photo-Initiator
<b>PMNCs</b>	Polymer-Matrix Nano-Composites
<b>ZnO</b>	Zinc Oxide
<b>VE</b>	Vinyl Ether
<b>TAS-PF6</b>	Triarylsulfonium hexafluorophosphate
<b>MEHQ</b>	4-Methoxyphenol
<b>SDS</b>	Sodium Dodecyl Sulfate
<b>H-NMR</b>	Proton Nuclear Magnetic Resonance
<b>ZCNPs</b>	zwitterionic Chitosan Nano-Particles
<b>PC</b>	Polycarbonate
<b>PTFE</b>	Polytetrafluoroethylene
<b>SEM</b>	Scanning electron microscopy
<b>FE-SEM</b>	Field emission Scanning electron microscopy
<b>TEM</b>	Transmission electron microscopy
<b>FT-IR</b>	Fourier transform infrared spectroscopy
<b>DSC</b>	Differential scanning calorimetry
<b>TPT</b>	Trimethylolpropane triacrylate
<b>TPET</b>	Trimethylolpropane ethoxylate triacrylate



# List of Symbols

$k_d$	Dissociation rate coefficient
$k_i$	Initiation rate coefficient
$k_{p1}$	Propagation rate coefficient
$k_{pn}$	General propagation rate coefficient
$k_{acc}$	Combination rate coefficient
$k_{ri}$	Re-beginning rate coefficient
$k_{dis}$	Disproportion rate coefficient
$k_p$	Propagation rate coefficient
$k_t$	Termination rate coefficient
$k_{tr}$	Transfer rate coefficient



# Bibliography

- Akgün, E., Hubbuch, J., and Wörner, M. (2013). Perspectives of aerosol-photopolymerization: Nanoscale polymer particles. *Chemical Engineering Science*, 101:248–252. doi: 10.1016/j.ces.2013.06.010.
- Akgün, E., Hubbuch, J., and Wörner, M. (2014a). Perspectives of Aerosol-Photopolymerization: Nanostructured Polymeric Particles. *Macromolecular Materials and Engineering*, 299:1316–132. doi: 10.1002/mame.201400032.
- Akgün, E., Hubbuch, J., and Wörner, M. (2014b). Perspectives of aerosol-photopolymerization: organic-inorganic hybrid nanoparticles. *Colloid and Polymer Science*, 292:1241–1247. doi: 10.1007/s00396-014-3175-2.
- Akgün, E., Muntean, A., Hubbuch, J., Wörner, M., and Sangermano, M. (2015). Cationic Aerosol Photopolymerization. *Macromolecular Materials and Engineering*, 300:136–139. doi: 10.1002/mame.201400211.
- Amato, D., Amato, D., Flyntb, A., and Patton, D. (2014). Functional, sub-100 nm polymer nanoparticles via thiol–ene miniemulsion photopolymerization. *Polymer Chemistry*, 6:5625–5632. doi: 10.1039/c4py01449a.
- Arshady, R. (1990). Albumin microspheres and microcapsules: Methodology of manufacturing techniques. *Journal of Controlled Release*, 14:111–131. doi: 10.1016/0168-3659(90)90149-N.
- Bell, S., Berdick, M., Holliday, W., and Kiritsis, G. (1970). Sustained relief analgesic compositions. doi: .
- Biskos, G., Vons, V., Yurteri, C., and Schmidt-Ott, A. (2008). Generation and Sizing of Particles for Aerosol-Based Nanotechnology. *KONA Powder and Particle Journal*, 26:13–35. doi: 10.14356/kona.26.2008006.
- Campos, E., Branquinho, J., Carreira, A.S. and Carvalho, A., Coimbra, P., Ferreira, P., and Gil, M. (2013). Designing polymeric microparticles for biomedical and industrial applications. *European Polymer Journal*, 49:2005–2021. doi: 10.1016/j.eurpolymj.2013.04.033.
- Cramer, N. and Bowman, C. (2001). Kinetics of Thiol–Ene and Thiol–Acrylate Photopolymerizations with Real-Time Fourier Transform Infrared. *Journal of Polymer Science*, 39:3311–3319.
- Decker, C., Bianchi, C., Decker, D., and Morel, F. (2001). Photoinitiated polymerization of vinyl ether-based systems. *Progress in Organic Coatings*, 42:253–266. doi: 10.1016/S0300-9440(01)00203-X.
- Ebewele, R. O. (2000). *Polymer Science and Technology*. Taylor and Francis Group, LLC.
- Eerikäinen, H. and Kauppinen, E. (2009). The Synthesis and Assembly of Polymeric Microparticles Using Microfluidics. *Advanced Materials*, 21:4071–4086. doi: 10.1002/adma.2008033863.
- Esen, C. and Schweiger, G. (1996). Preparation of Monodisperse Polymer Particles by Photopolymerization. *Journal of Colloid and Interface Science*, 179:276–280. doi: 10.1006/jcis.1996.0214.

- Esfandiari, P., Ligon, S., Lagref, J., Frantz, R., Cherkaoui, Z., and Liska, R. (2013). Efficient Stabilization of Thiol-ene Formulations in Radical Photo-polymerization. *Journal of Polymer Science*, 51:4261–4266. doi: 10.1002/pola.26848.
- Green, B. and Schleicher, L. (1957). Oil-containing microscopic capsules and method of making them. doi:.
- Hoon Byeon, J., Kulkarni, A., Kim, H., Thompson, D., and Roberts, J. (2014). Photoassisted One-Step Aerosol Fabrication of Zwitterionic Chitosan Nanoparticles. *Biomacromolecules*, 15:2320–2325. doi: /10.1021/bm5005417.
- Kawaguchi, H. (2000). Functional polymer microspheres. *Progress in Polymer Science*, 25:1171–1210. doi: 10.1016/S0079-6700(00)00024-1.
- Landfester, K. (2009). Miniemulsion Polymerization and the Structure of Polymer and Hybrid Nanoparticles. *Angewandte Chemie*, 48:4488–4507. doi: 10.1002/anie.200900723.
- Liu, D., Yu, B., Jiang, X., and Yin, J. (2013). Responsive Hybrid Microcapsules by the One-Step Interfacial Thiol-Ene Photopolymerization. *Langmuir*, 29:5307–5314. doi: org/10.1021/la400098c.
- Liu, W. (2006). Nanoparticles and Their Biological and Environmental Applications. *Journal of Bioscience and Bioengineering*, 102:1–7. doi: 10.1263/jbb.102.1.
- Mora-Huertas, C., Fessi, H., and Elaissari, A. (2010). Polymer-based nanocapsules for drug delivery. *International Journal of Pharmaceutics*, 385:113–142. doi: 10.1016/j.ijpharm.2009.10.018.
- Schorck, F., Luo, Y., Smulders, W., Russum1, J., Butté, A., and Fontenot, K. (2005). Miniemulsion Polymerization. *Adv Polym Sci*, 175:129–255. doi: 10.1007/b100115.
- Shin, D. and Oh, E.K. and Kim, S. (1996). Preparation of Polymer Particles in Aerosol-Phase Reaction. *Aerosol Science and Technology*, 24:243–254. doi: 10.1080/02786829608965369.
- Soppimath, K., Aminabhavia, T., Kulkarni, A., and Rudzinski, W. (2001). Biodegradable polymeric nanoparticles as drug delivery devices. *Journal of Controlled Release*, 70:1–20. doi: 10.1016/S0168-3659(00)00339-4.

# Acknowledgments

I would like to express my gratitude to Prof. Michael Wörner for his understanding, patience and kindness. I appreciated his continuous help during my long lab days and his assistance for everything I needed, from German life to lab work. He tried to give me all his knowledge about this work always with motivation and encouragement.

Vorrei ringraziare i Prof. Roberto Pisano e Marco Sangermano per avermi dato l'opportunità di lavorare a questa tesi. Ho apprezzato molto la vostra disponibilità ed il vostro interessamento durante tutto il lavoro. Vi ringrazio per le conoscenze che mi avete donato e per la pazienza che avete sempre mostrato nei miei confronti.

Un ringraziamento speciale va a Marco, il dottorando che ogni tesista desidera avere al proprio fianco. Grazie per tutti i preziosi consigli, per l'incoraggiamento e l'interesse verso di me e verso questo lavoro che hai mostrato dal primo all'ultimo giorno. Grazie per aver cercato di risolvere ogni problema, per avermi insegnato tanto e soprattutto per avermi sopportata.